공학박사 학위논문

Analyzing and Designing Price-based Power System Operation for Active Power with the Feedback Control Mechanism

피드백 제어 구조를 활용한 가격 기반

전력시스템 운영의 분석 및 설계에 관한 연구

2014년 2월

서울대학교 대학원

전기·컴퓨터공학부

진 영 규

Analyzing and Designing Price-based Power System Operation for Active Power with the Feedback Control Mechanism

지도 교수 윤 용 태

이 논문을 공학박사 학위논문으로 제출함
2013년 12월

서울대학교 대학원
전기·컴퓨터공학부
진 영 규

진영규의 공학박사 학위논문을 인준함
2013년 12월

위 원 장 _____ (인)

부위원장 _____ (인)

위 원 _____ (인)

위 원 _____ (인)

위 원 _____ (인)

Abstract

Analyzing and Designing Price-based Power System Operation for Active Power with the Feedback Control Mechanism

Young Gyu Jin

School of Electrical Engineering and Computer Science

The Graduate School

Seoul National University

In a decentralized and deregulated environment, price-based operation (PBO) is suggested as an alternative to the centralized scheme. In the PBO, time-varying prices coordinate independent suppliers and consumers who may try to maximize their own profit. The most important thing in the PBO is to determine the appropriate prices, but it is not an easy task. Thus, analyzing and designing methods for the PBO is necessary to guide the determination of the price signals and to provide insights for the dynamic results. In order to perform the analysis and the design considering the dynamic performance of the coordination in view of the frequency stability, various methods and structures for the PBO have been presented in this dissertation.

Firstly, the continuous-time model of the PBO is described under the assumptions that there are a large number of the participants and that the superposition of the asynchronous discrete responses of them can be

approximately represented as the continuous function. Then, the power market dynamics is formalized as the feedback control structure, and the PBO is interpreted as the controller within it. Then, the approximation method is composed to express the target system with a simple typical form. After determining the approximate target system, the basic tuning rule is derived by applying a selected controller tuning rule. In addition, the modified designing rule is composed by supplementing an asymmetric damping control to the basic tuning rule in order to enhance the dynamic characteristics for the frequency control.

As a method for further improving the dynamic performance in view of the frequency stability, a new structure for the PBO using price information as a kind of price offset is constructed. The effects of the price information on the maximum deviation of the energy imbalance are quantitatively analyzed. The analysis shows that the maximum deviation is likely to be reduced linearly to the difference between the price information and the system marginal price in the steady state. It is also found that the actual maximum deviation is the smallest when the price information is a little greater or less than the steady-state price.

Finally, a general framework for the optimal design of the PBO is constructed. Not only that the power/energy balancing and the congestion management functions are successfully performed within the framework, but it is also guaranteed that the converged values in the steady state should be equal to the optimal solutions of the OPF method. The framework is suitable in a decentralized environment in the sense that each congestion management controller can be separately designed and operated.

The effectiveness of the presented methods is verified by two case studies using the IEEE 39 bus network. The results show that the PBO designed by the designing rules is better than that without the application of them in view of the frequency stability. Moreover, the modified tuning rule performs even better than the basic tuning rule. The use of price information gives the considerable reduction of the energy imbalance regardless of whether the PBO is appropriately designed or not. In the case study for the framework, the fundamental property of it is verified that the converged values are all equal to the optimal solution irrespective of the specific design of the PBO, even though the time variation differs by the designs. A few kinds of the trade-off in the PBO are identified such as; between the recovery speed to the normal state and the smooth change of the variables such as the nodal prices; between the power/energy balancing and the congestion management functions.

Keywords: Congestion Management, Controller design, Electricity price, Frequency control, Optimal power flow, Power system operation.

Student Number: 2010-31001

Contents

List of Tables

List of Figures

Chapter 1. Introduction

1.1 Background

A few decades ago, almost all electric power systems throughout the world were operated by one controlling authority, which handles all aspects of generation, transmission and distribution. Although this centralized operation scheme with monopoly structure has a lot of advantages, many research results have pointed out the problems of this scheme [1-4]. Moreover, such a centralized operation can be confronted with difficulties when the number of components grows bigger with the introduction of new systems such as distributed generators and energy storage systems [3, 5]. Thus, there have been various types of restructuring and deregulation in the power industry up to recently, e.g., power pool model [6-8]. The main thrust of the most restructuring actions is to introduce competition. The competition within the market is able not only to reduce the cost of electricity consumption but also to induce better service for consumers. However, it may bring about many new technical issues in the operation of restructured power systems. Since power generations have been liberalized and privately owned in a deregulated environment, they tend to act in a way of maximizing their own profit and cannot be directly controlled anymore. Since there are naturally a large number of end customers, the same situation of profit pursuing and uncontrollability can happen to them. To deal with this problem, it is suggested to utilize the market mechanism.

Although there can be various structures of the market, the simplest one is the type of market composed of an energy market and an ancillary market depending on the type of the service [9]. The specific forms of transactions in the market can be realized through the bilateral contract, the auction procedures, and the real-time balancing. These kinds of transactions and the interaction between the components in the market are shown in Figure 1.1.

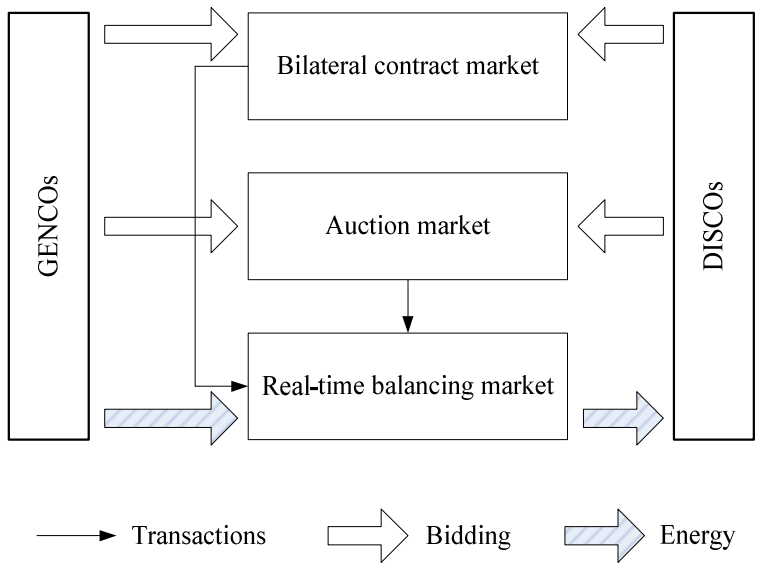

Figure 1.1 Market structure and interaction between the components in the market [9].

However, since the participants may exist who consume or supply differently with contracted volume, the imbalance between supply and demand is inevitable in the actual implementation of the transactions within the market. As a result, in order to maintain the security and the stability in the operation of deregulated power systems, the independent system operator

(ISO) has to function as the central entity which is responsible for the reliable system operation [10, 11]. The ISO performs reliability-related functions and market-related functions [10]. To be specific, the ISO can schedule and make provisions for the necessary functions through the market for the reliable real-time operation [9-11]. Especially for the real-time operation, the ISO should not only handle the imbalance between the real-time and scheduled quantities, but also perform real-time congestion management [10, 11]. However, as an alternative, the possibility of a price-based power system operation, which is abbreviated to price-based operation (PBO) in this dissertation, is also suggested. In the PBO, time-varying prices coordinate independent players who may be naturally non-cooperative [12-16]. In other words, electricity prices can be utilized as a kind of the control signal from the ISO to the participants within the PBO [11]. Thus, generation dispatch and direct load control in the existing centralized operation scheme are replaced with electricity prices or price-like control signals in the PBO, which are shown as conceptual diagrams for comparison purposes in Figure 1.2.

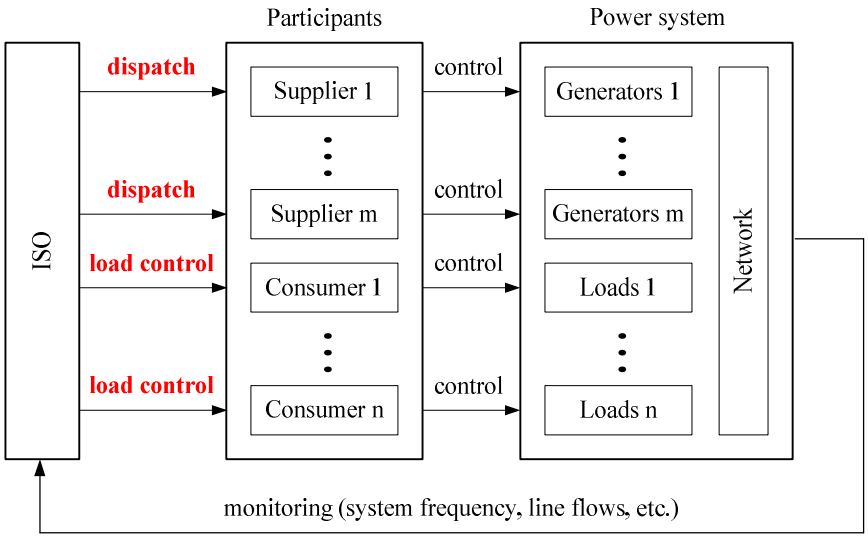

(a)

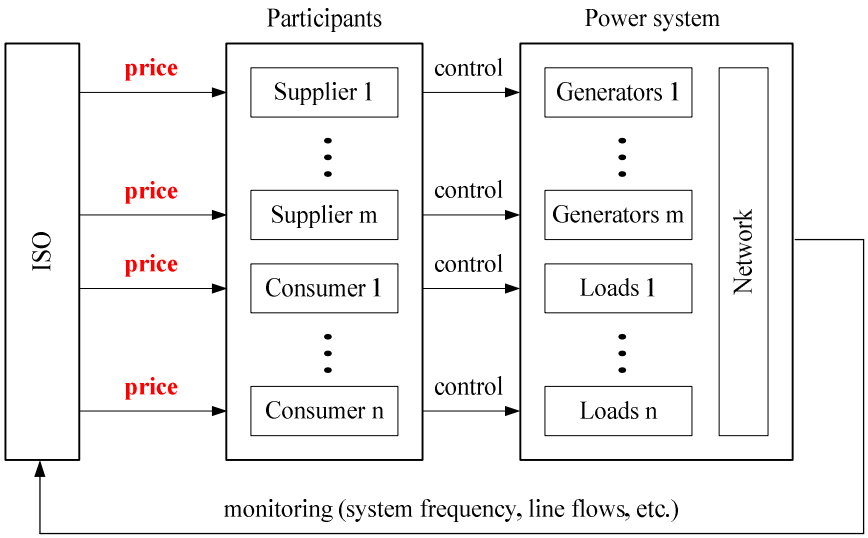

(b)

Figure 1.2 Conceptual diagrams of power system operation schemes. (a) Existing centralized operation. (b) Price-based operation.

1.2 Previous researches and limitations

There have been many studies on the PBO in various aspects. In [17] and [18], the power market is modeled by a set of differential equations which show the dynamic characteristics, and the stability is analyzed in a few typical cases. Modified dynamic equations are proposed in [19] to improve the stability. Possible dynamic responses of participants to electricity prices are considered in [20] and [21]. The effect of price signal delay on the stability is analyzed in [22], and the concepts of controllability and observability in the power market are also proposed in [14]. The research on the interconnected operation between power market dynamics and the physical power system is performed in [23]. In addition, [1] describes the possibility of congestion management by real-time price signal. As a specific implementation of the idea of using the real-time price in the congestion management function, the study in [24] proposes a specific congestion management scheme through different prices at each node, which is extended further in [25]. A method for real-time power system control including the congestion management by using the feedback control mechanism based on the OPF formulation is presented in [15].

The previous research results on the power market dynamics are able to provide insights based on the control system theories into the various situations that can happen in the implementation of the PBO. For example, a specific design of the PBO may cause an instability if there are two or more suppliers who exhibit economies of scale [20, 21]; the stability depends upon not only the value of time constants, but also the time delay of price signals

[20-22]; even though the power market dynamics itself is stable for the control scheme, the whole power system may be unstable when the stability is analyzed jointly with the physical systems [23]. These observations cannot be explained in static models, and the control system theories need to be used to sufficiently describe those dynamic properties [21].

However, the most critical drawback in the previous studies in [17-19, 22-25] based on the control theory in the continuous-time domain is that various aspects of the actual implementation in the real world are not explicitly considered. For example, in the real situation; the responses of the participants cannot be continuous; there is time delay of the responses occurred by the transmission of the price signal, time for decision, and time for action; time delays of the participant are all different from each other; the price signal is likely to be a discrete-time signal; the price signal can be asynchronously published so that the intervals of the consecutive price signals cannot necessarily be the same; the responses of the participants can also be asynchronous. In particular, the problem of delay was considered in [22], but the delay is equal for all participants and the price signal is published at the same instant so that the real situation is not properly reflected.

Aside from the difficulty in the actual implementation in the real world, there are also the limitations on the method itself for analyzing the PBO. In other words, the previous researches in [17-19, 22-25], in which power market dynamics are directly used, simply focused on the stability analysis based on the criteria such as eigenvalues. However, a transient characteristic is not considered in those studies, even though the transient characteristic is closely

related to the frequency deviation and the recovery time from the line congestion, which may cause the collapse of the whole power systems in extreme situation due to the failure of the component. Thus, it is not sufficient only to determine the stable region for the parameters of PBO. In other words, it is necessary to select the suitable values of the parameters in the stable region, which can reduce the frequency deviation and effectively manage the line congestion. Furthermore, an equilibrium price which is determined autonomously from the power market dynamics is treated with more importance in those studies, and the process of price changes is not properly considered. Thus, the possible methods for using electricity prices as the effective control signals are not fully investigated.

Particularly in [15], real-time control structure is proposed, in which the price controller is explicitly dependent on the status of the power systems. The price controller gets the information about the frequency deviation and the real power flow within the feedback loop, and it generates nodal prices for the power balancing and the congestion management. The structure is shown in Figure 1.3 and it is very similar to the framework for the PBO in this dissertation. However, the research in [15] does not give a specific configuration of the real-time price controller component. In addition, since the power systems are not separated into the individual components and not expressed in an explicit form, the structure in [15] has a limitation in applying design methods in a decentralized manner for enhancing the dynamic characteristics of the PBO.

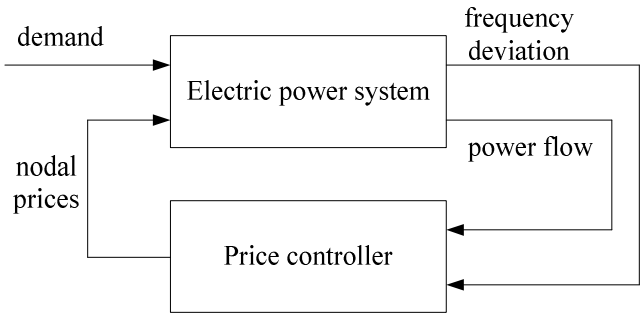

Figure 1.3 Structure of the PBO using real-time price control scheme within a feedback loop [15].

Finally, in the previous researches, the PBO is tightly interrelated with the dynamic behavior of the participants expressed by a set of differential equations, so that the PBO is not divided into the separate component to which various design techniques can be applied. As a result, a form of the PBO is limited to a certain type of controller expressed also by a differential equation, and the use of various types of controllers is fundamentally excluded in the preceding researches.

1.3 Objectives of the dissertation

As same as the ISO in the existing power system operation scheme should keep the balanced state and manage the line congestion, the main functions of the ISO in the PBO should still include keeping the system frequency to the nominal value and managing the line congestion. In other words, the ISO in the PBO needs to generate appropriate nodal prices for power/energy balancing and congestion management. Thus, designing the PBO is equivalent to making a method for generating proper nodal prices possibly by considering the participants' responses to the previously published nodal prices. However, considering the delayed and asynchronous responses of the participants in the real world, it becomes a challenging task to determine the values of the price signals and the time instant of publication of them. Thus, an analyzing method or an analysis tool is very necessary in the PBO to guide the determination of the appropriate price signals and to provide insights for the dynamic results according to the published price signals.

Since the success of the PBO is dependent on the spontaneous participation and the sufficient resources for the perfect competition, a certain design of the PBO cannot replace entirely the role of the current frequency and management schemes. In that case, the PBO can at least assist the frequency control functions performed by the primary and secondary control for reducing the frequency deviation [13]. For example, it is implemented in the current operation scheme by avoiding the line congestion in scheduling stage and by curtailing the load at some designated buses in real-time situation.

These are still meaningful operation strategies based on elaborate preparation. However, it seems that a supplementary method is necessary for handling unexpected situations in a systematic way and in a real-time basis. The PBO can be a candidate of the solution because it can effectively coordinate the actions of a large number of suppliers and consumers to solve the line congestion problem occurred by the sudden accidents such as a generation failure or a line fault.

In this dissertation, both inspired by the limitations of the previous researches and kept the goals of power system operation in mind, various methods and structures for designing a PBO have been presented to improve the dynamic performance in the load frequency control and the line congestion management functions. The presented methods and structures can be the effective components in the PBO. In other words, from designing methods and the structures for the PBO in this dissertation, the ISO may have help in determining the price signals and in finding the potential problems of a certain policy for the PBO on the aspect of the dynamic characteristics. Thus, the problems or the objectives that this dissertation focus on is to answer to the question of 'how to generate appropriate nodal prices depending on the condition of the power systems not only to satisfy the objectives of power system operation, but also to obtain the further reduction of frequency deviation and to make it easy to incorporate the improved design into the PBO'. The system frequency and actual power flow in the transmission lines can be considered as the typical conditions to be monitored. This main question can be specifically described as sub-questions like:

- Can the PBO be described as a typical feedback control structure?
- Can the PBO be mapped to a specific component of a modeled control structure?
- Can a rule for designing a PBO be composed?
- What are the effects of the appropriate design of a PBO?
- Is there any method to use available price information from the market in the design of the PBO?
- Can a general framework be composed, in which the PBO is not constrained to a specific form of the controller?
- Is the status in the steady-state from the PBO equal to the optimal solution of the existing power system operation schemes such as economic dispatch (ED) and optimal power flow (OPF).

1.4 Overview of the dissertation

The remainder of this dissertation is organized as follows. In Chapter 2, power market dynamics are described in detail. Most of the contents in Chapter 2 is a kind of summary of the previous researches mentioned above. At first, the PBO is described as the operation scheme by the ISO in the real world. And then, the continuous-time behavior of the aggregate participants is formed by the individual responses, which are inherently discrete and have different time delay. The power market dynamics are composed of the aggregate behavior of the participants based on the economic theory of the marginal cost and the marginal benefit. In particular, the power market dynamics in the case of one-supplier and one-consumer is described together with the introduction of important basic assumptions and equations. And then, extended cases of power market dynamics are explained, which include the case with multiple suppliers and consumers, the case using a modified price update method, and the case dealing with the line congestion.

The main contents of the dissertation are presented in from Chapter 3 to Chapter 6. In Chapter 3, power market dynamics are arranged as a typical feedback control structure based on which the PBO is designed as a form of the real-time feedback controller. A method for approximating the behavior of a large number of participants is proposed also in Chapter 2. The approximate target system from the methods in Chapter 2 is used in deriving the designing method for the PBO. Chapter 3 describes the proposed designing rules for the PBO, which include both a basic designing rule based on known controller

tuning method and a modified designing rule for improving the dynamic characteristics of the frequency deviation. Chapter 5 deals with the topic about the use of available price information. At first, available sources of price information are described. And then, the structure of the PBO is proposed, in which price information is used to improve the dynamic characteristics of the frequency deviation. The effect of price information on the frequency deviation is analyzed quantitatively, and the best price information is also suggested based on the analyzed effect. From Chapter 3 to Chapter 5, it is assumed that there is no line congestion and only the aspect of the system frequency is analyzed.

The congestion management together with the balancing of power and energy are considered in Chapter 6. Specifically, a general framework for the optimal design of the PBO which considers the power/energy balancing and the congestion management is proposed in Chapter 6. The proposed framework guarantees the optimality since it is based on the OPF solution. The substructures of the framework are derived from the part of the solution of OPF problem. In constructing the overall structure of the framework, it is particularly considered that any type of controller can be implemented in the PBO once it satisfies the convergence property. A simple example using the 6 bus network is given in Chapter 6 to demonstrate the suitability of the framework for the design of the PBO and to investigate the operation within the framework in detail.

Two case studies are performed by using the IEEE 39 bus network, which is a more realistic network model. The first case study is for the

verification of the contents in Chapter 3 (approximation methods), Chapter 4 (designing rules), Chapter 5 (use of price information). This case study considers only the aspect of the power/energy balancing or the system frequency. Thus, the line congestion is not considered so that the specific parameter values of the transmission lines of the IEEE 39 bus network are not used. In Chapter 7, the configuration and the results of this case study are described in detail. The second case study is for the verification of the framework in Chapter 6, and the configuration and the results are presented in Chapter 8. Since the line congestion is considered in the second case study, the line parameters such as reactances and power flow limits of IEEE 39 bus network need to be specified. Thus, the values of the line parameters used in the simulations are given in Chapter 8. Finally, conclusions and future works are given in Chapter 9.

Chapter 2. Power Market Dynamics

In this chapter, the price-based operation (PBO) is introduced and compared with the existing centralized operation and the market-oriented operation. The first thing necessary for analyzing and designing the PBO is to define the model for the behavior of the participants in response to the price signal. In this dissertation, the continuous-time model is selected. Thus, a method for linking a large number of asynchronous and discrete actions to the continuous function is described. And then, as a sort of the summary of the previous researches, the concept of the power market dynamics is introduced as a specific continuous-time model for the behavior of the participants, and other research results based on the power market dynamics are described.

2.1 Concept of the PBO

In the existing power system operation scheme, demand for electricity is considered as a price-inelastic variable to be forecasted, and electricity generation is elaborately scheduled or planned to meet varying demand and to maintain the security of the power systems. The practice of generation provision is composed of energy dispatch and ancillary service [9-11]. The energy dispatch is based on the forecasted demand and the optimization methods such as the economic dispatch (ED) and the optimal power flow (OPF) methods [26, 27]. The ancillary service is prepared to maintain the

balanced state from the error of demand forecast and to keep the security of the power systems from unexpected failures of the system components. The ancillary service can be divided into primary, secondary, and tertiary control according to necessary time for the activation of reserve services [28]; or they can be divided into regulation, spinning, non-spinning, and other types of reserves according to the capability and the status of generators for the ancillary service [29].

In the centralized operation by the vertically integrated utility (VIU), both the energy and the ancillary services can be procured by the VIU with planning for available resources under control. In the market environment, need for the energy balancing and the ancillary service is satisfied by the bidding process in the energy market and the ancillary service market, respectively [9, 10]. On the contrary, the classification between the energy and the ancillary service is meaningless any longer in the PBO. In other words, the provision of the energy balancing service and the ancillary service are achieved by the same method of increasing or decreasing the price signal. In addition, the prices are determined in real-time from the current status of the power systems so that they are not scheduled by stages in advance.

2.2 Continuous-time model of the PBO

In order to determine the price appropriately in the PBO, explicit model for the behavior of the participants in response to the price signal is required. However, it is very difficult to define the model for the participants' behaviors because the time delays of the responses of the participants are all different from each other due to necessary time interval for the transmission, decision, and action. Moreover, both the price signal and the responses of the participants are asynchronous and discrete. However, the publication of the price signals is not limited at the specific time instants with the same intervals, and there are a large number of participants. Then, it may be possible that a sequence of the price signals and the behaviors of the aggregate participants are represented as the continuous functions.

Firstly, a set of asynchronous discrete price signals are combined with respect to the same time axis. Then, they can be approximately represented as a continuous function. For example, let us assume that, as shown as the solid lines in Figure 2.1(a), a sequence of price signals is published to the participant group A, and another sequence of price signals is published to the participant group B. It should be noted from Figure 2.1(a) that the intervals between the price signals are all different. Since there are many participants, the time instants of the publication of the price signals can cover the entire time axis, so that total sequences of published price signals to all participants can be combined into the continuous function, as shown as the solid curve in Figure 2.1(b).

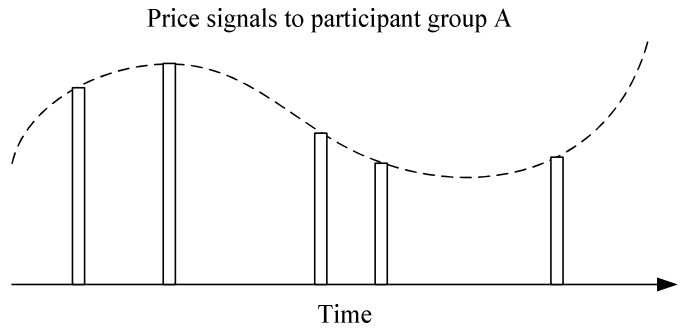

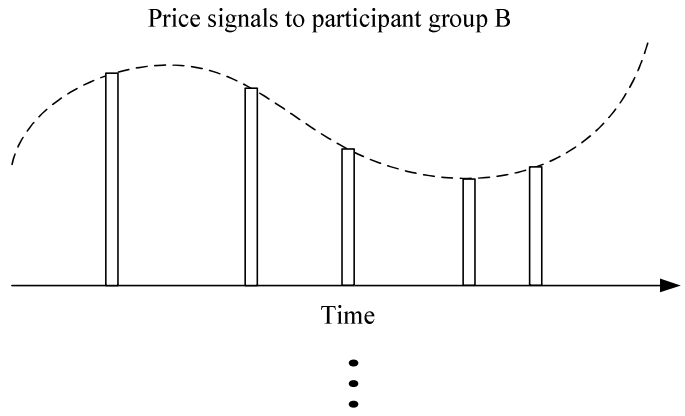

(a)

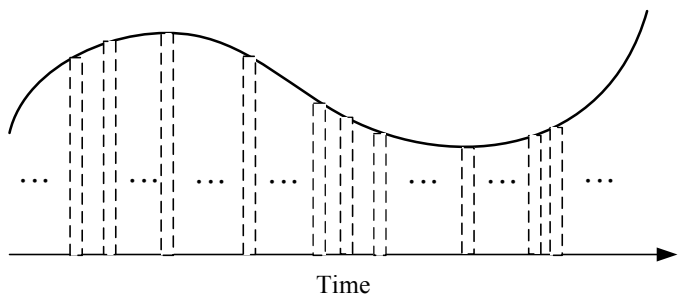

(b)

Figure 2.1 Composition of the continuous-time price signal. (a) Asynchronous discrete price signals to each participant group. (b) Combined continuous-time price signal.

Next, aggregation of the asynchronous discrete responses to the price signal of the participants with different values of time delay can result in the continuous variation of electricity generation or consumption. For example, let us assume that, as shown in Figure 2.2(a), the price signal rises like the step function. And then, the consumers decrease their electricity consumption in response to the increased price. As given in Figure 2.2(b), the amount of decreased consumption and the time instant of decrease are all different from each consumer due to different time delay and different response strategy to the price signal. Since there are a large number of consumers, the summation of successive changes of consumption may approximately constitute the continuous variation of consumption as shown in Figure 2.2(c).

When only the step change of the price signal as shown in Figure 2.2(a) is considered, time delay right after the instant of the step change is inevitable. However, for the continuous price signal as shown in Figure 2.1(b), the first-time delay cannot be identified due to the superposition of a set of continuous behavior of the participants. This superposition is similar to convolution integral. Consequently, the aggregate behavior of a large number of participants in response to a sequence of asynchronous price signals can be approximately modeled as the continuous variation of generation and consumption in response to the continuous prices.

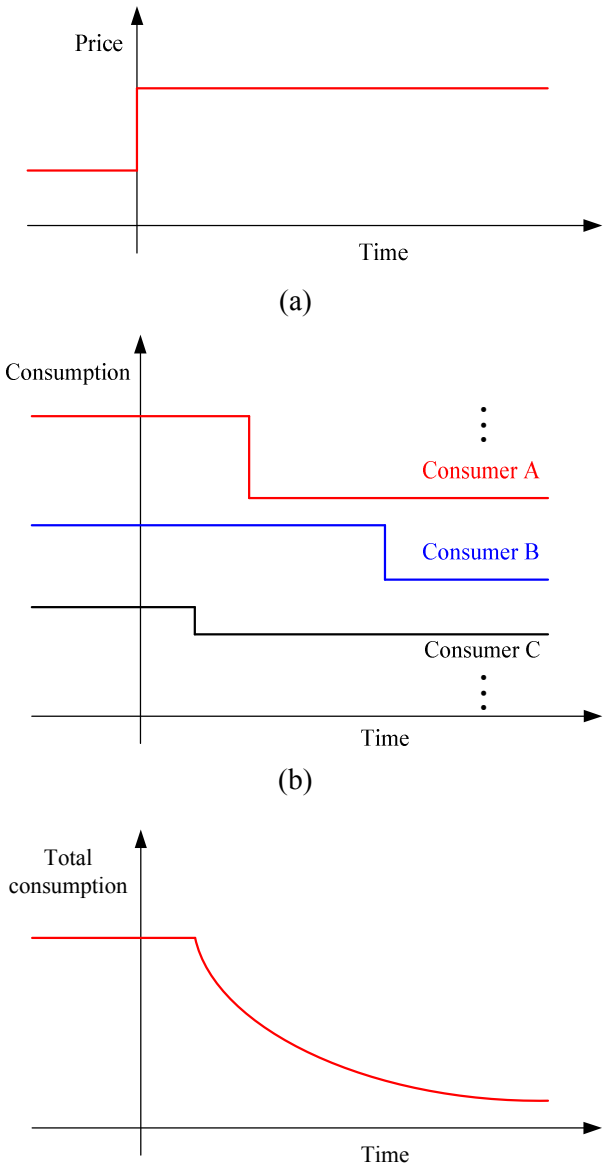

Figure 2.2 Composition of the continuous behavior of aggregate consumers. (a) Step increase of price signal. (b) Discrete changes of consumption of each consumer with different time delay. (c) Combined continuous-time response to the price signal.

2.3 Basic power market dynamics

Although the aggregate behavior of the participants and the price signal can approximately be represented as the continuous functions, the derivation of the specific continuous model is a challenging task. This requires an extensive empirical research, which is beyond the scope of this dissertation. Instead, the power market dynamics model in the previous studies is borrowed.

However, it should be noted that there is a limitation on modeling the behavior of the participants and the published price signals by the ISO in the real world with the power market dynamics in the continuous-time domain. In particular, when a sudden change occurs such as step decrease of generation due to a generation failure, the continuous-time model based on the power market dynamics cannot exactly capture the discontinuous phenomenon. In addition, all the variables, including the amount of generation and consumption, the energy imbalance, and the price signal, are instantaneously synchronized with respect to the time instant of the step change. Then, the initial time delay of the response to the price signal cannot be avoided. Nonetheless, the analysis based on the power market dynamics can provide the insights for the dynamic phenomena in the PBO. Furthermore, designing methods based on them can guide how to manage the sudden failure of the components in order to maintain the security of the power systems in the PBO.

The basic power market dynamics model is introduced at first in [17]. The purpose of the use of the dynamics is to investigate the impact of various policies for the ISO on the dynamic behavior of the power system market. In

particular, the most important assumption underlying the power market dynamics is the perfect competition. The specific assumptions are as follows:

- (A-1) Marginal production costs are the linear functions of the power generation with a positive slope.
- (A-2) Marginal benefits are the linear functions of the power consumption with a negative slope.
- (A-3) Responses of both suppliers and consumers to prices are not instantaneous, but represented as the first-order differential equations.
- (A-4) There is no energy storage so that supply and demand should be balanced.
- (A-5) There is no line congestion.
- (A-6) There are no losses.

The assumptions in (A-1) and (A-2) mean that the cost of generation and the benefit of consumption can have the form of quadratic function [27, 30]. Then, from (A-1) and (A-2), the marginal cost of the *i*-th supplier (MC_i) and the marginal benefit of the *j*-th consumer (MB_j) can be represented as the functions of $P_{g,i}$ and $P_{d,j}$

$$MC_i\left(P_{g,i}\right)=b_{g,i}+c_{g,i}P_{g,i},\quad MB_j\left(P_{d,j}\right)=b_{d,j}+c_{d,j}P_{d,j} \tag{2.1}$$

where $P_{g,i}$ and $P_{d,j}$ are the quantity of generation and consumption for the *i*-th supplier and the *j*-th consumer, respectively; $b_{g,i}$, $c_{g,i}$, $b_{d,j}$, and $c_{d,j}$

are constants determined by the cost and benefit functions. From the assumptions for the slope of the linear functions, $c_{g,i}$ is greater than zero and $c_{d,j}$ is less than zero.

In the situation of perfect competition, each individual participant adjusts the quantity of generation/consumption according to the level of price compared to the marginal cost/benefit. To be specific, suppliers increase the quantity of generation if the price is greater than the marginal cost and decrease the generation in the opposite case; consumers decrease the electricity consumption if the price is greater than the marginal benefit and increase the consumption in the opposite case. In the steady state, both the marginal cost and the marginal benefit should be equal to the system marginal price. Then, the differential equations for the dynamic behavior of the participants considering the assumption (A-3) can be represented as

$$\begin{aligned} \tau_{g,i}\dot{P}_{g,i} &= \lambda - \left(b_{g,i} + c_{g,i}P_{g,i}\right), \quad i = 1,\cdots,m \\ \tau_{d,j}\dot{P}_{d,j} &= \left(b_{d,j} + c_{d,j}P_{d,j}\right) - \lambda, \quad j = 1,\cdots,n \end{aligned} \tag{2.2}$$

where λ is a price; *m* and *n* are the number of suppliers and consumers; $\tau_{g,i}$ and $\tau_{d,j}$ are the strategic coefficients for the *i*-th supplier and the *j*-th consumer, respectively. It can be seen from (2.2) that both the marginal cost and the marginal benefit are equal to the price in the steady state. In (2.2), the units of $P_{g,i}$ and $P_{d,j}$ are per unit (p.u.) with respect to a specified system base; the unit of λ is \$/MWh; the unit of $\tau_{g,i}$ and $\tau_{d,j}$ is sec·\$/MWh or min·\$/MWh. Whereas the unit of normal time constants is time, i.e., seconds or minutes, the units of $\tau_{g,i}$ and $\tau_{d,j}$ are not just the time dimension since

they implicitly include a conversion procedure between the electric power and the monetary value. Meanwhile, $\tau_{g,i}$ and $\tau_{d,j}$ determine the strategy of the participants in response to the price signal. Thus, $\tau_{g,i}$ and $\tau_{d,j}$ are named as the strategic coefficients in this dissertation, even though they play a role of normal time constants in the dynamic equations in (2.2) and they are indicated as just time constants in the previous researches.

The assumption in (A-4) can be represented as

$$\sum_{i=1}^{m} P_{g,i} = \sum_{j=1}^{n} P_{d,j} \tag{2.3}$$

However, it is impossible to satisfy the power balance condition of (2.3) at every moment. Thus, power imbalance at some instants should be properly handled so that the power imbalance also should be included in the market dynamics. The power imbalance can be represented as the equation like

$$\dot{E} = \sum_{i=1}^{m} P_{g,i} - \sum_{j=1}^{n} P_{d,j} \tag{2.4}$$

where E means the energy imbalance or the cumulative power imbalance. It should be noted that E becomes zero in the steady state so that the power balance condition of (2.3) is satisfied. In the meanwhile, since it is assumed that there is no energy storage, a suitable physical system which corresponds to the variable E cannot be designated in the real world. Thus, the energy imbalance appears as a form of the frequency deviation of the power systems. The frequency deviation approximately has a linear relation with the energy imbalance as follows [23, 31]

$$\Delta f = \left(\frac{f_0}{2H_T S_T} \right) \cdot E = L_f E \tag{2.5}$$

where Δf is the frequency deviation, f_0 is the nominal frequency, H_T is the weighted average of inertia constants, and S_T is the total rating. The position of the energy imbalance in the structure of the primary control loop of the power systems is shown in Figure 2.3. Although the energy imbalance is explicitly indicated after the integrator in Figure 2.3, the actual data monitored or measured from the generator is the frequency. Thus, the energy imbalance is an intermediate variable and it seems unsuitable to use it in the real-world applications. However, the frequency may become rather an inappropriate variable on the consumer side since the frequency is not measured and power consumption is recorded by using the meter at home. Thus, in the market dynamics in which the response of the consumers should also be considered, the energy imbalance can be a suitable variable to be computed from the data of power supply and power consumption.

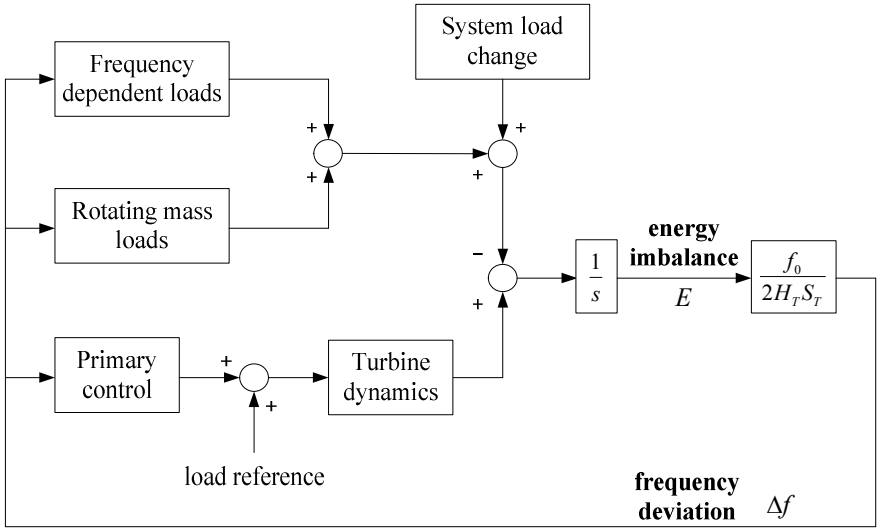

Figure 2.3 Relation between the energy imbalance and the frequency deviation in the primary control scheme [31].

The assumptions (A-5) and (A-6) mean that only the power balance condition of (2.3) from supply and demand is considered. Thus, another equation is not constructed from two assumptions. Then, the power market dynamics for *m*-suppliers and *n*-consumers can be represented as a set of differential equations like [17]

$$\begin{aligned} \tau_{g,i}\dot{P}_{g,i} &= \lambda - \left(b_{g,i} + c_{g,i}P_{g,i}\right), \quad i = 1,\cdots,m \\ \tau_{d,j}\dot{P}_{d,j} &= \left(b_{d,j} + c_{d,j}P_{d,j}\right) - \lambda, \quad j = 1,\cdots,n \\ \dot{E} &= \sum_{i=1}^{m} P_{g,i} - \sum_{j=1}^{n} P_{d,j} \end{aligned} \tag{2.6}$$

2.4 Price update method

The equilibrium price λ_{SS} of (2.6) can be determined definitely by being equal to zero on the left-hand side as

$$\lambda_{SS} = \frac{\sum_{i=1}^{m}\left(b_{g,i} / c_{g,i}\right) - \sum_{j=1}^{n}\left(b_{d,j} / c_{d,j}\right)}{\sum_{i=1}^{m}\left(1 / c_{g,i}\right) - \sum_{j=1}^{n}\left(1 / c_{d,j}\right)} \tag{2.7}$$

Then, the power balance condition can be satisfied by continuously publishing the equilibrium price λ_{SS}. However, this does not guarantee that the energy imbalance E becomes zero in the steady state, even though it remains constant. This means that the frequency deviation cannot be removed or the system frequency cannot be maintained to its nominal value. Since the frequency control is one of the most important goals of the power system operation, the energy imbalance E should be made to zero by appropriately adjusting the prices. Thus, the price update equation is a fundamental component in the PBO.

The scope of the term 'PBO' may include the market dynamics in (2.6). However, since the essential function of the PBO is generating the appropriate price signals in the power system operation, the price update equation can be considered as equivalent to the PBO in the narrow sense. This view is accepted in this research, and the price update method and the PBO will appear as the same thing in the following development of the dissertation without an explicit mention.

In [17], a simple price update method is introduced. The form of the method is also a differential equation as

$$\tau_\lambda \dot{\lambda} = -E \tag{2.8}$$

where τ_λ is an operational coefficient for the price update. Different from $\tau_{g,i}$ and $\tau_{d,j}$ in (2.2), the unit of τ_λ is sec·J/$/MWh or min·J/$/MWh. Implicitly, τ_λ has a conversion procedure between the energy and the monetary value. In addition, τ_λ relates to an operational policy of the ISO in the PBO. Thus, τ_λ is named as the operational coefficient for the price update in this dissertation, even though it becomes a normal time constant in the price update method and it is used as just a time constant in the previous researches. Then, it is certain from (2.8) that the energy imbalance becomes zero in the steady state. However, the study in [17] shows that a simple combination of (2.6) and (2.8) cannot satisfy the stability condition. Thus, it is asserted that a supplementary price signal should be used, so that the whole power market dynamics including the price update equation should be composed as

$$\begin{aligned} \tau_g \dot{P}_g &= \lambda - \left(b_g + c_g P_g\right) - kE \\ \tau_d \dot{P}_d &= \left(b_d + c_d P_d\right) - \lambda \\ \dot{E} &= P_g - P_d \\ \tau_\lambda \dot{\lambda} &= -E \end{aligned} \tag{2.9}$$

where k is a constant gain. Since '$-kE$' is added to satisfy the stability condition, it is named as 'stabilizing signal' and can be interpreted as a kind of 'bias' for the suppliers. The unit of k should be $/MWh/J in order for '$-kE$' to be in the same unit of $/MWh as the unit of price. It should be noted that

the supplementary price signal '$-kE$' is added only to the equations for the suppliers. This is because only suppliers react to the energy imbalance or the frequency deviation, and the consumers seldom adjust their consumption pattern in response to it.

In [19], a modified stabilizing signal is proposed to improve the stability characteristics, which is represented as

$$\tau_g \dot{P}_g = \lambda - \left(b_g + c_g P_g\right) - kE - k_d \dot{E} \tag{2.10}$$

where k_d is another constant gain in unit of sec·$/MWh/J or min·$/MWh/J. The additional stabilizing term '$k_d \dot{E}$' can be seen as a derivative control in managing the energy imbalance. In general, PID controller can show better control performance than PI controller in some applications [32, 33]. For the same reason, a larger stable region can be achieved in the parameter space by using the modified stabilizing signal, as shown in Figure 2.4.

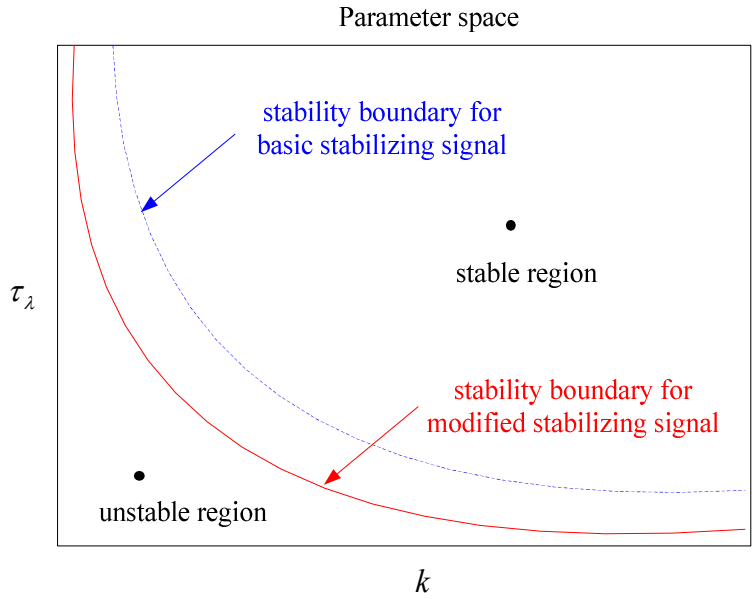

Figure 2.4 Improved stability characteristics of the modified stabilizing signal [19].

2.5 Stability analysis

Since the power market dynamics are expressed as a set of differential equation of (2.9), the control system theories are used in the stability analysis. Although there are a few methods for checking the stability such as Lyapuov functions [34, 35], a simple method based on eigenvalues can be used because (2.9) is a linear system. In general, the number of suppliers and consumers is not so small that eigenvalues should be determined by the numerical methods. However, analytical results can exhibit important insights on the stability. Thus, it is significant to analyze an impractical situation with a small number of participants. Some observations which are explicitly stated in [17] are as follows:

- Energy imbalance does not change the equilibrium point of the power market dynamics as long as it is eventually driven to zero.
- Permanent energy imbalance is caused without a price update method based on the feedback mechanism, which may make the whole power market dynamics unstable.
- Unsuitable choice of feedback gain, strategic coefficients and operational coefficient may result in the instability.
- The larger the feedback gain for the price is, the more the possibility of instability becomes.
- The smaller the operational coefficient for the price update is, the more the possibility of instability becomes.
- The type of instability is an oscillatory instability.

2.6 Consideration of line congestion

Line congestions impose additional constraints on the power market dynamics. However, there are no dynamics in the case of the line congestion. In other words, the form of the additional constraints is not a differential equation, but an algebraic equation [17, 24]. The algebraic equation can be expressed as a linear equation, of which the coefficients are determined by the sensitivity of generation/consumption to the line flow, or so-called power transfer distribution factors (PTDF) [36].

Let us assume that the congestion occurs in the transmission line designated as the number *l*. Then, the linear equation for the constraint can be represented as

$$S_{l,g1}P_{g,1} + \cdots + S_{l,gm}P_{g,m} + S_{l,d,}P_{d,1} + \cdots + S_{l,dn}P_{d,n} = r_l \tag{2.11}$$

where $S_{l,gi}$ and $S_{l,dj}$ are sensitivities of $P_{g,i}$ and $P_{d,j}$ on the active power flow in the line *l*, respectively; r_l is a slack variable. As a general case with n_s congested lines, (2.11) can be expressed as a system of equations like:

$$\begin{bmatrix} S_{1,g1} & \cdots & S_{m,gm} & S_{1,d1} & \cdots & S_{1,dn} \\ \vdots & & \vdots & \vdots & & \vdots \\ S_{n_s,g1} & \cdots & S_{n_s,gm} & S_{n_s,d1} & \cdots & S_{n_s,dn} \end{bmatrix} \begin{bmatrix} P_{g,1} \\ \vdots \\ P_{g,m} \\ P_{d,1} \\ \vdots \\ P_{d,n} \end{bmatrix} = \begin{bmatrix} r_1 \\ r_2 \\ \vdots \\ r_{n_s} \end{bmatrix} \tag{2.12}$$

A combination of (2.9) and (2.12) composes a differential algebraic equation (DAE). However, DAE is not a suitable form for the stability analysis. Thus,

Lagrange multiplier μ is introduced to construct a set of differential equations for the stability analysis. In an economic sense, Lagrange multiplier means the congestion price or the shadow price. Then, power market dynamics with the line congestions can be represented as

$$\begin{bmatrix} \mathbf{T_1} & \mathbf{0} \\ \mathbf{0} & \mathbf{T_2} \end{bmatrix} \begin{bmatrix} \dot{\mathbf{P}} \\ \dot{\mathbf{\Lambda}} \end{bmatrix} = \begin{bmatrix} \mathbf{C} & \mathbf{S}^T \\ \mathbf{S} & \mathbf{0} \end{bmatrix} \begin{bmatrix} \mathbf{P} \\ \mathbf{\Lambda} \end{bmatrix} + \begin{bmatrix} \mathbf{B} \\ \mathbf{R} \end{bmatrix} \tag{2.13}$$

where

$$\mathbf{T_1} = \begin{bmatrix} \tau_{g,1} & & & & & & \\ & \ddots & & & & & \\ & & \tau_{g,m} & & & & \\ & & & \tau_{d,1} & & & \\ & & & & \ddots & & \\ & & & & & \tau_{d,n} \end{bmatrix}$$

$$\mathbf{T_2} = \begin{bmatrix} \tau_{\lambda} & & & \\ & 0 & & \\ & & \ddots & \\ & & & 0 \end{bmatrix}$$

$$\mathbf{P} = \begin{bmatrix} P_{g,1} \\ \vdots \\ P_{g,m} \\ P_{d,1} \\ \vdots \\ P_{d,n} \end{bmatrix}, \qquad \mathbf{\Lambda} = \begin{bmatrix} \lambda \\ \mu_1 \\ \vdots \\ \mu_{n_s} \end{bmatrix},$$

$$\mathbf{C} = \begin{bmatrix} -c_{g,1} & & & & & \\ & \ddots & & & \mathbf{0} & \\ & & -c_{g,m} & & & \\ & & & c_{d,1} & & \\ & \mathbf{0} & & & \ddots & \\ & & & & & c_{d,n} \end{bmatrix}$$

$$\mathbf{S} = \begin{bmatrix} 1 & \cdots & 1 & -1 & \cdots & -1 \\ S_{1,g1} & \cdots & S_{1,gm} & S_{1,d1} & \cdots & S_{1,dn} \\ \vdots & & \vdots & \vdots & & \vdots \\ S_{n_s,g1} & \cdots & S_{n_s,gm} & S_{n_s,d1} & \cdots & S_{n_s,dn} \end{bmatrix}$$

$$\mathbf{B} = \begin{bmatrix} -b_{g,1} \\ \vdots \\ -b_{g,m} \\ b_{d,1} \\ \vdots \\ b_{d,n} \end{bmatrix}, \qquad \mathbf{R} = \begin{bmatrix} 0 \\ r_1 \\ \vdots \\ r_{n_s} \end{bmatrix},$$

The system in (2.13) as well as in (2.9) is a higher order system. Thus, even though the eigenvalue method can be used in the stability analysis, eigenvalues should be numerically determined. However, an analytic expression for the eigenvalues can give more insights on the dynamic behavior also in this case of power market dynamics with line congestion. Thus, it is meaningful to investigate a small example. Some observations which are explicitly stated in [17] are as follows:

- As the number of congested lines increases, the number of eigenvalues decreases.
- If the power market dynamics are stable without congestion, the stability holds when the line congestion occurs.
- Line congestion may significantly shift the equilibrium point.
- The value of $P_{g,i}$ or $P_{d,j}$ in the steady state can be negative. The negative value means that the quantity of the corresponding generation or demand should be fixed to zero.
- The operating cost increases when the line congestion occurs.

There is another approach to addressing the line congestion management together with the power/energy balancing [15]. Different from the previously mentioned approach that the line congestion imposes an algebraic constraint, the line congestion is composed into the differential equation with a special form in another method as

$$\begin{pmatrix} \dot{x}_{\lambda_0} \\ \dot{x}_{\Delta\lambda} \\ \dot{x}_{\mu} \end{pmatrix} = \begin{pmatrix} 0 & 0 & 0 \\ 0 & -K_\Delta B_\Delta & -K_\Delta L_\Delta^T \\ 0 & 0 & 0 \end{pmatrix} \begin{pmatrix} x_{\lambda_0} \\ x_{\Delta\lambda} \\ x_{\mu} \end{pmatrix} + \begin{pmatrix} -k_f \mathbf{1}_n^T & 0 \\ 0 & 0 \\ 0 & K_p \end{pmatrix} \begin{pmatrix} \Delta f \\ \Delta p_L + w \end{pmatrix}$$
$$\lambda = \begin{pmatrix} 1 & 0 & 0 \\ \mathbf{1}_{n-1} & I_{n-1} & 0 \end{pmatrix} \begin{pmatrix} x_{\lambda_0} \\ x_{\Delta\lambda} \\ x_{\mu} \end{pmatrix} \tag{2.14}$$

where B_Δ is a submatrix of the susceptance matrix B obtained by removing the first column and the first row of B; L_Δ is a submatrix of L obtained by removing the first column of L, where L is an appropriately

defined matrix for the relation between the power angles and the power flow limits; x_{λ_0}, $x_{\Delta\lambda}$, and x_μ are controller states; K_Δ, K_p, and k_f are controller gains; Δf is the frequency deviation; Δp_L is the line overflow; λ is the nodal price. The variable w in (2.14) is a solution of the subproblem made from the condition that w and $(K_o x_\mu + \Delta p_L + w)$ are perpendicular to each other, where K_o is another controller gain. It is asserted as the advantage of this method in [15] that it does not require knowledge of the power market dynamics. However, this holds only when the convergence to the OPF solution is guaranteed. If we want the controller gains to be determined, the power market dynamics should also be considered. Thus, even in the simulation of [15], knowledge of power market dynamics is assumed by taking the parameters from [23]. Consequently, although the congestion management is handled by a particular set of differential equations without an explicit inclusion of the power market dynamics as in (2.14), the parameters of the market dynamics cannot help but to be considered in the application of the method.

Chapter 3. Structure of the PBO

When analyzing and designing the PBO based on the power market dynamics, it may be one of the simple methods to perform the tasks on the dynamics equations themselves. However, a certain modification of the original problem can make the solution of it much simpler. As well-known examples, Laplace transform enables the simple operation of time-domain functions, and Fourier transform enables the simple analysis on the frequency response. In a similar fashion, analyzing and designing the PBO can be easier if the power market dynamics are properly represented. In this dissertation, considering that there are a lot of research results in the control engineering field for a long time, the PBO and the power market dynamics are represented as the typical feedback control problem. The feedback control structure of the PBO is described in this chapter. In addition, a method for simplifying a complex system is also presented in order to take advantage of various techniques based on the simple systems with typical forms.

3.1 Feedback control structure of the PBO

From the viewpoint of the control engineering, the power market dynamics in (2.9) can be seen as the typical feedback control system. To be specific, the price-responsive participants can be considered as a controlled system, and the price update method or the PBO can be mapped to a controller. The most

common reference signal may be the nominal frequency of the power systems. The process within the arrangement of the PBO as a feedback control system can be described as follows. The controller (PBO) generates the control signal (real-time electricity prices) and provides the control signal to the controlled system (participants or electric power system). Then, the controlled system reacts to the control signal, and the output signal (system frequency) is observed and feedbacked into the controller. Finally, the controller (PBO) adjusts the control signal by comparing the feedbacked output signal to the reference value (nominal frequency).

From the relationship in (2.5), the goal of keeping the frequency to the nominal value is equivalent to driving the energy imbalance to zero. Thus, as the output variable and the reference value, the system frequency and the nominal frequency can be replaced with the energy imbalance and zero value, respectively. Then, the interpretation of the PBO in a typical feedback control structure can be represented as a block diagram as shown in Figure 3.1.

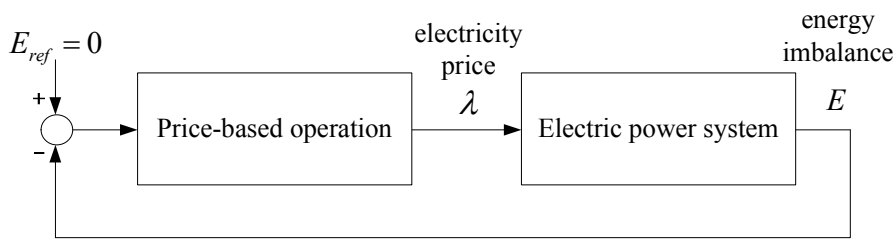

Figure 3.1 Feedback control structure of PBO.

Since the most important function in the PBO is the determination of electricity prices as a kind of control signal, it can be seen from Figure 3.1 that the PBO is located exactly in the same position of the controller in the feedback control structure. Then, the PBO becomes equivalent to the controller in the feedback control structure. Thus, they are interchangeably used as the expressions with the same meaning hereafter in this dissertation without explicit mention. Consequently, designing the PBO is equivalent to designing the controller. For example, if the controller has a form of PID control, the design of the PBO becomes determining the parameters of PID control, that is, the proportional, integral, and derivative gains. Moreover, the most important thing is that the price update method or the PBO is explicitly separated from the dynamic behavior of the participants, so that the PBO is not restricted to a form of differential equation as in (2.9). Thus, like the controller design is one of the major problems in control engineering, designing the PBO possibly can be an important research topic in the area of power system operation.

3.2 Representation of electric power systems

Once the power market dynamics are arranged as the feedback control structure, designing the PBO becomes the controller design problem. In order for that, the target system based on which the design process is performed should be specified. A form of the target system can be derived from (2.9). However, in view of the PBO, it is unfair for only the suppliers to have an additional obligation to keep system stable in a decentralized environment based on competition. On the contrary, it is more suitable to provide the same prices to both sides of suppliers and consumers. Thus, (2.6) will be used instead of (2.9) in deriving the form of the target system. The equations of (2.6) are rewritten here for convenience.

$$\begin{aligned} \tau_{g,i}\dot{P}_{g,i} &= \lambda - \left(b_{g,i} + c_{g,i}P_{g,i}\right), \quad i = 1,\cdots,m \\ \tau_{d,j}\dot{P}_{d,j} &= \left(b_{d,j} + c_{d,j}P_{d,j}\right) - \lambda, \quad j = 1,\cdots,n \\ \dot{E} &= \sum_{i=1}^{m} P_{g,i} - \sum_{j=1}^{n} P_{d,j} \end{aligned} \tag{3.1}$$

Instability caused by the elimination of the stabilizing signal can be resolved by an appropriate design of the PBO. This is possible due to the separation of the PBO as an individual component as shown in Figure 3.1.

The first step in the derivation of the target system is to form the constant terms $b_{g,i}$ and $b_{d,j}$, which do not change with respect to the price, into a disturbance. Mathematically, the disturbance can be added to the control signal or to the output of the target system. In the dissertation, it is selected to compose the constant terms into an output disturbance. Then, the transfer

function of the output disturbance $D(s)$ can be expressed as

$$D(s) = \sum_{i=1}^{m} \frac{-b_{g,i}}{s^2(\tau_{g,i}s + c_{g,i})} + \sum_{j=1}^{n} \frac{-b_{d,j}}{s^2(\tau_{d,j}s - c_{d,j})} \tag{3.2}$$

It should be noted that $D(s)$ has double integrator terms of $1/s^2$ since there are two integral steps within the process from the constant terms ($b_{g,i}$ and $b_{d,j}$) to the output or the energy imbalance (E).

The next step is to form the remaining terms as the target system for designing the PBO. Then, the transfer function of the target system $H(s)$ can be represented as

$$H(s) = \sum_{i=1}^{m} \frac{1}{s(\tau_{g,i}s + c_{g,i})} + \sum_{j=1}^{n} \frac{1}{s(\tau_{d,j}s - c_{d,j})} \tag{3.3}$$

It should be noted that $H(s)$ has single integrator terms of $1/s$ since the integral operation is done once in the conversion from the power into the energy imbalance.

Then, the electric power systems in Figure 3.1 can be divided into the target system and the output disturbance, which are represented as block diagrams as in Figure 3.2. The parameters related to $D(s)$ and $H(s)$ are also explicitly specified in Figure 3.2. The detailed representation of the target system $H(s)$ with block diagrams is given in Figure 3.3. Although the disturbance $D(s)$ constitutes the energy imbalance and consequently affects the stability and the control performance of the PBO, it is irrelevant to include the disturbance which does not respond to the control signal or the price. Thus, only the target system of (3.3) can be considered in designing the PBO.

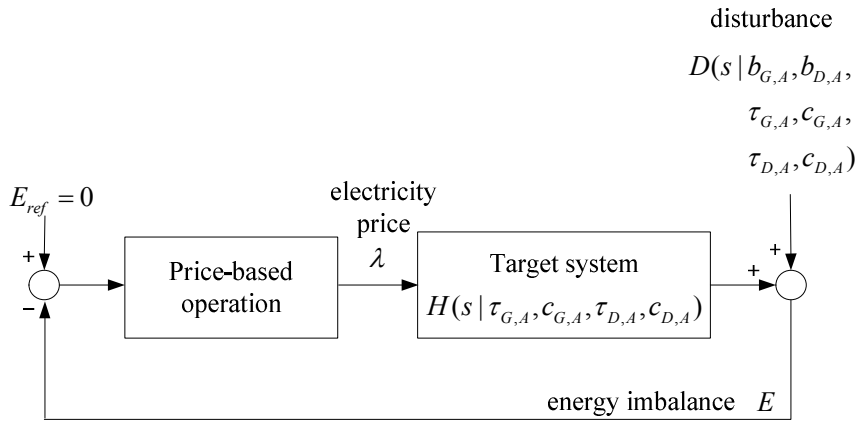

Figure 3.2 Feedback control structure of the PBO with explicitly specified parameters of the target system and the disturbance.

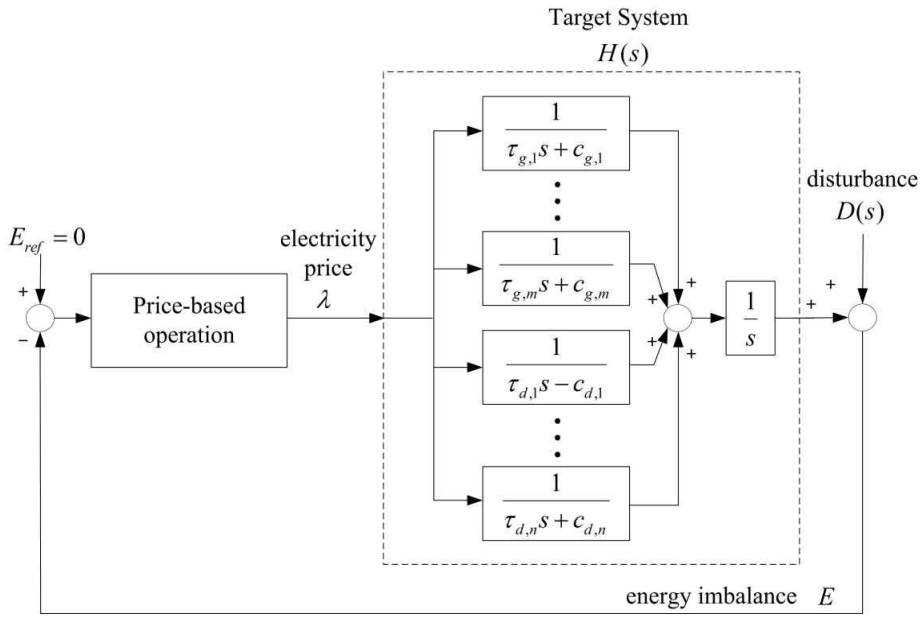

Figure 3.3 Detailed representation of the target system $H(s)$ within the feedback control structure.

3.3 Approximation of the target system

Since there are generally a large number of suppliers and consumers, the target system in (3.3) becomes a very higher order system. Thus, it is rather complicated to design the PBO for the target system with an original form of (3.3). This makes it a necessary step to approximate the target system in (3.3) to the system with a simpler form.

As the simplest method for the approximation, the dominant pole method can be considered [37]. However, if there are many poles of a similar size, which may happen within the target system of (3.3), just selecting one dominant pole may lose the subtle interaction between the participants. Meanwhile, it can be seen that the target system in (3.3) is a linear combination of simple systems with the same form of the transfer function. Thus, by exploiting fully the property of the system, a little modified dominant pole approximation method, which is named as a solution method in the dissertation, can be derived as described below.

The purpose of the approximation is to find an approximate target system with a form of

$$\tilde{H}(s) = \frac{1}{s(\tau_A s + c_A)} \tag{3.4}$$

The integral term $1/s$ is a common factor of (3.3) and (3.4). Thus, it is suitable that the approximation is focused on converting the combination of the first-order systems into one first-order system. By setting aside the common integral term in (3.3), the remaining first-order terms $\hat{H}(s)$ can be

expressed as

$$\hat{H}(s) = \sum_{i=1}^{m} \frac{1}{\tau_{g,i} s + c_{g,i}} + \sum_{j=1}^{n} \frac{1}{\tau_{d,j} s - c_{d,j}} \tag{3.5}$$

Let an approximate first-order system for (3.5) be denoted as $\tilde{\hat{H}}(s)$ with a form of

$$\tilde{\hat{H}}(s) = \frac{1}{\tau_A s + c_A} \tag{3.6}$$

As same as [37], c_A can be determined by equating the DC gain. Then, c_A becomes

$$c_A = 1 / \left(\sum_{i=1}^{m} \frac{1}{c_{g,i}} + \sum_{j=1}^{n} \frac{1}{-c_{d,j}} \right) \tag{3.7}$$

The value of τ_A can be determined by using the definition of the time constant. The unit step response of (3.5) can be determined as

$$\begin{aligned} \hat{h}(t) * u(t) = \Bigg\{ & \left(\sum_{i=1}^{m} \frac{1}{c_{g,i}} + \sum_{j=1}^{n} \frac{1}{-c_{d,j}} \right) \\ & - \left(\sum_{i=1}^{m} \frac{1}{c_{g,i}} e^{-t/\left(\tau_{g,i}/c_{g,i}\right)} + \sum_{j=1}^{n} \frac{1}{-c_{d,j}} e^{-t/\left(-\tau_{d,j}/c_{d,j}\right)} \right) \Bigg\} \cdot u(t) \end{aligned} \tag{3.8}$$

and the unit step response of (3.6) becomes

$$\tilde{\hat{h}}(t) * u(t) = \left\{ \frac{1}{c_A} - \frac{1}{c_A} e^{-t/\left(\tau_A/c_A\right)} \right\} u(t) \tag{3.9}$$

Because the time constant of (3.6) is τ_A / c_A, the value of τ_A can be determined by equating the function values of (3.8) and (3.9) at $t = \tau_A / c_A$ as follows

$$\hat{h}(t) * u(t)\Big|_{t=\tau_A/c_A} = \tilde{\tilde{h}}(t) * u(t)\Big|_{t=\tau_A/c_A} \tag{3.10}$$

Then, by substituting c_A in (3.7) into (3.10), τ_A becomes the solution of the equation as

$$\sum_{i=1}^{m} \frac{1}{c_{g,i}} e^{-\left(\frac{\tau_A}{c_A}\right)/\left(\frac{\tau_{g,i}}{c_{g,i}}\right)} + \sum_{j=1}^{n} \frac{1}{-c_{d,j}} e^{\left(\frac{\tau_A}{c_A}\right)/\left(\frac{\tau_{d,j}}{c_{d,j}}\right)} = \frac{1}{c_A} e^{-1} \tag{3.11}$$

The equation (3.11) is a nonlinear one so that a numerical method should be used to compute a solution. However, since the terms on the left-hand side of (3.11) are monotonically decreasing functions, it is guaranteed that there is only one solution. Thus, the proposed solution method for approximation does not cause the complexity which arises from the multiple roots. This property results from the simple form of the target system in (3.3). Therefore, at least for the target system in (3.3), the accuracy of approximation is better than the basic dominant pole method in terms of the similarity of unit step response.

Chapter 4. Designing Rules for the PBO

If a generation failure occurs, the amount of electricity supply suddenly decreases and the frequency or the energy imbalance starts to fall below the reference value. In the PBO, the fault situation is resolved by increasing the price. Then, according to the power market dynamics, the generation increases and the consumption decreases due to the increased price signal, and finally the balanced state is recovered. However, it is still a difficult problem to determine how much the price should be increased.

For example, if the price rises too large, the increase of generation becomes so greater than the decrease of consumption that the frequency imbalance passes over the reference value. When this over-recovery repeats, the oscillation of the frequency occurs, even though it finally converges to the reference value. On the contrary, if the price rises too small, the time duration until the recovery to the balanced state becomes too long, even if the oscillation does not occur. These aspects of overshoot and recovery time should also be considered in designing the controller in the feedback control structure. Naturally, there are a lot of studies on the methods of tuning the controller for achieving the proper dynamic performance. Similar to the controller tuning rules, designing rules for the PBO are presented in this chapter in order to enhance the dynamic characteristics particularly of the frequency or the energy imbalance [38]. The designing rules in this chapter are neither the only option nor the optimal ones. However, these rules may

provide some insights and guides to composing the operation policy of the ISO or determining the appropriate prices in the PBO. Moreover, these rules can be the basic design of the PBO, from which other improved designs of the PBO are derived and to which the improved ones are compared in further researches.

4.1 Selection of a controller form for the PBO

If the stabilizing signal for the suppliers in (2.9) is included in the price update method, the price update equation can be written as

$$\tau_\lambda \dot{\lambda} = -E - k\tau_\lambda \dot{E} \tag{4.1}$$

The price update equation (4.1) is not a formal expression of the differential equation, since there is a derivative term in the right-hand side. However, the equation (4.1) is expressed informally on purpose to derive the relation with PID control. By the application of Laplace transform, (4.1) can be represented as

$$\tau_\lambda s\lambda(s) = -E(s) - k\tau_\lambda sE(s) \tag{4.2}$$

The reference value of the energy imbalance E is zero, that is $E_{ref} = 0$. Then, $\lambda(s)$ can be arranged as

$$\lambda(s) = k\left\{1 + \frac{1}{k\tau_\lambda s}\right\}\left\{E_{ref}(s) - E(s)\right\} = G(s)\cdot\left\{E_{ref}(s) - E(s)\right\} \tag{4.3}$$

Meanwhile, PID controller has a typical form of

$$G_{PID}(s) = K_P\left(1 + \frac{1}{T_I s} + T_D s\right) \tag{4.4}$$

where K_P, T_I, and T_D are the proportional gain, the integral time, and the derivative time, respectively. Then, it can be seen by comparing (4.3) to (4.4) that the price-update method in (4.1) is equivalent to PI controller with $K_P = k$ and $T_I = k\tau_\lambda$. Similarly to the modified price update method in [19], the price update equation in (2.10) can be expressed informally as

$$\tau_\lambda \dot{\lambda} = -E - k\tau_\lambda \dot{E} - k_d \tau_\lambda \ddot{E} \tag{4.5}$$

By applying the Laplace transform to (4.5) gives

$$\tau_\lambda s\lambda(s) = -E(s) - k\tau_\lambda sE(s) - k_d \tau_\lambda s^2 E(s) \tag{4.6}$$

By arranging (4.6) with respect to $\lambda(s)$ and applying the condition of $E_{ref} = 0$, the following expression can be obtained:

$$\begin{aligned} \lambda(s) &= k\left\{1 + \frac{1}{k\tau_\lambda s} + \frac{k_d}{k}s\right\}\left\{E_{ref}(s) - E(s)\right\} \\ &= G(s)\cdot\left\{E_{ref}(s) - E(s)\right\} \end{aligned} \tag{4.7}$$

Then, the price update method in (4.5) is identical to PID controller with $K_p = k$, $T_I = k\tau_\lambda$, and $T_D = k_d / k$. Thus, it can be seen that the price update methods in [17] and [19] have a form of PI controller although there is no explicit mention about PID controller.

Since the PBO is an individual component in the feedback control structure as shown in Figure 3.1, theoretically, any kind of controller can be

applied as a specific design of the PBO. However, if the PBO can have various forms, the design process should also be performed individually according to the particular form. This means that general designing rules cannot be derived. On the contrary, there have been a lot of researches on designing or tuning methods of PID controller. Thus, rather generalized designing rules for the PBO can be obtained if PID controller with a form of (4.4) is selected as the PBO. For this reason, the designing rules for the PBO in this dissertation are also based on PID controller. The feedback control structure is shown in Figure 4.1, in which the use of PID controller is explicitly indicated in the position of the PBO. However, the strength of the feedback control structure of the PBO is that a form of the PBO is not restricted to a particular design. Thus, in order to verify this merit, a modified designing rule is also composed in the section 4.4 as the improved design for the PBO different from the typical PID controller.

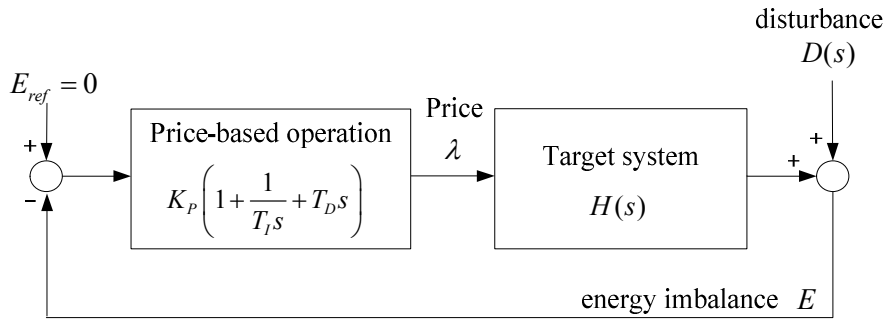

Figure 4.1 Feedback control structure of the PBO with PID controller used as the PBO.

4.2 Selection of tuning rule

Once the PID controller is selected as a form of the PBO, various tuning rules can be applied to determine the parameters of it. The most well-known tuning rule is Ziegler-Nichols PID tuning rule [39]. There are two methods of Ziegler-Nichols tuning rules, which are shown in Table 4.1 and Table 4.2 [32]. However, the target system in (3.3) or the approximate target system in (3.4) has an integrator and does not have a critical gain value. These correspond to the conditions in which either the first method or the second method of Ziegler-Nichols tuning rule cannot be applied [32]. Thus, the Ziegler-Nichols tuning rules should be unavoidably excluded from possible methods for the design of the PBO.

As an alternative, other tuning methods are examined including pole-placement method [40], internal model control method [41, 42], and direct synthesis method [43]. Among the methods, the PID tuning rule in [41], which is known for the better performance in the integrating process, is selected in this dissertation as the reference designing rule for the PBO. Another reason for selecting the rule in [41] is that it has a parameter adjusting the speed of a closed-loop response. This feature means that the constraint on the response speed of the physical power systems can be possibly satisfied by adjusting the parameter of the designing rule for the PBO. In other words, if the response of the physical systems is considerably slow, then better performance in the dynamic behavior and the stability can be achieved by properly making the speed parameter small.

Table 4.1 First method of Ziegler-Nichols tuning rule (L: delay time, T: time constant) [23].

Type of controller	K_P	T_I	T_D
P	T/L	-	-
PI	$0.9T/L$	$L/0.3$	-
PID	$1.2T/L$	$2L$	$0.5L$

Table 4.2 Second method of Ziegler-Nichols tuning rule (K_{cr}: critical gain, P_{cr}: critical period) [23].

Type of controller	K_P	T_I	T_D
P	$0.5K_{cr}$	-	-
PI	$0.45K_{cr}$	$(1/1.2)P_{cr}$	-
PID	$0.6K_{cr}$	$0.5P_{cr}$	$0.125P_{cr}$

The tuning rules in [41] cover a few fundamental types of the system, which are given in Table 4.3. The parameters in Table 4.3 are intermediate ones, and the relation of them with the parameters of PID controller in (4.4) is as follows:

$$K_P = k_c\left(1+\frac{\tau_D}{\tau_I}\right), \quad T_I = \tau_I\left(1+\frac{\tau_D}{\tau_I}\right), \quad T_D = \frac{\tau_D}{1+\frac{\tau_D}{\tau_I}} \tag{4.8}$$

The term τ_c in Table 4.3 is a desired closed-loop parameter and becomes the design parameter for the PBO, which adjusts the response speed.

Table 4.3 Selected PID tuning rules for designing the PBO [41].

Type of system	$H(s)$	k_c	τ_I	τ_D
First order	$k\frac{e^{-\theta s}}{\tau_1 s+1}$	$\frac{1}{k}\frac{\tau_1}{(\tau_c+\theta)}$	$\min\{\tau_1, 4(\tau_c+\theta)\}$	-
Second order	$k\frac{e^{-\theta s}}{(\tau_1 s+1)(\tau_2 s+1)}$	$\frac{1}{k}\frac{\tau_1}{(\tau_c+\theta)}$	$\min\{\tau_1, 4(\tau_c+\theta)\}$	τ_2
Pure time delay	$ke^{-\theta s}$	0	0	-
Integrating	$k\frac{e^{-\theta s}}{s}$	$\frac{1}{k}\frac{1}{(\tau_c+\theta)}$	$4(\tau_c+\theta)$	-
Integrating with lag	$k\frac{e^{-\theta s}}{s(\tau_2 s+1)}$	$\frac{1}{k}\frac{1}{(\tau_c+\theta)}$	$4(\tau_c+\theta)$	τ_2
Double integrating	$k\frac{e^{-\theta s}}{s^2}$	$\frac{1}{k}\frac{1}{4(\tau_c+\theta)^2}$	$4(\tau_c+\theta)$	$4(\tau_c+\theta)$

4.3 Basic designing rule

Since the approximate target system is the first-order system as shown in (3.4), the tuning rule for the integrating system with a lag in Table 4.3 can be used for composing the designing rule for the PBO. Then, from Table 4.3 and the equation (4.8), the following basic designing rule can be obtained:

$$K_P = \frac{c_A}{\tau_c} + \frac{\tau_A}{4\tau_c^2}, \quad T_I = 4\tau_c + \frac{\tau_A}{c_A}, \quad T_D = \frac{1}{\frac{c_A}{\tau_A} + \frac{1}{4\tau_c}} \tag{4.9}$$

If τ_A / c_A is too large, e.g., $\tau_A / c_A > 10$, the approximate target system in (3.4) can be further simplified as a double integrating system of

$$\tilde{H}(s) = \frac{1}{\tau_A s^2} \tag{4.10}$$

Then, the following designing rule can be applied instead of (4.9):

$$K_P = \frac{\tau_A}{2\tau_c^2}, \quad T_I = 8\tau_c, \quad T_D = 2\tau_c \tag{4.11}$$

Since the speed of response depends on the parameter τ_c, the choice of τ_c determines the magnitude of the frequency deviation and the time necessary for the frequency to be recovered. Considering the tight criteria for the frequency [44, 45], a smaller value of τ_c is favored. However, if τ_c is too small, the oscillation can happen in the response, and the system can be unstable due to the large value of gain. Thus, a suitable value of τ_c can be determined by a trade-off between the fast response (smaller value) and the robustness (larger value) [41]. The stability issue in the case of the rapid

response is also suggested in [17]. Thus, there is a limit on how far τ_c can be smaller simultaneously satisfying the stability condition, so that τ_c should be carefully determined.

Meanwhile, as indicated in (2.5) and mentioned in Section 3.1, the energy imbalance and the frequency deviation can be replaced with each other by multiplying an appropriate gain constant. However, when the basic designing rule in (4.9) or (4.11) is adjusted with respect to the frequency deviation, the gain constant should be carefully considered. Specifically, if the frequency deviation is used instead of the energy imbalance, the structure in Figure 4.1 can be represented as shown in Figure 4.2. It can be seen from Figure 4.2 that the gain constant is included in the target system on which the designing rule is based. Thus, in the case when the frequency deviation is used as an output variable, the rule in (4.9) is modified as

$$K_P = \frac{1}{L_f}\left(\frac{c_A}{\tau_c} + \frac{\tau_A}{4\tau_c^2}\right), \quad T_I = 4\tau_c + \frac{\tau_A}{c_A}, \quad T_D = \frac{1}{\frac{c_A}{\tau_A} + \frac{1}{4\tau_c}} \tag{4.12}$$

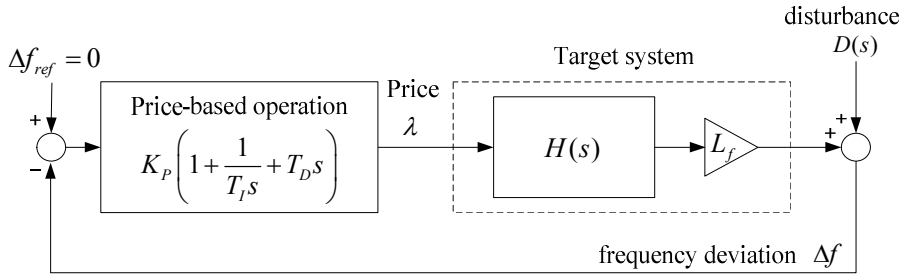

Figure 4.2 Feedback control structure of the PBO with respect to the frequency deviation instead of the energy imbalance.

and the rule for a large value of τ_A / c_A in (4.11) is changed as

$$K_P = \frac{\tau_A}{2L_f \tau_c^2}, \quad T_I = 8\tau_c, \quad T_D = 2\tau_c \tag{4.13}$$

It should be noted from (4.12) and (4.13) that the gain constant L_f affects only the proportional gain K_P because of the form of PID controller in (4.4). Furthermore, there is canceling of the gain constant L_f within the feedback loop. Thus, when the designing rule in (4.9), (4.1), (4.12), or (4.13) is used as the specific design of the PBO, the generated prices are all equal regardless that the output variable is the energy imbalance or the frequency deviation.

4.4 Modified designing rule

4.4.1 Additional component from asymmetric damping

In the existing centralized operation scheme, the frequency is managed in stages for different time scales [26, 31]. Among the steps, the primary control fast prevents the further frequency deviation by rapidly changing the valve position. And then, the secondary control, or automatic generation control (AGC), recovers the frequency to the nominal value by resetting the reference mechanical power. Considering the stability of power system and the goal of the operation in terms of frequency deviation, it is necessary in the PBO to stop the variation of frequency deviation or the energy imbalance as fast as possible.

Picking up an idea from the primary control, a method is composed to use an additional price signal stopping the further variation of the energy imbalance at the moment of the event such as the generation failure or the abrupt demand change for short duration. This is similar to damping control. In view of PID control, it can be considered as a proportional control making the time derivative of the energy imbalance close to zero. The final price λ provided to the participants is obtained by summing the price of basic PID control, denoted as λ_{PID}, and the price of the additional damping control, denoted as λ_{Damp}. Then, the problem naturally arises how to determine the proportional gain of the damping control. Again, it is possible to resort to the tuning rule in Table 4.3. However, in this case, the target system is not $\tilde{H}(s)$

in (3.4) but $\hat{\tilde{H}}(s)$ in (3.6) because the output variable is the derivative of the energy imbalance. Then, the tuning rule of the proportional gain for the first-order system in Table 4.3 can be applied for determining the gain of the additional damping. Thus, the proportional gain $K_{P,Damp}$ can be determined as

$$K_{P,Damp} = \frac{\tau_A}{\tau_{c,damp}} \tag{4.14}$$

where $\tau_{c,damp}$ is another desired parameter for damping. This modified configuration of the PBO is represented in Figure 4.3. Since the damping control is added for the fast response at the moment of an event, the value of $\tau_{c,damp}$ is recommended to be smaller than τ_c to obtain better dynamic performance in the variation of the energy imbalance.

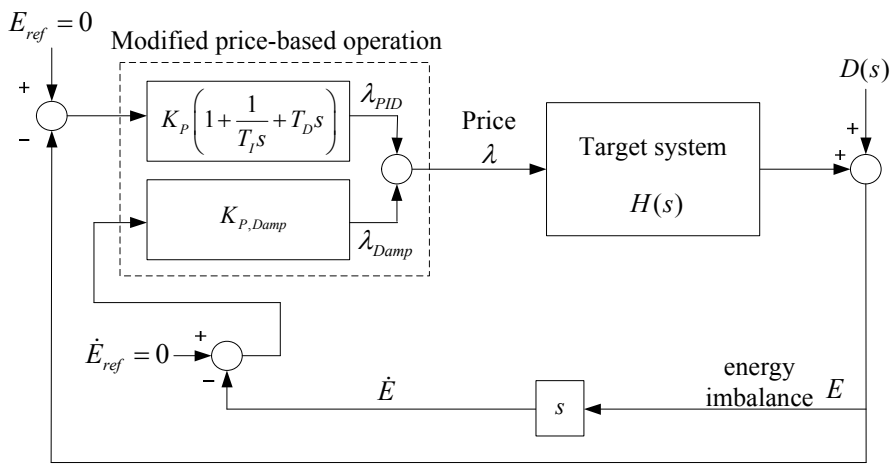

Figure 4.3 Feedback control structure of the modified designing rule for the PBO.

For the first-order system with a form of $\hat{\tilde{H}}(s)$, the proportional gain does not change even if τ_A / c_A is too large. Thus, $K_{P,Damp}$ does not change depending on τ_A / c_A as does in the case of (4.9) and (4.11). However, there is one thing to be taken care of when the additional damping control is applied. If it is applied in the pure form, it functions against the normal process of reducing the energy imbalance by the basic PID controller when the signs of E and $\dot{E}$ are reversed. In other words, when E is positive, it is getting worse than the basic designing rule if $\dot{E}$ negative because the additional damping control impedes the desirable function of the negative $\dot{E}$ for reducing the energy imbalance. This reasoning identically applies to the case when E is negative and $\dot{E}$ is positive. Thus, the additional damping is necessary when both E and $\dot{E}$ are positive or negative. As a result, in order to obtain the expected effect of reducing the energy imbalance, the additional damping control should be used asymmetrically considering the signs of E and $\dot{E}$, which results in the following conditional gain

$$K_{P,Damp} = \begin{cases} \dfrac{\tau_A}{\tau_{c,damp}} & \text{if } \operatorname{sgn}(E \cdot \dot{E}) > 0 \\ 0 & \text{otherwise} \end{cases} \tag{4.15}$$

4.4.2 Specific form of the modified designing rule

The proportional control for $\dot{E}$ is equivalent to the derivative control for E. Thus, (4.15) can be combined into (4.9) or (4.11). Then, the modified designing rule with an additional damping control in (4.9) can be arranged as

$$K_P = \frac{c_A}{\tau_c} + \frac{\tau_A}{4\tau_c^2}, \quad T_I = 4\tau_c + \frac{\tau_A}{c_A},$$
$$T_D = \begin{cases} \dfrac{1}{\dfrac{c_A}{\tau_A} + \dfrac{1}{4\tau_c}} \cdot \left(1 + \dfrac{\tau_c}{\tau_{c,damp}}\right) & \text{if } \mathrm{sgn}(E \cdot \dot{E}) > 0 \\ \dfrac{1}{\dfrac{c_A}{\tau_A} + \dfrac{1}{4\tau_c}} & \text{otherwise} \end{cases} \tag{4.16}$$

and the rule in (4.11) in the case of the large value of τ_A / c_A can be similarly modified as

$$K_P = \frac{\tau_A}{2\tau_c^2}, \quad T_I = 8\tau_c,$$
$$T_D = \begin{cases} 2\tau_c \cdot \left(1 + \dfrac{\tau_c}{\tau_{c,damp}}\right) & \text{if } \mathrm{sgn}(E \cdot \dot{E}) > 0 \\ 2\tau_c & \text{otherwise} \end{cases} \tag{4.17}$$

It can be seen from (4.16) and (4.17) that the derivative time or the gain of derivative control increases during the interval of applying the additional damping control. The benefits of the modified designing rule are not only the reduction of energy imbalance, but also the mitigation of an oscillation resulted from the small value of τ_c. Specifically, because there is no integral gain term in the damping controller, an overshoot in the unit step response

does not occur and the oscillation is not caused even for a small value of $\tau_{c,damp}$ unlike the case of τ_c. This property enables the modified designing rule to deal with rapid changes of the power imbalance between supply and demand by setting $\tau_{c,damp}$ as a small value, which is particularly necessary for the frequency regulation function.

Finally, it is necessary how the modified designing rules in (4.16) and (4.17) change when the frequency deviation is used as the output variable instead of the energy imbalance. The feedback control structure using the frequency deviation is given in Figure 4.4. As can be seen from Figure 4.4, there also occurs canceling of the gain constant L_f within the feedback loop so that L_f affects only the proportional gain K_P. Certainly, the branch condition of $\text{sgn}(E \cdot \dot{E}) > 0$ should be replaced with $\text{sgn}(\Delta f \cdot \Delta \dot{f}) > 0$.

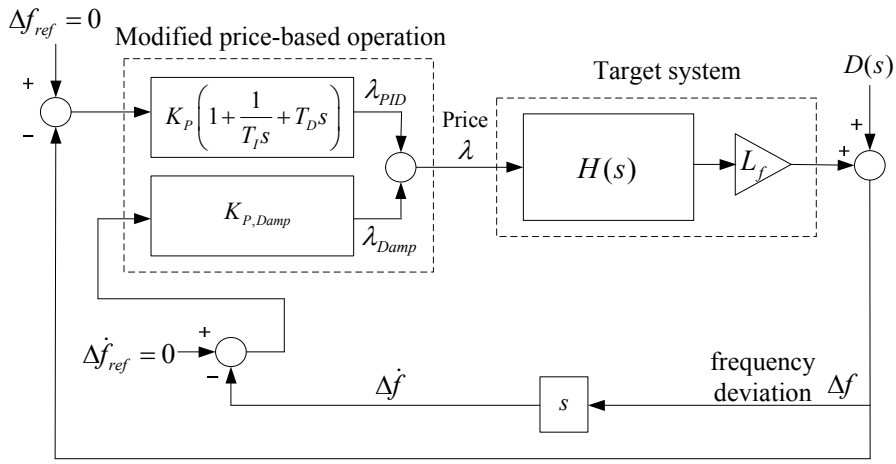

Figure 4.4 Feedback control structure of the modified designing rule for the PBO with respect to the frequency deviation instead of the energy imbalance.

Consequently, in the case when the frequency deviation is used as an output variable, the rule in (4.16) is can be expressed as

$$K_P = \frac{1}{L_f}\left(\frac{c_A}{\tau_c} + \frac{\tau_A}{4\tau_c^2}\right), \quad T_I = 4\tau_c + \frac{\tau_A}{c_A},$$
$$T_D = \begin{cases} \dfrac{1}{\dfrac{c_A}{\tau_A} + \dfrac{1}{4\tau_c}} \cdot \left(1 + \dfrac{\tau_c}{\tau_{c,damp}}\right) & \text{if } \operatorname{sgn}(\Delta f \cdot \Delta \dot{f}) > 0 \\ \dfrac{1}{\dfrac{c_A}{\tau_A} + \dfrac{1}{4\tau_c}} & \text{otherwise} \end{cases} \tag{4.18}$$

and the rule for a large value of τ_A / c_A in (4.17) should be modified as

$$K_P = \frac{\tau_A}{2L_f\tau_c^2}, \quad T_I = 8\tau_c,$$
$$T_D = \begin{cases} 2\tau_c \cdot \left(1 + \dfrac{\tau_c}{\tau_{c,damp}}\right) & \text{if } \operatorname{sgn}(\Delta f \cdot \Delta \dot{f}) > 0 \\ 2\tau_c & \text{otherwise} \end{cases} \tag{4.19}$$

Chapter 5. Use of Price Information

When the demand for electricity increases, the equilibrium price rises. It is unusual to exactly know the equilibrium price in advance. Thus, a kind of trials and errors for determining the equilibrium price are unavoidably experienced. However, regardless of the fact that the equilibrium price cannot be known in advance, the activities based on the equilibrium price are being conducted in the real world. In other words, the transactions based on the expected equilibrium price take place in the futures market, and various techniques for forecasting it are developed. Then, it is likely to get some benefits from the price information in those activities when it is used in the process of determining the price signal in the PBO. Thus, a structure for using the price information in the PBO is developed, and the benefit of using the price information is quantitatively analyzed in this chapter.

5.1 Structure of the PBO using price information

The derivation of the structure of the PBO using price information starts from the power market dynamics in (3.1), which is rewritten here for convenience as

$$\begin{aligned}
\tau_{g,i}\dot{P}_{g,i} &= \lambda - \left(b_{g,i} + c_{g,i}P_{g,i}\right), \quad i = 1,\cdots,m \\
\tau_{d,j}\dot{P}_{d,j} &= \left(b_{d,j} + c_{d,j}P_{d,j}\right) - \lambda, \quad j = 1,\cdots,n \\
\dot{E} &= \sum_{i=1}^{m} P_{g,i} - \sum_{j=1}^{n} P_{d,j}
\end{aligned} \tag{5.1}$$

If it is assumed that the electricity price in the steady state, denoted as λ_{SS}, is known in advance, then the variables $P_{g,i}$, $P_{d,j}$, and E in (5.1) converge to the particular steady-state values by continuously providing λ_{SS} to the participants. However, it cannot be guaranteed that E becomes zero in the steady state when only λ_{SS} is provided. This means that the frequency of the power system remains deviated from the nominal value. Thus, except for λ_{SS}, an additional time-varying price signal generated from the feedback control mechanism is still needed in order to ensure that E becomes zero.

Nonetheless, the knowledge of λ_{SS} can be a valuable information, and it is meaningful to achieve the desirable effect by devising a method for using it. For this purpose, considering that λ_{SS} is a constant, a method is composed in which λ_{SS} functions as a constant price offset that is added to the prices generated from the feedback mechanism. However, the constant price offset cannot necessarily be equal to λ_{SS}, and it cannot be λ_{SS} in a practical sense. Thus, the price offset is denoted as λ_0 instead of λ_{SS}. Then, a new structure of the PBO using price information as a price offset can be composed as shown in Figure 5.1.

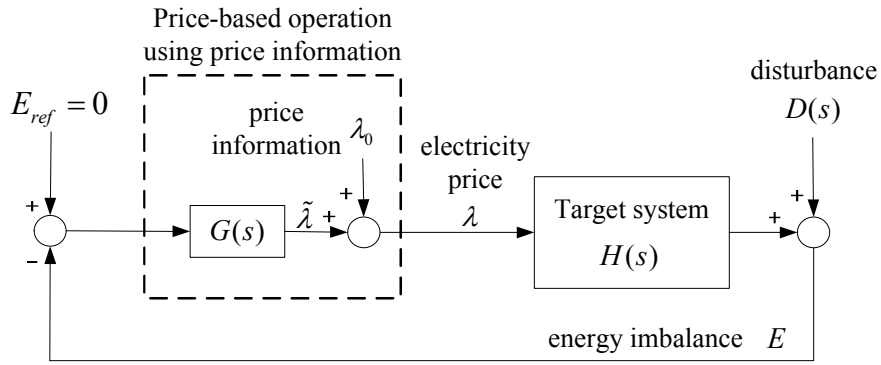

Figure 5.1 Structure of the PBO using price information as a price offset.

5.2 Available sources of price information

Although it cannot be guaranteed that E becomes zero in the steady state by using only λ_{SS}, it is able to prevent the energy imbalance from further going away from the reference value of zero. Thus, the expected desirable effect of using the price information is to reduce the variation of the energy imbalance, that is, to reduce the frequency deviation. Then, it can be easily thought that the variation of the energy imbalance decreases more if λ_0 is closer to λ_{SS}. If the power market dynamics in (5.1) are known in advance, λ_{SS} can be easily computed from (2.7). However, as mentioned earlier, it is likely that the strategies of the participants expressed as in (5.1) are unknown particularly in a decentralized environment. Thus, other sources of price information are necessary for the new structure of the PBO in Figure 5.1 to be applied to practical applications.

Considering the practical applications, it is desirable that the price information is easily accessible. Moreover, the accuracy of the price information needs to be high to some degree compared to the actual system marginal price. One of the sources which meet these conditions is the price obtained from the futures market for electricity. Under well-operated market circumstance, it is known that the futures market price converges to a spot price at the delivery period [46]. In particular, the results from the empirical analysis of Nord Pool Power Exchange show that the error is around 8 % compared to the settled spot price when a month-ahead hourly price in the market is used as a forecasted value [47].

Another available source of the price information is an estimated electricity price from various forecasting methods [48, 49]. The estimated price is determined from a set of price data in the past. This is a meaningful source in the situation without the well-operated market. The simplest estimated price may be the price of past itself, e.g., the price of yesterday. However, it can be distorted by unexpected disturbance such as a dramatic change of the weather condition and a large scale of fault in the power systems. Thus, advanced techniques such as time-series analysis are needed to smooth the abrupt variation of price [50]. There is an empirical study which shows that the next-day price forecasted by time-series model is not significantly different with spot prices, and the daily mean error is only around 4% [49].

5.3 Quantitative effects of price information

If the price information affects the variation of the energy imbalance and the desirable effect becomes greater if the price information is closer to λ_{SS}, it is necessary to perform the quantitative analysis with respect to the accuracy of the price information compared to λ_{SS}.

At first, let new variables be defined as follows

$$\begin{aligned} \tilde{P}_{g,i} &= P_{g,i} - P_{gSS,i}, \quad \tilde{P}_{d,j} = P_{d,j} - P_{dSS,j} \\ \tilde{\lambda} &= \lambda - \lambda_0, \qquad\quad \tilde{E} = E \end{aligned} \tag{5.2}$$

where $P_{gSS,i}$ and $P_{dSS,j}$ are the amount of generation of the *i*-th supplier and consumption of the *j*-th consumer in the steady state, respectively. Then, (5.1) can be represented with these new variables as

$$\begin{aligned} \tau_{g,i}\dot{\tilde{P}}_{g,i} &= -b_{g,i} - c_{g,i}(\tilde{P}_{g,i} + P_{gSS,i}) + (\tilde{\lambda} + \lambda_0) \\ \tau_{d,j}\dot{\tilde{P}}_{d,j} &= b_{d,j} + c_{d,j}(\tilde{P}_{d,j} + P_{dSS,j}) - (\tilde{\lambda} + \lambda_0) \\ \dot{\tilde{E}} &= \sum_i (\tilde{P}_{g,i} + P_{gSS,i}) - \sum_j (\tilde{P}_{d,j} + P_{dSS,j}) \end{aligned} \tag{5.3}$$

By setting the values of time derivative to zero in (5.1), the following relationship can be derived

$$\begin{aligned} 0 &= -b_{g,i} - c_{g,i}P_{gSS,i} + \lambda_{SS} \\ 0 &= b_{d,j} + c_{d,j}P_{dSS,j} - \lambda_{SS} \\ 0 &= \sum_i P_{gSS,i} - \sum_j P_{dSS,j} \end{aligned} \tag{5.4}$$

Let λ_ε denote the difference between the price information and the system marginal price in the steady state, which is defined as

$$\lambda_{\varepsilon} = \lambda_0 - \lambda_{SS} \tag{5.5}$$

Then, by substituting (5.5) into (5.3) and using the relationship in (5.4), the original market dynamics in (5.1) can be expressed with new variables as

$$\begin{aligned} \tau_{g,i}\dot{\tilde{P}}_{g,i} &= -c_{g,i}\tilde{P}_{g,i} + (\tilde{\lambda} + \lambda_{\varepsilon}) \\ \tau_{d,j}\dot{\tilde{P}}_{d,j} &= c_{d,j}\tilde{P}_{d,j} - (\tilde{\lambda} + \lambda_{\varepsilon}) \\ \dot{\tilde{E}} &= \sum_i \tilde{P}_{g,i} - \sum_j \tilde{P}_{d,j} \end{aligned} \tag{5.6}$$

where the initial values of variables are

$$\tilde{P}^0_{g,i} = -\tilde{P}_{gSS,i}, \quad \tilde{P}^0_{d,j} = -\tilde{P}_{dSS,j}, \quad \tilde{E}^0 = 0 \tag{5.7}$$

From the superposition property of linear systems, the energy imbalance of (5.6) can be separated into two parts like

$$\tilde{E}(t) = \tilde{E}_{Init}(t) + \tilde{E}_{Diff}(t) \tag{5.8}$$

where $\tilde{E}_{Init}(t)$ is the contribution of the initial value in (5.7), and $\tilde{E}_{Diff}(t)$ is the contribution of λ_{ε} on the energy imbalance. By deriving the closed-loop response from the structure in Figure 5.1 and using the dynamic equations in (5.6), Laplace transform of $\tilde{E}_{Init}(t)$ can be determined as

$$\tilde{E}_{Init}(s) = \frac{\tilde{E}_{Nat}(s)}{1 + G(s)\tilde{H}(s)} \tag{5.9}$$

where $\tilde{E}_{Nat}(s)$ is the natural response by the initial values in (5.7), which can be represented as

$$\begin{aligned}\tilde{E}_{Nat}(s) &= \sum_{i=1}^{m} \frac{\tau_{g,i}\tilde{P}^{0}_{g,i}}{s(\tau_{g,i}s + c_{g,i})} - \sum_{j=1}^{n} \frac{\tau_{d,j}\tilde{P}^{0}_{g,i}}{s(\tau_{d,j}s - c_{d,j})} \\ &= \sum_{i=1}^{m} \frac{-\tau_{g,i}P_{gSS,i}}{s(\tau_{g,i}s + c_{g,i})} - \sum_{j=1}^{n} \frac{-\tau_{d,j}P_{dSS,j}}{s(\tau_{d,j}s - c_{d,j})}\end{aligned} \tag{5.10}$$

In (5.9), $\tilde{H}(s)$ is an open-loop transfer function when λ_{ε} is excluded, which can be written as

$$\tilde{H}(s) = \sum_{i=1}^{m} \frac{1}{s(\tau_{g,i}s + c_{g,i})} + \sum_{j=1}^{n} \frac{1}{s(\tau_{d,j}s - c_{d,j})} \tag{5.11}$$

Similarly, Laplace transform of $\tilde{E}_{Diff}(t)$ for the closed-loop response, or $\tilde{E}_{Diff}(s)$, can be arranged as

$$\tilde{E}_{Diff}(s) = \frac{\tilde{D}(s)}{1 + G(s)\tilde{H}(s)} \tag{5.12}$$

where $\tilde{D}(s)$ is an open-loop transfer function related to λ_{ε} as

$$\tilde{D}(s) = \frac{\lambda_{\varepsilon}}{s} \cdot \left(\sum_{i=1}^{m} \frac{1}{s(\tau_{g,i}s + c_{g,i})} + \sum_{j=1}^{n} \frac{1}{s(\tau_{d,j}s - c_{d,j})} \right) \tag{5.13}$$

Then, from (5.13), $\tilde{E}_{Diff}(s)$ can be expressed with respect to λ_{ε} as

$$\tilde{E}_{Diff}(s) = \lambda_{\varepsilon} \cdot \tilde{E}^{N}_{Diff}(s) \tag{5.14}$$

where $\tilde{E}^{N}_{Diff}(s)$ is a normalized transfer function according to λ_{ε}. Let

$\tilde{E}_{Init,\max}$ and $\tilde{E}^{N}_{Diff,\max}$ denote a maximum absolute deviation of $\tilde{E}_{Init}(t)$ and $\tilde{E}_{Diff}(t)$ from zero for $t \geq 0$, respectively;

$$\tilde{E}_{Init,\max} = \max_{t\geq 0} \left|\tilde{E}_{Init}(t)\right|, \quad \tilde{E}^{N}_{Diff,\max} = \max_{t\geq 0} \left|\tilde{E}^{N}_{Diff}(t)\right| \tag{5.15}$$

Then, the following inequality relationship can be formed

$$\begin{aligned} \tilde{E}_{\max} &= \max_{t\geq 0} \left|\tilde{E}(t)\right| = \max_{t\geq 0} \left|\tilde{E}_{Init}(t) + \tilde{E}_{Diff}(t)\right| \\ &\leq \max_{t\geq 0} \left|\tilde{E}_{Init}(t)\right| + \max_{t\geq 0} \left|\tilde{E}_{Diff}(t)\right| \\ &= \tilde{E}_{Init,\max} + \left|\lambda_{\varepsilon}\right| \cdot \tilde{E}^{N}_{Diff,\max} \end{aligned} \tag{5.16}$$

where $\tilde{E}_{\max}$ is the maximum absolute deviation of $\tilde{E}(t)$ from zero. Then, $\tilde{E}_{Init,\max} + \left|\lambda_{\varepsilon}\right| \cdot \tilde{E}^{N}_{Diff,\max}$ becomes the upper bound of $\tilde{E}_{\max}$ when the accuracy of price information is λ_{ε}. Consequently, the reduction of the energy imbalance can be obtained by using suitable price information within the structure in Figure 5.1. Furthermore, since $\tilde{E}_{Init,\max}$ and $\tilde{E}^{N}_{Diff,\max}$ are related to the specific design of the PBO $G(s)$ as can be seen from (5.9) and (5.12), it can be asserted that $\tilde{E}_{Init,\max}$ and $\tilde{E}^{N}_{Diff,\max}$ can be reduced by the proper design of the PBO.

5.4 Acceptable range of price information

When there is no available price information, it is reasonable that λ_0 should be set to zero. Moreover, although negative electricity prices can occur under some conditions [51, 52], they are positive in normal cases. Thus, the lower bound for the acceptable range of the price information λ_0 can be carefully determined as zero. However, the upper bound of the acceptable range should be determined by considering $\tilde{E}(t)$. In Figure 5.2, the shaded area (A) and (B) indicate the possible values of $\tilde{E}_{\max}$ according to λ_ε, and the solid line denotes the upper bound of $\tilde{E}_{\max}$ as given in (5.16). Without any price information, λ_0 is set to zero and the accuracy of it becomes $\lambda_\varepsilon = -\lambda_{SS}$. In that situation, the upper bound of $\tilde{E}_{\max}$ is determined from (5.16) as $\tilde{E}_{Init,\max} + |\lambda_{SS}| \cdot \tilde{E}_{Diff,\max}$. If λ_ε is larger than λ_{SS}, there is a chance that $\tilde{E}_{\max}$ is greater than $\tilde{E}_{Init,\max} + |\lambda_{SS}| \cdot \tilde{E}_{Diff,\max}$, as represented as a shaded area (B) with cross stripes in Figure 5.2. In other words, when λ_ε is larger than λ_{SS}, it cannot be guaranteed that the use of price information gives a reduction of the energy imbalance compared to the case without it. Thus, the upper bound of the acceptable range for λ_0 can be determined as $2\lambda_{SS}$. As a result, the acceptable range of the price information for achieving the desirable effect of reducing the energy imbalance becomes

$$0 \le \lambda_0 \le 2\lambda_{SS} \tag{5.17}$$

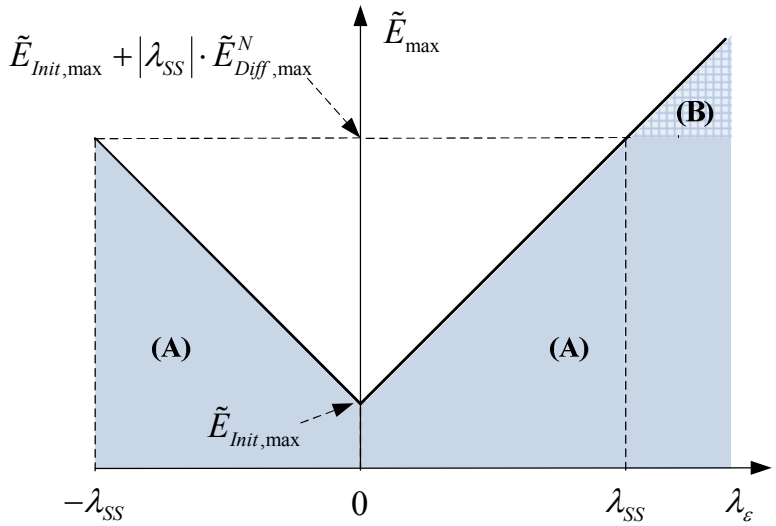

Figure 5.2 The upper bound of $\tilde{E}_{\max}$ (solid lines) and the area for possible values of $\tilde{E}_{\max}$ (shaded area) according to λ_{ε}.

5.5 Price information with the smallest deviation

It can be simply speculated from (5.16) that the smallest value of $\tilde{E}_{\max}$ may be obtained when the price information is exact, namely $\lambda_\varepsilon = 0$. However, since (5.16) specifies the upper bound, it cannot be ruled out that the smallest absolute deviation of $\tilde{E}_{\max}$ may appear when λ_ε is not equal to zero. The main reason for this situation is that the cancelling effect between $\tilde{E}_{Init}(t)$ and $\tilde{E}_{Diff}(t)$ makes it difficult to predict the actual variation of $\tilde{E}_{\max}$ according to λ_ε. To be specific, when $|\lambda_\varepsilon|$ is large, $\tilde{E}_{Diff}(t)$ dominates $\tilde{E}(t)$, so that the cancelling effect is not large. In other words, it holds when $|\lambda_\varepsilon|$ is large that the effect of reducing the energy imbalance is greater according as λ_0 is closer to λ_{SS}. However, when $|\lambda_\varepsilon|$ is suitably small, the cancelling effect considerably affects the value of $\tilde{E}_{\max}$, so that $\tilde{E}_{\max}$ for a certain value of $\lambda_0 \neq \lambda_{SS}$ can be the smallest one among the range in (5.17).

The cancelling effect can be specifically described by the following example. Let us assume that $\tilde{E}_{Init}(t)$ and $\tilde{E}_{Diff}(t)$ have the forms as shown in Figure 5.3(a). It is also assumed that the magnitude of $\tilde{E}_{Init,\max}$ is approximately ten times bigger than that of $\tilde{E}^N_{Diff,\max}$. Then, $\tilde{E}(t)$ can be created from (5.8) for various values of λ_ε. The resultant graphs of $\tilde{E}(t)$ are shown in Figure 5.3(b). Because of the cancelling effect between $\tilde{E}_{Init}(t)$ and $\tilde{E}_{Diff}(t)$, the value of $\tilde{E}_{\max}$ for $\lambda_\varepsilon = 0.1$ is smaller than that for $\lambda_\varepsilon = 0$.

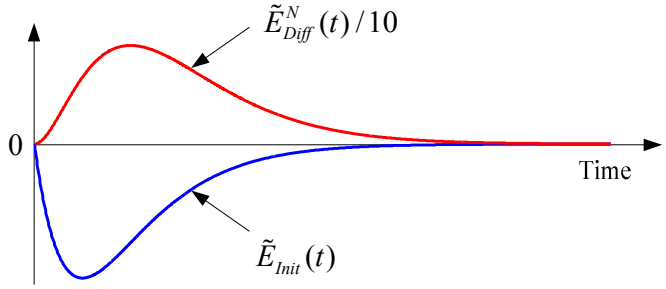

(a)

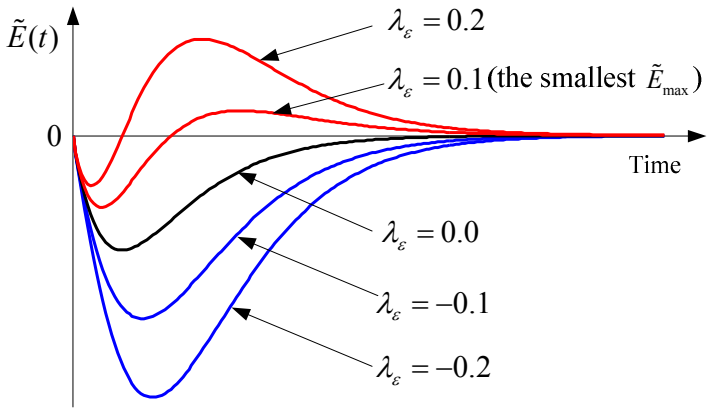

(b)

Figure 5.3 Example of the cancellation effect between $\tilde{E}_{Init}(t)$ and $\tilde{E}_{Diff}(t)$. (a) Function values of $\tilde{E}_{Init}(t)$ and $\tilde{E}_{Diff}(t)$. (b) Time variation of the energy imbalance $\tilde{E}(t)$ for some values of λ_ε.

In this example, $\tilde{E}_{Init}(t)$ and $\tilde{E}_{Diff}(t)$ appear on the opposite sides of zero so that $\tilde{E}_{\max}$ is the smallest when λ_{ε} is slightly larger than zero. On the contrary, if $\tilde{E}_{Init}(t)$ and $\tilde{E}_{Diff}(t)$ appear on the same sides, $\tilde{E}_{\max}$ may become the smallest when λ_{ε} is slightly smaller than zero. This shows an interesting point that some accuracy error of the price information compared to the actual system marginal price in the steady state can result in rather a more reduction of the energy imbalance or better performance in terms of the frequency stability.

Chapter 6. Framework for Balancing and Congestion Management

In this chapter, the congestion management in the PBO is considered. When the congestion occurs in a transmission line, the amount of generation and consumption at some buses in the network should be changed. This is because the power flow in the transmission line is a dependent variable on net power of the buses. Then, like the balance of the power is accomplished by the appropriate price signals, the congestion can also be relieved by controlling the price at each bus in the PBO. Thus, it becomes an important problem how to determine the price at each bus, or the nodal prices, in the PBO.

Meanwhile, there is a well-known OPF method for the congestion management function. This means that the optimal nodal prices exist in a certain situation when the congestion occurs. In other words, a set of nodal prices may not be optimal, even though the congestion is resolved by the nodal prices. This situation can happen in the feedback control model of the PBO. If the nodal prices are generated from the feedback controllers without an elaborately designed structure, the situation may happen when the congestion is resolved at a moment but the nodal prices at the moment are not equal to the optimal ones. However, it is annoying to verify the optimality of the nodal prices at every situation. Thus, a general structure or a framework of the PBO is introduced in this chapter, which guarantees the optimality as well as provides the elementary balancing and congestion management functions.

6.1 Optimal power flow method

The methods for the PBO in this dissertation basically try to be based on the optimality conditions as same as the most schemes for power system operation do. Among the techniques currently used, the optimal power flow (OPF) method is the most well-known method for achieving the optimality in the power system operation considering both the power balancing and the congestion management. Thus, it is a suitable choice that the derivation of the framework for the optimal PBO with congestion management should start from the OPF formulation.

The formulation of OPF used in the dissertation is based on the following assumptions: the power flow is calculated by DC power flow method [26]; there is no loss in transmission lines; bus 1 is a slack bus so that $\theta_1 = 0$. Then, the OPF problem can be formulated as the following optimization problem

$$\min_{\mathbf{P_g},\mathbf{P_d}} \left\{ F\left(\mathbf{P_g},\mathbf{P_d}\right) \right\} = \min_{\mathbf{P_g},\mathbf{P_d}} \left\{ \sum_{k=1}^{n_b} C_{g,k}\left(P_{g,k}\right) - \sum_{k=1}^{n_b} U_{d,k}\left(P_{d,k}\right) \right\} \tag{6.1}$$

subject to the power balancing equation

$$\mathbf{1}^T \mathbf{P} = P_1 + P_2 + \cdots + P_{n_b} = 0 \tag{6.2}$$

and the load flow equations at each bus

$$\hat{\mathbf{B}}\hat{\boldsymbol{\theta}} = \left[\mathbf{B}_2 \quad \mathbf{B}_3 \quad \cdots \quad \mathbf{B}_{\mathbf{n_b}} \right] \cdot \hat{\boldsymbol{\theta}} = \mathbf{P} \tag{6.3}$$

and the transmission line constraints at each branch

$$-\mathbf{P}_{\mathbf{f}}^{\max} \le \mathbf{P}_{\mathbf{f}} \le \mathbf{P}_{\mathbf{f}}^{\max} \tag{6.4}$$

where the meanings of the variables are

F : total cost function.

$C_{g,k}$: cost function of generation at the bus k.

$U_{d,k}$: utility or benefit function of consumption at the bus k.

n_b : number of the buses.

n_l : number of the transmission lines or the branches.

$\mathbf{P}_{\mathbf{g}} = \left[P_{g,1}, \cdots, P_{g,n_b} \right]^T$: amount of generation, $n_b \times 1$ vector.

$\mathbf{P}_{\mathrm{d}} = \left[P_{d,1}, \cdots, P_{d,n_b} \right]^T$: amount of consumption, $n_b \times 1$ vector.

$P_{g,k}$: amount of generation at the bus k.

$P_{d,k}$: amount of consumption at the bus k.

$\mathbf{P} = \mathbf{P}_{\mathbf{g}} - \mathbf{P}_{\mathbf{d}}$: net power injection, $n_b \times 1$ vector.

$P_k = P_{g,k} - P_{d,k}$: net power injection at the bus k.

$\mathbf{B}$: line susceptance matrix for DC power flow, $n_b \times n_b$ matrix.

$\mathbf{B}_{\mathbf{k}}$: k-th column of line susceptance matrix $\mathbf{B}$, $n_b \times 1$ vector.

$\hat{\mathbf{B}}$: modified line susceptance matrix composed by eliminating the column of slack bus from $\mathbf{B}$, $n_b \times (n_b - 1)$ matrix.

$\hat{\boldsymbol{\theta}} = \left[\theta_2 \quad \theta_3 \quad \cdots \quad \theta_{n_b} \right]$: relative phase angle to the slack bus assumed as the bus 1, $(n_b - 1) \times 1$ vector.

θ_k : relative phase angle of the bus k to the slack bus.

$\mathbf{P_f} = \begin{bmatrix} P_{f,1} & P_{f,2} & \cdots & P_{f,n_l} \end{bmatrix}$: active power flow, $n_l \times 1$ vector.

$P_{f,l}$: active power flow of the line *l*.

$\mathbf{P_f^{max}} = \begin{bmatrix} P_{f,1}^{\max} & P_{f,2}^{\max} & \cdots & P_{f,n_l}^{\max} \end{bmatrix}$: active power flow limit, $n_l \times 1$ vector.

$P_{f,l}^{\max}$: active power flow limit of the line *l*.

$\mathbf{1}$: column vector of the appropriate size with all the elements being equal to 1.

By the assumption of DC power flow, the active power flow from the bus i to j, denoted as $P_f^{i,j}$, is determined by

$$P_f^{i,j} = \frac{\theta_i - \theta_j}{x_{i,j}} \tag{6.5}$$

where $x_{i,j}$ is the inductive reactance in p.u. of the transmission line connecting the bus *i* and *j*. Then, $\mathbf{P_f}$ can be represented in terms of the relative phase angles $\hat{\boldsymbol{\theta}}$ as

$$\mathbf{P_f} = \mathbf{X}^{-1}\hat{\mathbf{A}}\hat{\boldsymbol{\theta}} \tag{6.6}$$

where $\mathbf{X}$ is the reactance matrix of dimension $n_l \times n_l$, which is defined as $\mathbf{X} = \text{diag}\left[x_{i,j} \right]$; $\hat{\mathbf{A}}$ is the branch-to-node incidence matrix of dimension $n_l \times (n_b - 1)$.

Let $\mathbf{z}$ be defined as $\mathbf{z}^T = \begin{bmatrix} \mathbf{P_g}^T & \mathbf{P_d}^T \end{bmatrix}$. Then, the Lagrangian function L can be obtained from (6.1)-(6.4) and (6.6) as

$$\begin{aligned} L\left(\mathbf{z}, \lambda_P, \boldsymbol{\lambda}_\mathbf{0}, \boldsymbol{\mu}_+, \boldsymbol{\mu}_-\right) &= F(\mathbf{z}) + \lambda_P(-\mathbf{1}^T\mathbf{P}) + \boldsymbol{\lambda}_\mathbf{0}^T\left(\hat{\mathbf{B}}\hat{\boldsymbol{\theta}} - \mathbf{P}\right) \\ &+ \boldsymbol{\mu}_+^T\left(\mathbf{X}^{-1}\hat{\mathbf{A}}\hat{\boldsymbol{\theta}} - \mathbf{P}_\mathbf{f}^{\max}\right) + \boldsymbol{\mu}_-^T\left(-\mathbf{X}^{-1}\hat{\mathbf{A}}\hat{\boldsymbol{\theta}} - \mathbf{P}_\mathbf{f}^{\max}\right) \end{aligned} \tag{6.7}$$

where λ_P is Lagrange multiplier associated with equality constraint for the power balancing in (6.2); $\boldsymbol{\lambda}_\mathbf{0}$ is Lagrange multipliers associated with the equality constraint on the power flow in (6.3) except for the slack bus; $\boldsymbol{\mu}_+$ and $\boldsymbol{\mu}_-$ are Lagrange multipliers associated with the inequality constraints on the power flow in (6.4) except for the slack bus. Then, the optimality conditions can be determined from Karush-Kuhn-Tucker (KKT) conditions [53] as

$$\frac{\partial L}{\partial \mathbf{z}} = \frac{\partial F(\mathbf{z})}{\partial \mathbf{z}} - \lambda_P\mathbf{1} - \boldsymbol{\lambda}_\mathbf{0} = \frac{\partial F(\mathbf{z})}{\partial \mathbf{z}} - \boldsymbol{\rho} = \mathbf{0} \tag{6.8-a}$$

$$\frac{\partial L}{\partial \hat{\boldsymbol{\theta}}} = \hat{\mathbf{B}}^T\boldsymbol{\lambda}_\mathbf{0} + \hat{\mathbf{A}}^T\mathbf{X}^{-1}\boldsymbol{\mu}_+ - \hat{\mathbf{A}}^T\mathbf{X}^{-1}\boldsymbol{\mu}_- = \mathbf{0} \tag{6.8-b}$$

$$\frac{\partial L}{\partial \lambda_P} = -\mathbf{1}^T\mathbf{P} = \mathbf{0} \tag{6.8-c}$$

$$\frac{\partial L}{\partial \boldsymbol{\lambda}_\mathbf{0}} = \hat{\mathbf{B}}\hat{\boldsymbol{\theta}} - \mathbf{P} = \mathbf{0} \tag{6.8-d}$$

$$\frac{\partial L}{\partial \boldsymbol{\mu}_+} = \mathbf{X}^{-1}\hat{\mathbf{A}}\hat{\boldsymbol{\theta}} - \mathbf{P}_\mathbf{f}^{\max} \le \mathbf{0} \tag{6.8-e}$$

$$\frac{\partial L}{\partial \boldsymbol{\mu}_-} = -\mathbf{X}^{-1}\hat{\mathbf{A}}\hat{\boldsymbol{\theta}} - \mathbf{P}_\mathbf{f}^{\max} \le \mathbf{0} \tag{6.8-f}$$

$$\boldsymbol{\mu}_+^T\left(\mathbf{X}^{-1}\hat{\mathbf{A}}\hat{\boldsymbol{\theta}} - \mathbf{P}_\mathbf{f}^{\max}\right) = \mathbf{0}, \quad \boldsymbol{\mu}_+ \ge \mathbf{0} \tag{6.8-g}$$

$$\boldsymbol{\mu}_-^T\left(-\mathbf{X}^{-1}\hat{\mathbf{A}}\hat{\boldsymbol{\theta}} - \mathbf{P}_\mathbf{f}^{\max}\right) = \mathbf{0}, \quad \boldsymbol{\mu}_- \ge \mathbf{0} \tag{6.8-h}$$

The optimal nodal prices are composed of Lagrange multipliers λ_P and $\boldsymbol{\lambda}_\boldsymbol{\theta}$ that satisfy the set of conditions in (6.8). The specific equation for determining the nodal prices can be written as

$$\boldsymbol{\rho} = \lambda_P \mathbf{1} + \boldsymbol{\lambda}_\boldsymbol{\theta} \tag{6.9}$$

where $\boldsymbol{\rho}$ is a $n_b \times 1$ vector consisting of ρ_k's or the nodal prices at the bus *k*. The terms $\boldsymbol{\mu}_+$ and $\boldsymbol{\mu}_-$ are so-called congestion prices, which means the possible cost reduction that would be achieved when the maximum transfer limit of the corresponding line increases by one unit. If there is no congestion, all elements of $\boldsymbol{\mu}_+$ and $\boldsymbol{\mu}_-$ are zero. Then, $\boldsymbol{\lambda}_\boldsymbol{\theta}$ becomes a zero vector from (6.8-b), which means that the nodal prices are all equal.

For the line constraints in (6.8-e)-(6.8-h), there is no such case in which the constraints of the positive and negative flow limits are violated at the same time. Besides, the sign of power flow depends on the defined direction of it. Thus, without any loss of generality, the positive maximum power flow will be considered as the inequality constraints. Then, (6.8-f) and (6.8-h) are naturally met, and $\boldsymbol{\mu}_-$ is always equal to zero. Accordingly, for the simplicity of expressions, $\boldsymbol{\mu}$ will be used instead of $\boldsymbol{\mu}_+$ in the following description.

Consequently, (6.8-a), (6.8-b), (6.8-c), (6.8-d), (6.8-e) and (6.8-h) constitute the optimal conditions, which are considered in the following composition of the framework for the design of the optimal PBO with congestion management.

6.2 Substructures of the framework

6.2.1 Marginal price

The condition (6.8-a) means that the marginal cost of generation and the marginal benefit of consumption are identical to the nodal prices of the corresponding buses at the optimal operating point. This condition can be satisfied by the power market dynamics themselves. In this description of the framework, the criteria for separating the participants are the nodes or the buses in the network. Thus, the power market dynamics in (3.1) can be expressed with respect to the bus like

$$\begin{aligned} \tau_{g,k}\dot{P}_{g,k} &= -b_{g,k} - c_{g,k}P_{g,k} + \rho_k \\ \tau_{d,k}\dot{P}_{d,k} &= b_{d,k} + c_{d,k}P_{g,k} - \rho_k \qquad \left(k = 1, \cdots, n_b\right) \\ \dot{E} &= \sum_{k=1}^{n_b}\left(P_{g,k} - P_{d,k}\right) \end{aligned} \tag{6.10}$$

Then, it can be seen from (6.10) that the marginal cost and the marginal benefit should be equal to nodal prices of the corresponding buses in the steady state, which means the satisfaction of the condition (6.8-a).

6.2.2 Balancing of power and energy

The condition of power/energy balancing is related to (6.8-c). If the supply is greater than the demand, $\mathbf{1}^T\mathbf{P}$ becomes positive. In the opposite case, $\mathbf{1}^T\mathbf{P}$ becomes negative. Then, (6.8-c) can be met by adding the following dynamic equation for the power/energy balancing to (6.10)

$$\dot{E} = \mathbf{1}^T \mathbf{P} \tag{6.11}$$

and by performing the control action to drive the energy imbalance E to zero. This is equivalent to the typical feedback control structure in Figure 3.1 and Figure 3.2. However, the PBO is specifically divided into the power/energy balancing and the congestion management functions in this framework. Thus, the substructure of the framework for the power/energy balancing can be represented by indicating the exact function of the block as shown in Figure 6.1.

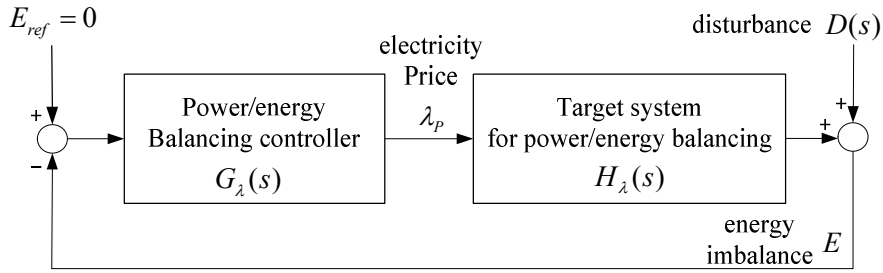

Figure 6.1 Substructure of the framework for the power/energy balancing.

Once the balancing condition is represented as a feedback control problem, the performance of the PBO is dependent on the design or tuning of the controller. The target system for the design of the power/energy balancing controller is same as the expression in (3.3) except that the different subscripts are used for indicating the buses. Thus, the disturbance $D(s)$ in (3.2) should be modified as

$$D(s) = \sum_{k=1}^{n_b} \left\{ \frac{-b_{g,k}}{s^2(\tau_{g,k}s + c_{g,k})} + \frac{-b_{d,k}}{s^2(\tau_{d,k}s - c_{d,k})} \right\} \tag{6.12}$$

and the target system $H(s)$ in (3.3) should be replaced with the target system for the power/energy balancing $H_\lambda(s)$, which is expressed as

$$H_\lambda(s) = \sum_{k=1}^{n_b} \left\{ \frac{1}{s(\tau_{g,k}s + c_{g,k})} + \frac{1}{s(\tau_{d,k}s - c_{d,k})} \right\} \tag{6.13}$$

Similar to the procedure in Chapter 3, the target system for the power/energy balancing can be represented in the case of price inelastic demand as

$$H_\lambda(s) = \sum_{k=1}^{n_b} \left\{ \frac{1}{s(\tau_{g,k}s + c_{g,k})} \right\} \tag{6.14}$$

Thus, $H_\lambda(s)$ in (6.13) or (6.14) is the target system for the design or tuning of the real-time power/energy balancing controller $G_\lambda(s)$. In other words, now that the target system is determined, the approximation methods in Chapter 3 and the design methods in Chapter 4 can be applied to the designing process of $G_\lambda(s)$.

6.2.3 Nodal prices and congestion prices

According to (6.8-b), there is a relationship between the Lagrange multipliers $\boldsymbol{\lambda_0}$ and the congestion price $\boldsymbol{\mu}$ to ensure the optimal operation, which can be re-written as

$$\hat{\mathbf{B}}^T\boldsymbol{\lambda}_\mathbf{0} + \hat{\mathbf{A}}^T\mathbf{X}^{-1}\boldsymbol{\mu} = \mathbf{0} \tag{6.15}$$

If there is no congestion, $\boldsymbol{\mu}$ is equal to $\mathbf{0}$. Then, $\boldsymbol{\lambda}_\mathbf{0}$ also becomes $\mathbf{0}$ and all the nodal prices are equal to each other from (6.9). If congestion occurs, the element of $\boldsymbol{\mu}$ corresponding to the congested line becomes positive. Let $\hat{\mathbf{B}}^T$ be expressed as

$$\hat{\mathbf{B}}^T = \begin{bmatrix} \hat{\mathbf{b}}_\mathbf{1} & \hat{\mathbf{B}}' \end{bmatrix} \tag{6.16}$$

where $\hat{\mathbf{b}}_\mathbf{1}$ is the first column of $\hat{\mathbf{B}}^T$ corresponding to the slack bus, which is a $(n_b - 1)\times 1$ vector; $\hat{\mathbf{B}}'$ is the modified line susceptance matrix composed by eliminating the row and the column of slack bus from $\mathbf{B}$, which is a $(n_b - 1)\times(n_b - 1)$ matrix. Similarly, let $\boldsymbol{\lambda}_\mathbf{0}$ be represented as a combination of the components for the slack bus and the others like

$$\boldsymbol{\lambda}_\mathbf{0}^T = \begin{bmatrix} \lambda_{\theta,1} & \hat{\boldsymbol{\lambda}}_\mathbf{0}^T \end{bmatrix} \tag{6.17}$$

where $\lambda_{\theta,1}$ is the Lagrange multiplier for the bus 1 or the slack bus; $\hat{\boldsymbol{\lambda}}_\mathbf{0}$ is a set of Lagrange multipliers associated with the equality constraint on the power flow except for the slack bus, which is a $(n_b - 1)\times 1$ vector. Then, (6.15) can be represented as

$$\lambda_{\theta,1}\hat{\mathbf{b}}_\mathbf{1} + \hat{\mathbf{B}}'\hat{\boldsymbol{\lambda}}_\mathbf{0} + \hat{\mathbf{A}}^T\mathbf{X}^{-1}\boldsymbol{\mu} = \mathbf{0} \tag{6.18}$$

Let $\hat{\boldsymbol{\lambda}}_{\mathbf{0}}$ be expressed as

$$\hat{\boldsymbol{\lambda}}_{\mathbf{0}} = \lambda_{\theta,1}\mathbf{1} + \boldsymbol{\lambda}_{\Delta} \tag{6.19}$$

where $\boldsymbol{\lambda}_{\Delta}$ the difference vector of $\hat{\boldsymbol{\lambda}}_{\mathbf{0}}$ from $\lambda_{\theta,1}$. Then, (6.18) can be arranged by substituting (6.19) into it as

$$\lambda_{\theta,1}\left(\hat{\mathbf{b}}_{\mathbf{1}} + \hat{\mathbf{B}}'\mathbf{1}\right) + \hat{\mathbf{B}}'\boldsymbol{\lambda}_{\Delta} + \hat{\mathbf{A}}^{T}\mathbf{X}^{-1}\boldsymbol{\mu} = \mathbf{0} \tag{6.20}$$

The elements of the term $\left(\hat{\mathbf{b}}_{\mathbf{1}} + \hat{\mathbf{B}}'\mathbf{1}\right)$ in (6.20) mean the sum of elements of each row of $\mathbf{B}$ except the slack bus. By definition, they are all equal to zero. Thus, (6.20) becomes

$$\hat{\mathbf{B}}'\boldsymbol{\lambda}_{\Delta} + \hat{\mathbf{A}}^{T}\mathbf{X}^{-1}\boldsymbol{\mu} = \mathbf{0} \tag{6.21}$$

If the inverse of $\hat{\mathbf{B}}'$ is pre-multiplied to (6.21), the following relationship can be derived

$$\begin{aligned} \boldsymbol{\lambda}_{\Delta} &= -\left(\hat{\mathbf{B}}'\right)^{-1}\hat{\mathbf{A}}^{T}\mathbf{X}^{-1}\boldsymbol{\mu} \\ &= -\left\{\mathbf{X}^{-1}\hat{\mathbf{A}}\left(\hat{\mathbf{B}}'\right)^{-1}\right\}^{T}\boldsymbol{\mu} \end{aligned} \tag{6.22}$$

where $\mathbf{X}^{-1}\hat{\mathbf{A}}\left(\hat{\mathbf{B}}'\right)^{-1}$ is the power transfer distribution factor (PTDF) except for the assigned slack bus [36], and the dimension of it is $n_l \times \left(n_b - 1\right)$. The variable $\lambda_{\theta,1}$ is equivalent to the price information λ_0 in Chapter 5 in that $\lambda_{\theta,1}$ only shifts the value of λ_P and does not affect the optimal condition. Thus, if it is assumed that there is no available price information, zero can be

assigned to $\lambda_{\theta,1}$ for simplicity. Then, from (6.9), (6.17), (6.19), and (6.22), the optimal nodal prices can be determined as

$$\begin{aligned}\boldsymbol{\rho} &= \begin{bmatrix}\rho_1 \\ \hat{\boldsymbol{\rho}}\end{bmatrix} = \lambda_P \mathbf{1}_{n_b} + \begin{bmatrix}\lambda_{\theta,1} \\ \hat{\boldsymbol{\lambda}}_{\boldsymbol{\theta}}\end{bmatrix} = \lambda_P \mathbf{1}_{n_b} + \begin{bmatrix}0 \\ \boldsymbol{\lambda}_{\boldsymbol{\Lambda}}\end{bmatrix} \\ &= \begin{bmatrix}\lambda_P \\ \lambda_P \mathbf{1}_{n_b-1} - \left\{\mathbf{X}^{-1}\hat{\mathbf{A}}\left(\hat{\mathbf{B}}'\right)^{-1}\right\}^T \boldsymbol{\mu}\end{bmatrix} = \lambda_P \mathbf{1}_{n_b} - \mathbf{S}^T \begin{bmatrix}0 \\ \boldsymbol{\mu}\end{bmatrix}\end{aligned} \tag{6.23}$$

where $\mathbf{S} = [\mathbf{S_1}\ \mathbf{S_2}\ \cdots\ \mathbf{S_{n_b}}] = [S_{l,k}]$ is a $n_l \times n_b$ matrix of power transfer distribution factors, which consists of the elements $S_{l,k}$ defined as the sensitivity of the power flow in the line l to the net amount of power generation or consumption at the bus k.

By examining the form of (6.23), $(-\mathbf{S}^T\boldsymbol{\mu})$ can be considered as a disturbance added to the controller output λ_P in view of the control engineering. This interpretation is used in the composition of the substructure for the relationship between the nodal prices and the congestion prices, which is shown in Figure 6.2. Different from Figure 6.1, the target system $H_\lambda(s)$ and disturbance $D(s)$ are not represented as separate blocks for simplicity in Figure 6.2 since the focus of Figure 6.2 is on the composition of nodal prices, not on the representation of the electric power system. Consequently, the optimal condition in (6.8-b) can be satisfied by subtracting the congestion price multiplied by PTDF from the nodal price of the slack bus.

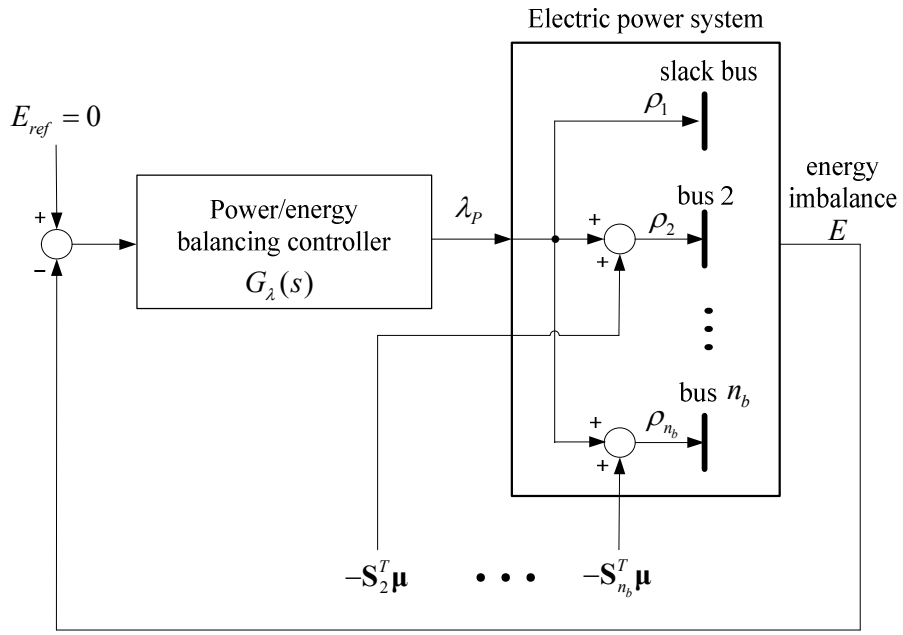

Figure 6.2 Substructure of the framework for the relationship between the nodal prices and the congestion prices.

6.2.4 Line congestion management

The management of line congestions can also be represented as a feedback control problem. However, the congestion management controller is individually assigned to each line so that the number of feedback control structure should be equal to the number of the transmission lines. For the line l, the congestion price μ_l is designated as the output of the congestion management controller, and the output of the system becomes the variation of power flow due to the congestion price. Contrary to the fact that the reference is always set to zero for the power/energy balancing, the reference of the

congestion management controller is conditional and time-varying. The term 'conditional' means that the reference is set to zero in the normal situation without congestion, but it changes into the difference between the maximum power flow limit and the part of actual power flow induced by λ_P. The term 'time-varying' indicates that the reference varies because the part of actual power flow induced by λ_P changes in time. Then, the role of the controller for managing the line congestion becomes equivalent to reducing the actual power flow over the maximum flow limit by generating the appropriate congestion price μ_l. Let $P_{f,l}^{\lambda}$ and $P_{f,l}^{\mu}$ denote the part of power flow the in line l induced by λ_P and μ_l, respectively. Then, when there occurs the congestion, the error input into the congestion management controller becomes

$$\left(P_{f,l}^{\max} - P_{f,l}^{\lambda}\right) - P_{f,l}^{\mu} \tag{6.24}$$

where the terms within the parenthesis constitute the time-varying reference mentioned above.

The target system for the design of the congestion management controller can be determined from (6.13) or (6.14). In the process from μ_l to $P_{f,l}^{\mu}$, the multiplication by the negative PTDF occurs at first to convert μ_l into the nodal prices as shown in (6.23) and Figure 6.2. This induces the variation of power injection at each node by the transfer function in (6.13) or (6.14). Finally, the variation of power injection is multiplied by the corresponding element of PTDF again, and the result value transfers into the variation of

power flow in the line *l*. Thus, the target system for managing the congestion in the transmission line *l* can be represented as

$$H_{\mu,l}(s) = \sum_{k=1}^{n_b} \left\{ \frac{-S_{l,k}^2}{\tau_{g,k}s + c_{g,k}} + \frac{-S_{l,k}^2}{\tau_{d,k}s - c_{d,k}} \right\} \tag{6.25}$$

For inelastic demand to price, it can be written as

$$H_{\mu,l}(s) = \sum_{i=1}^{n_b} \left\{ \frac{-S_{l,k}^2}{\tau_{g,k}s + c_{g,k}} \right\} \tag{6.26}$$

The negative signs before $S_{l,k}$ in (6.25) and (6.26) mean that the positive congestion price needs to be generated when the power flow is greater than the maximum power flow limit, that is, when the input to the congestion management controller is negative. This configuration of the feedback control problem for managing the congestion in the line *l* is shown in Figure 6.3.

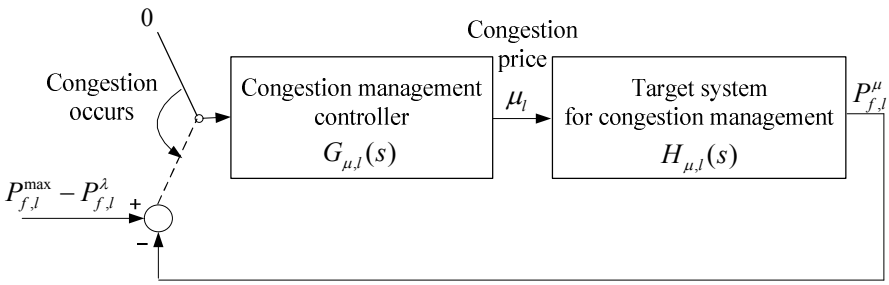

Figure 6.3 Substructure of the framework for the management of line congestion.

As described in Chapter 3 and Chapter 4, the appropriate design of the congestion management controller also can be determined by; firstly, approximating the target system in (6.25) or (6.26) into a system with a simple form; secondly, applying the controller tuning rule to the approximate system. However, by comparing (6.25) and (6.26) with (6.13) and (6.14), it can be seen that the target system for managing the congestion can be obtained from (6.13) and (6.14) by eliminating the integrator and multiplying the negative square of the corresponding element of PTDF. Then, it seems all right that the design methods for the power/energy balancing controller as given in (4.9), (4.11), (4.16), and (4.17) may be applied also to the design of the congestion management controller. However, the target systems in (6.25) and (6.26) correspond to the first-order system in Table 4.3. Thus, it can be determined from Table 4.3 that the congestion management controller is not PID control but PI control with τ_D being equal to zero. Then, a designing rule for the congestion management controller $G_{\mu.l}(s)$ of the line l can be derived as

$$K_P = -\frac{\tau_A}{\tau_c}, \quad T_I = \min\left\{\frac{\tau_A}{c_A},\ 4\tau_c\right\}, \quad T_D = 0 \tag{6.27}$$

However, the tunings rule in Table 3 are based on the individual target system. This suggests that, when a lot of target systems are interrelated as in this framework, it can be another option to design other controllers based on one selected design of a reference controller. Thus, as a design method for the framework in the dissertation, it is proposed to select the balancing controller as the reference design since the number of the balancing controller is one and

there are a large number of congestion management controllers. Then, the basic designing rule in (4.9) can be modified for the congestion management controller $G_{\mu.l}(s)$ of the line *l* as

$$K_P = -k_L\left(\frac{c_A}{\tau_c}+\frac{\tau_A}{4\tau_c^2}\right),\quad T_I = 4\tau_c+\frac{\tau_A}{c_A},\quad T_D = 0 \tag{6.28}$$

where $k_L > 0$ is a gain factor of the congestion management controllers compared to the power/energy balancing controller, which may become another design parameter. Similarly, if τ_A / c_A is too large, e.g., $\tau_A / c_A > 10$, the basic designing rule in (4.10) can be changed as

$$K_P = k_L\left(\frac{\tau_A}{2\tau_c^2}\right),\quad T_I = 8\tau_c,\quad T_D = 0 \tag{6.29}$$

Since the derivative time for the congestion management controller is equal to zero, the modified designing rule in (4.16) or (4.17) for the congestion management controllers has the same form as (6.28) or (6.29). It should be noted that there is a minus sign before k_L because it is defined as positive. Normally, the value of $S_{l,k}^2$ in (6.25) and (6.26) is smaller than one by the definition of PTDF [36]. Thus, the value of k_L is likely to be greater than one since the proportional gain is inversely proportional to the numerator of the target system.

6.3 Overall structure of the framework

The overall structure of the proposed framework for the optimal design of the real-time PBO can be obtained by combining the sub-structures in Figure 6.1-Figure 6.3. However, some modification should be made by investigating the availability of output signals in Figure 6.3. In other words, although (6.24) may be reasonable in expression, it cannot be used in real-world applications because $P_{f,l}^{\lambda}$ and $P_{f,l}^{\mu}$ are not measurable quantities. For transforming Figure 6.3 into the form with measurable variables, the actual power flow $P_{f,l}$ should be represented as

$$P_{f,l} = P_{f,l}^{\lambda} + P_{f,l}^{\mu} \tag{6.30}$$

Then, (6.24) can be written as

$$P_{f,l}^{\max} - P_{f,l} \tag{6.31}$$

Since $P_{f,l}$ is a measurable quantity, (6.31) can be used in practical applications. Thus, the overall structure of the framework with the physically available quantities can be constructed as shown in Figure 6.4.

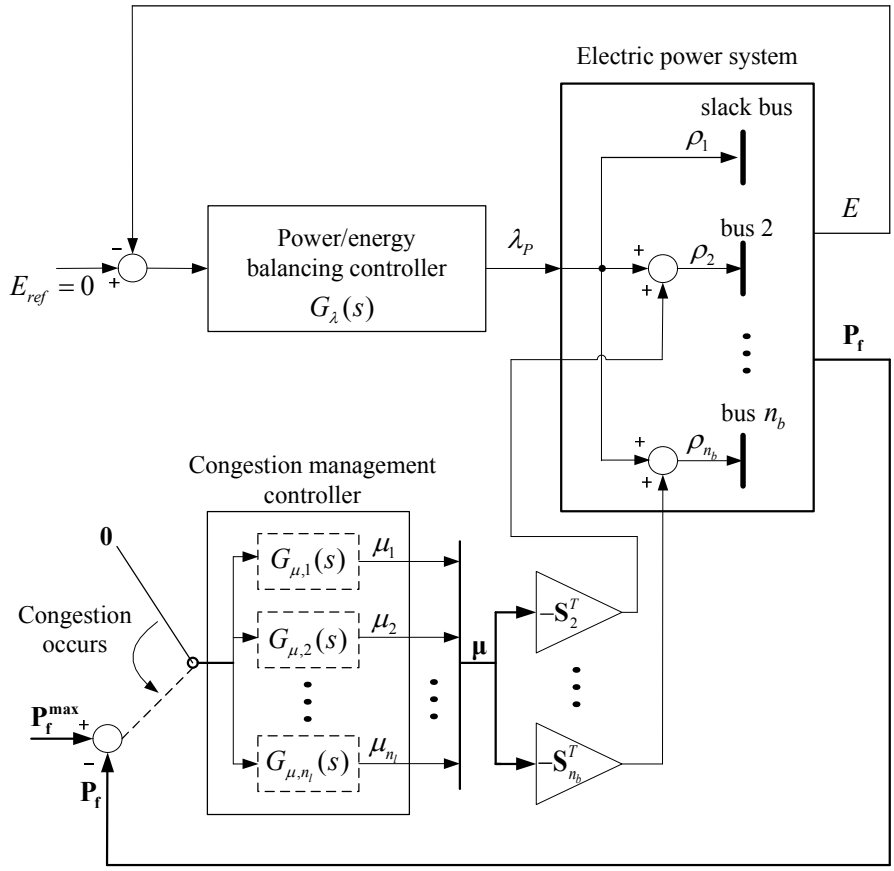

Figure 6.4 Overall structure of the framework for the optimal design of the PBO.

6.4 Example

6.4.1 Simulation settings

The proposed framework for the optimal design of the PBO is simulated and verified with a simple 6-bus network in [26], as shown in Figure 6.5. The values of line reactance of the corresponding lines are also indicated in Figure 6.5.

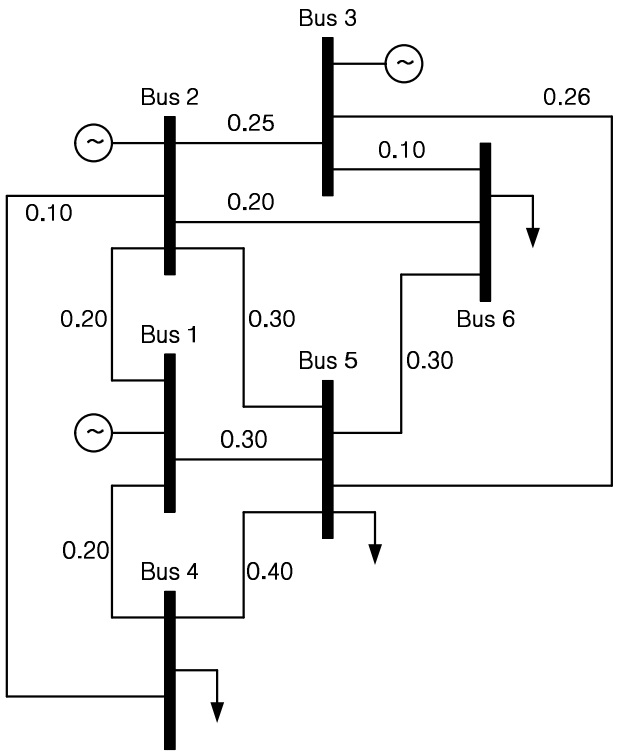

Figure 6.5 Six-bus network used in the example together with the values of line reactance [26].

Then, the line susceptance matrix **B** can be determined as follows

$$\mathbf{B} = \begin{bmatrix} 13.33 & -5 & 0 & -5 & -3.33 & 0 \\ -5 & 27.33 & -4 & -10 & -3.33 & -5 \\ 0 & -4 & 17.85 & 0 & -3.85 & -10 \\ -5 & -10 & 0 & 17.50 & -2.5 & 0 \\ -3.33 & -3.33 & -3.85 & -2.5 & 16.34 & -3.33 \\ 0 & -5 & -10 & 0 & -3.33 & 18.33 \end{bmatrix} \tag{6.32}$$

The buses 1, 2, and 3 are the generator buses, and the others are the load buses. The slack bus is assumed as the bus 1. Then, the PTDF matrix **S** can be determined as

$$\begin{array}{c} \text{bus } 1 \quad\quad 2 \quad\quad 3 \quad\quad 4 \quad\quad 5 \quad\quad 6 \\ \mathbf{S} = \begin{bmatrix} 0 & -0.4706 & -0.4026 & -0.3149 & -0.3217 & -0.4064 \\ 0 & -0.3149 & -0.2949 & -0.5044 & -0.2711 & -0.2960 \\ 0 & -0.2145 & -0.3026 & -0.1807 & -0.4072 & -0.2976 \\ 0 & 0.0544 & -0.3416 & 0.0160 & -0.1057 & -0.1907 \\ 0 & 0.3115 & 0.2154 & -0.3790 & 0.1013 & 0.2208 \\ 0 & 0.0993 & -0.0342 & 0.0292 & -0.1927 & -0.0266 \\ 0 & 0.0642 & -0.2422 & 0.0189 & -0.1246 & -0.4100 \\ 0 & 0.0622 & 0.2890 & 0.0183 & -0.1207 & 0.1526 \\ 0 & -0.0077 & 0.3695 & -0.0023 & 0.0150 & -0.3433 \\ 0 & -0.0034 & -0.0795 & 0.1166 & -0.1698 & -0.0752 \\ 0 & -0.0565 & -0.1273 & -0.0166 & 0.1096 & -0.2467 \end{bmatrix} \begin{array}{l} \text{line } 1-2 \\ \text{line } 1-4 \\ \text{line } 1-5 \\ \text{line } 2-3 \\ \text{line } 2-4 \\ \text{line } 2-5 \\ \text{line } 2-6 \\ \text{line } 3-5 \\ \text{line } 3-6 \\ \text{line } 4-5 \\ \text{line } 5-6 \end{array} \end{array} \tag{6.33}$$

It should be noted from (6.33) that the elements for the bus 1 (the first column) are all equal to zero because the bus 1 is assumed as the slack bus. The plus sign means that the increase of the power at the bus also increases the active power flow in the corresponding transmission line; the minus sign means the other way.

The generation cost functions of the buses 1, 2, and 3 are taken also from [26], which is given as

$$\begin{aligned} C_{g,1}(P_{g,1}) &= 213.1 + 11.669P_{g,1} + 0.00533P_{g,1}^2 \\ C_{g,2}(P_{g,2}) &= 200.0 + 10.333P_{g,2} + 0.00889P_{g,2}^2 \\ C_{g,3}(P_{g,3}) &= 240.0 + 20.833P_{g,3} + 0.00741P_{g,3}^2 \end{aligned} \tag{6.34}$$

The strategic coefficients of each generation are set as

$$\tau_{g,1} = 0.1, \quad \tau_{g,2} = 0.3, \quad \tau_{g,3} = 0.2 \tag{6.35}$$

The generation limits are set as

$$0 \le P_{g,1} \le 200, \quad 0 \le P_{g,2} \le 200, \quad 0 \le P_{g,3} \le 70 \tag{6.36}$$

The demand is assumed as inelastic to the electricity prices. The initial values of demand for the bus 4 ($P_{d,4}$), bus 5 ($P_{d,5}$) and bus 6 ($P_{d,6}$) before the simulation scenario are set as

$$P_{d,4} = 70, \quad P_{d,5} = 70, \quad P_{d,6} = 0 \tag{6.37}$$

The demand of the bus 6 ($P_{d,6}$) changes to 70 at the specified time defined in the simulation scenario. The unit for power is assumed as MW.

The simulation scenario with three events at the specified time instants is constructed as shown in Figure 6.6. Three events have corresponding purposes. Event I is designed to show that the power/energy balancing controller can manage a sudden power mismatch. Event II is designed to verify that the line congestion controller well manages the congestion in the framework. At last, Event III is designed to demonstrate that the multiple congestions can be handled within the proposed framework.

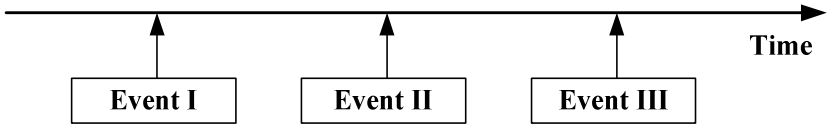

- **Event I (t=50 min)**
  - Sudden increase of demand at bus 6
- **Event II (t=100 min)**
  - Decease of maximum transfer limit in the line between bus 3 and 6 from 100MW to 30MW
- **Event III (t=150 min)**
  - Decease of maximum transfer limit in the line between bus 1 and 4 from 100MW to 20MW

Figure 6.6 Simulation scenario of the example for the verification of the framework.

Four cases of the simulation are formed according to the forms of the balancing and congestion management controllers. These cases consist of a combination of both tuned and not-tuned designs for the purpose that any design of controllers and any combination of them result in the optimal steady state once the convergence property is satisfied within the proposed framework. The parameters of the power/energy balancing controller in Case I and Case II are taken from [17, 19], which is represented as

$$G_{\lambda}(s) = 0.1 \times \left(1 + \frac{1}{10s} + 3s \right) \tag{6.38}$$

The form of the controller in (6.38) corresponds to the case without tuning for the power/energy balancing function. In Case II, the gains for the line

congestion controllers are determined from designing procedure by deciding an appropriate value of k_L. As an example of the possible selection methods for k_L, the value of k_L is determined heuristically from the values of $S_{l,k}$. To be specific, since the congestion occurs in the line from the bus 3 to 6 and the line from bus 1 to 4 as given in the scenario in Figure 6.6, the values of $S_{l,k}$ for two lines with respect to the generator buses except for the slack bus can be found in (6.33) as

$$\begin{aligned} S_{2,3-6} &= -0.77\times10^{-2}, \quad S_{3,3-6} = 0.37 \\ S_{2,1-4} &= -0.31, \qquad\quad S_{3,1-4} = -0.29 \end{aligned} \tag{6.39}$$

And then, the values of k_L for two lines are selected as the average of square values of $S_{l,k}$:

$$\begin{aligned} k_{L,3-6} &= \frac{2}{S_{2,3-6}^2 + S_{3,3-6}^2} = 14.64 \\ k_{L,1-4} &= \frac{2}{S_{2,1-4}^2 + S_{3,1-4}^2} = 10.74 \end{aligned} \tag{6.40}$$

Then, the congestion management controllers in Case II are determined by multiplying the negative of k_L to $G_\lambda(s)$ except for the derivative control as

$$\begin{aligned} G_{\mu,3to6}(s) &= -k_{L,3-6}G_\lambda(s\,|\,T_D = 0) = -1.46\times\left(1+\frac{1}{10s}\right) \\ G_{\mu,1to4}(s) &= -k_{L,1-4}G_\lambda(s\,|\,T_D = 0) = -1.07\times\left(1+\frac{1}{10s}\right) \end{aligned} \tag{6.41}$$

In Case III, only the balancing controller is designed by the tuning rule. The approximate system can be determined by the approximation method as

$$\tilde{H}(s) = \frac{1}{s(0.0562s + 0.0046)} \tag{6.42}$$

Then, the power/energy balancing controller can be determined by the basic designing rule in Chapter 4 for $\tau_c = 0.5$ minutes as

$$G_\lambda(s) = 0.11 \times \left(1 + \frac{1}{4s} + 1s\right) \tag{6.43}$$

In Case IV, both the balancing controller and the congestion management controllers are tuned. Then, similarly as the procedure for (6.41), the congestion management controllers can be composed from the balancing controller in (6.43) as

$$\begin{aligned} G_{\mu,3to6}(s) &= -k_{L,3-6} G_\lambda(s \,|\, T_D = 0) = -1.65 \times \left(1 + \frac{1}{4s}\right) \\ G_{\mu,1to4}(s) &= -k_{L,1-4} G_\lambda(s \,|\, T_D = 0) = -1.21 \times \left(1 + \frac{1}{4s}\right) \end{aligned} \tag{6.44}$$

The specific forms of the controllers of the power/energy balancing controllers and the congestion management controllers for four cases are summarized in Table 6.1.

Table 6.1 Controllers for balancing and managing congestion used in the example for the framework.

	Power/energy balancing controller $G_{\lambda}(s)$	Congestion management controllers	
		$G_{\mu,3-6}(s)$	$G_{\mu,1-4}(s)$
Case I	$0.1\times\left(1+\frac{1}{10s}+3s\right)$	$0.1\times\left(1+\frac{1}{10s}+3s\right)$	
Case II		$-1.46\times\left(1+\frac{1}{10s}\right)$	$-1.07\times\left(1+\frac{1}{10s}\right)$
Case III	$0.11\times\left(1+\frac{1}{4s}+1s\right)$	$0.11\times\left(1+\frac{1}{4s}+1s\right)$	
Case III		$-1.65\times\left(1+\frac{1}{4s}\right)$	$-1.21\times\left(1+\frac{1}{4s}\right)$

6.4.2 Simulation results

The simulation results are shown in from Figure 6.7 to Figure 6.10; the energy imbalance is in Figure 6.7; the generations at three generator buses are in Figure 6.8; the power flows both in the line 3-6 and the line 1-4 are in Figure 6.9; the nodal prices of three generator buses are in Figure 6.10. Since there is no congestion during $t \le 100$, the difference in the results is due to the power/energy balancing controller. In other words, the variation during

$t \leq 100$ in Case I and Case III are identical to Case II and Case IV, respectively. Thus, the graphs for Case II and Case IV override those for Case I and Case III, respectively, in all figures from Figure 6.7 to Figure 6.10. It can be seen from the figures that the steady-state values in all cases show the trend of approaching and converging to the same values in the framework, although the speed and the shape of convergence are all different according to the specific forms of the controllers. These converged values are verified as being equal to those from the OPF tool [54], which shows the optimality characteristic of the framework. Especially for the nodal prices, the steady-state values after three events for all cases are compared to the values from OPF method, which is represented in Figure 6.11.

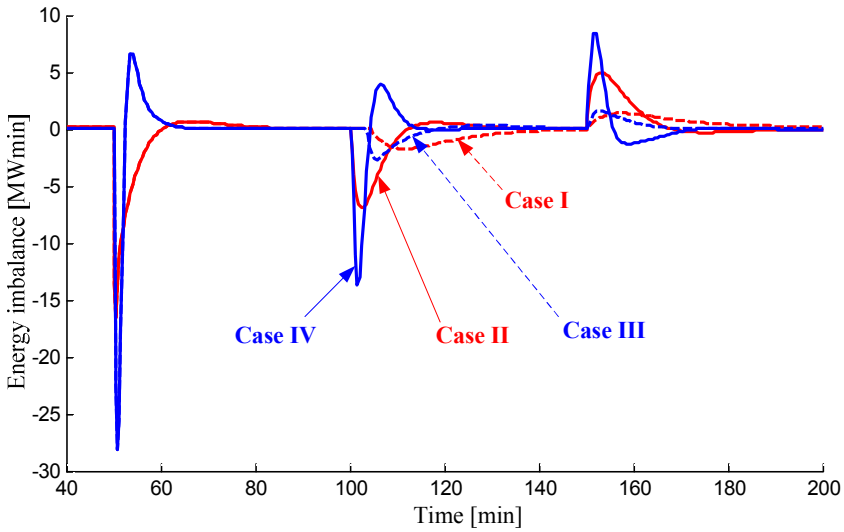

Figure 6.7 Simulation results of the example for the framework: energy imbalance.

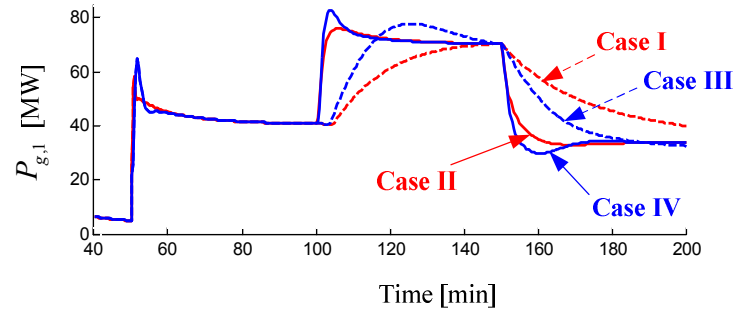

(a)

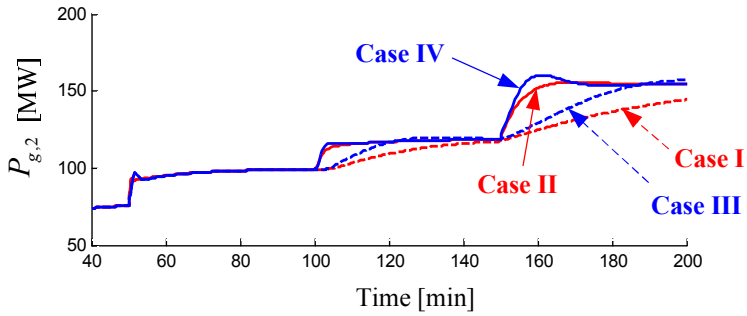

(b)

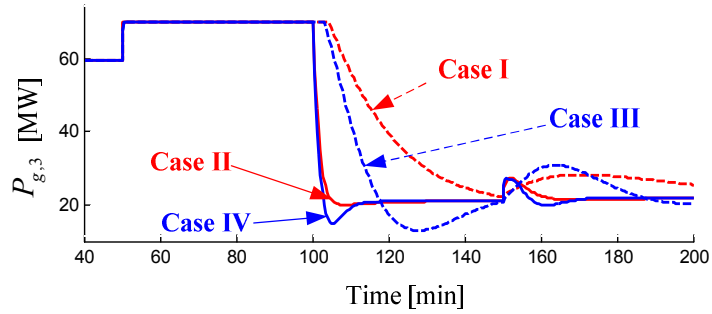

(c)

Figure 6.8 Simulation results of the example for the framework: the amount of generations. (a) Generation at bus 1. (b) Generation at bus 2. (c) Generation at bus 3.

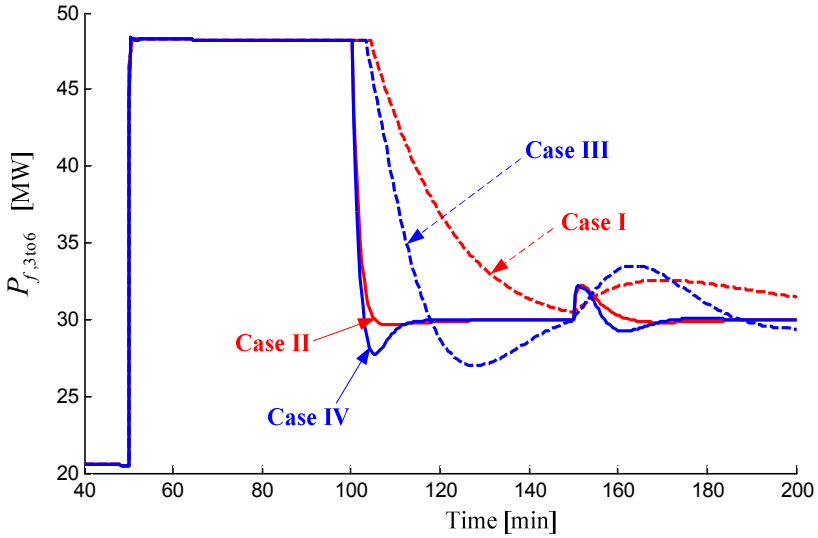

(a)

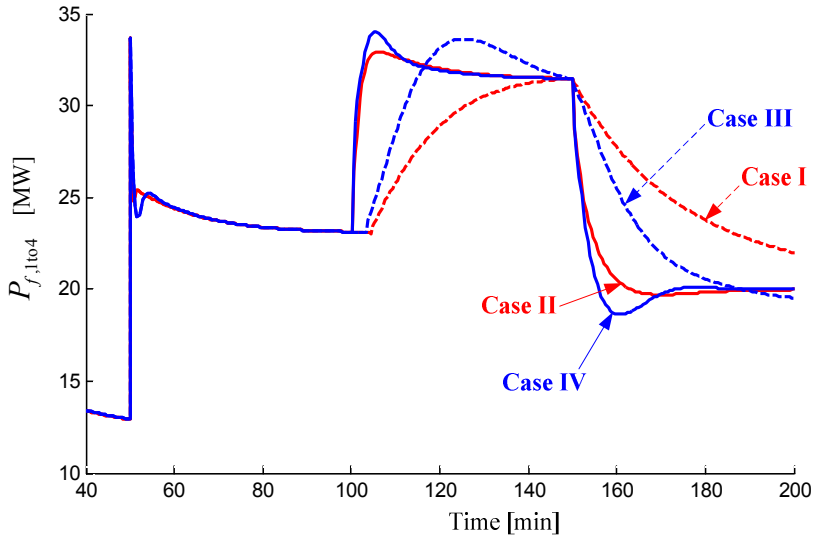

(b)

Figure 6.9 Simulation results of the example for the framework: power flows. (a) Power flow in the line from bus 3 to bus 6. (b) Power flow in the line from bus 1 to bus 4.

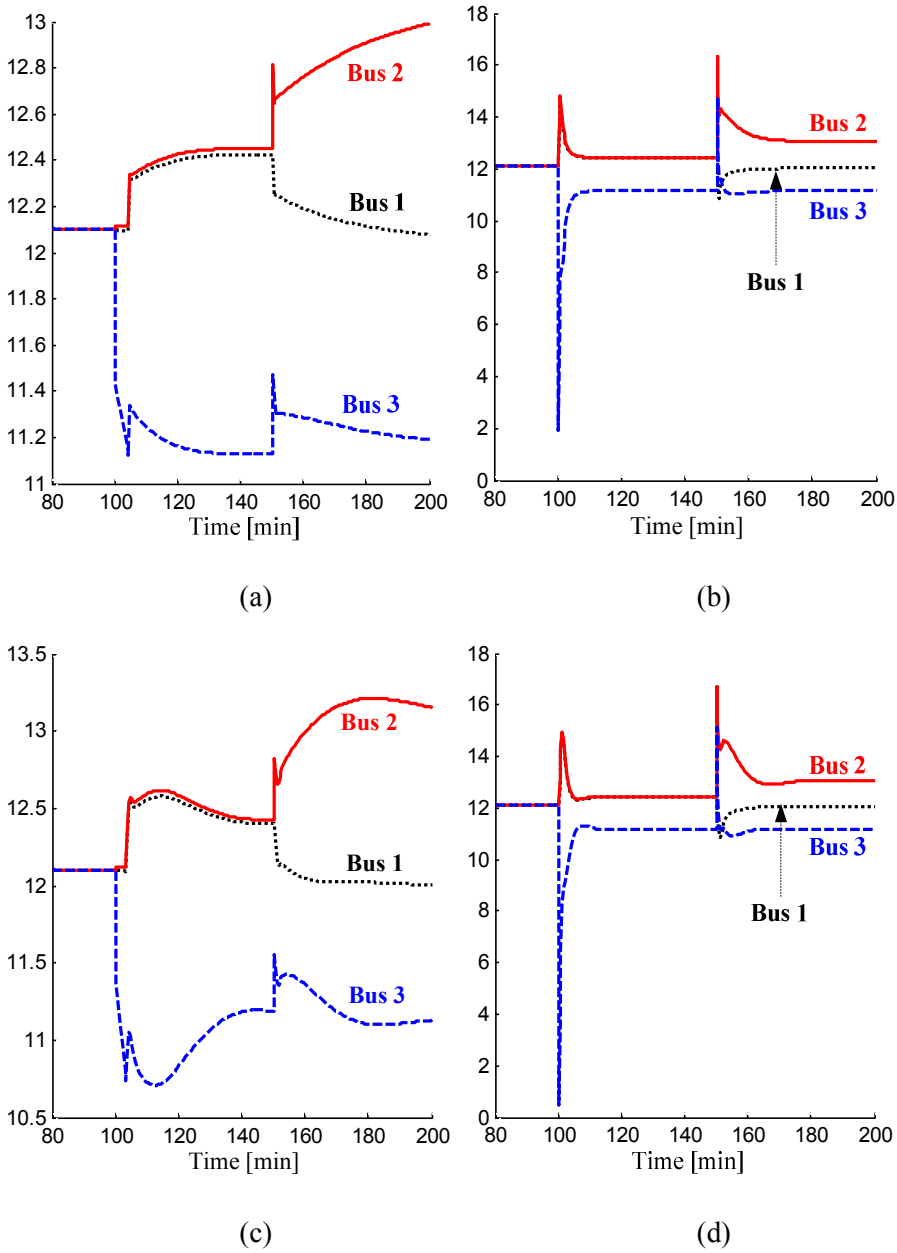

Figure 6.10 Simulation results of the example for the framework: nodal prices.

(a) Case I. (b) Case II. (c) Case III. (d) Case IV.

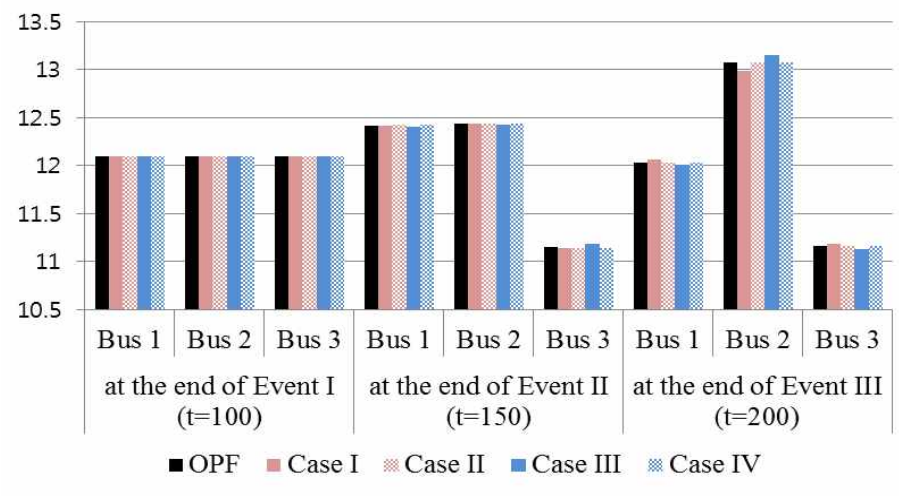

Figure 6.11 Simulation results of the example for the framework: nodal prices in the steady state compared to the optimal solution from the OPF method.

It can be seen from Figure 6.7 that, in time intervals of $100 < t \leq 150$ and $150 < t \leq 200$ with the congestion, the speed of convergence to zero for Case I and Case III is rather slower that Case II and Case III. This is due to the effects of designing the power/energy balancing controller. However, the maximum deviation of the energy imbalance for Case I and Case III without tuning of the congestion management controllers is much smaller than that for Case II and Case IV with tuning. This result is caused by the fact that congestion prices function as a disturbance to the output from the balancing controller as can be seen from Figure 6.2. Thus, the appropriately designed congestion management controllers may rather produce more severe disturbances due to the higher peak of congestion price for resolving the congestion faster. These results suggest that there should be a trade-off in

view of the frequency stability among the power/energy balancing controller and the congestion management controllers. Thus, if different organizations are in charge of the power/energy imbalance and the congestion management, close cooperation between them should be important for the stable operation of the whole power systems based on the real-time nodal prices.

It can be seen from Figure 6.9 that the violation of the power flow limit is resolved faster in Case II and Case IV than in Case I and Case III, respectively. This means that the abrupt increase in the power flow due to the unexpected situation such as a generation failure or a line trip can be handled more appropriately by designing the congestion management function. However, the faster recovery to the normal operation can be achieved at the expense of higher peak in the nodal prices at the instant of the event, which can be seen in Figure 6.10 at $t = 100$ and $t = 150$ for Case II and Case IV compared to Case I and Case III. In terms of the stable operation, the aspect of the physical power system is more important than the aspect of the economic prices. Thus, it may be more desirable, to some extent, to relieve the problematic situation of the physical power systems by inducing even rather an abrupt variation of the nodal prices.

Chapter 7. Case Study I

In this chapter, various methods described in Chapter 3 (approximation methods), Chapter 4 (designing rules), and Chapter 5 (use of price information) are simulated and verified. The simulations are based on the IEEE 39 bus network [55]. However, since the line congestion is not considered, the specific network model is not used in this case study. In other words, only the power market dynamics of the participants in the IEEE 39 bus network are used in this case study. The simulations considering the line congestion and using the specific network parameters are covered in the next chapter.

7.1 Common configuration

The common condition in the simulations for the approximation methods, the designing rules, and the use of price information is the power market dynamics. The specific simulation settings which are different from each other are given in the corresponding subsections. It is assumed that the participants consist of ten suppliers and seventeen consumers in the power market dynamics. The parameter values are taken from [23], which are given in Table 7.1. This market dynamics model is constructed by assuming that the steady-state price should be around \$40/MWh [23]. The strategic coefficients $\tau_{g,i}$

and $\tau_{d,j}$ are determined so that the ramp rate for the suppliers and the consumer should be usually within the range of 1~20 MW/min [23]. Different from the physical generators of the suppliers, there is no physical ramp rate for the consumers. However, similar ramp rates for the consumers are also assumed for the complete power market dynamics model. The values of $b_{g,i}$, $c_{g,i}$, $b_{d,j}$, and $c_{d,j}$ are assumed to be computed from the quadratic cost and benefit functions, even though the specific forms of the function are not given. The system base of the parameters is assumed as 100 MW.

Table 7.1 Parameters for the dynamic behavior of 10 suppliers and 17 consumers.

Participants dynamics					
$\tau_{g,i}$ (min)	$c_{g,i}$ ($/MW^{2}h)	$b_{g,i}$ ($/MWh)	$\tau_{d,j}$ (min)	$c_{d,j}$ ($/MW^{2}h)	$b_{d,j}$ ($/MWh)
35/60	0.8	30.00	150/60	-0.8	42.58
35/60	0.7	35.99	150/60	-0.7	43.50
25/60	0.7	35.45	150/60	-0.6	41.40
30/60	0.8	34.94	155/60	-0.6	43.13
25/60	0.8	35.94	150/60	-0.8	40.07
30/60	0.8	34.80	150/60	-0.8	42.56
30/60	1.0	34.40	155/60	-0.7	42.31
30/60	0.8	35.68	150/60	-0.6	40.95
30/60	0.8	33.36	155/60	-0.8	45.44
35/60	0.6	34.00	150/60	-0.7	41.92
			150/60	-0.7	41.73
			155/60	-0.6	41.85
			155/60	-0.6	41.34
			150/60	-0.7	40.97
			150/60	-0.7	41.97
			150/60	-0.8	41.65
			160/60	-0.7	41.98

7.2 Approximation of the target system

From (3.7) and (3.11), the approximate system for the market dynamics in Table 7.1 can be determined as

$$\tilde{H}(s) = \frac{1}{s(0.0597s + 0.0266)} \tag{7.1}$$

The unit step response of the approximate system in (7.1) is shown in Fig. 7.1. For comparison reasons, the responses of the actual system and the approximate system from the dominant pole method in [36] are also included in Fig. 7.1. Since there are seventeen participants, the actual target system in (3.3) also has a considerable number of the poles even considering the repetition of the poles. Thus, it is not sufficient to select a dominant pole, although the target system in (3.3) looks simple in its combination form. As a result, as can be seen from Figure 7.1 that the response of the proposed approximation method is considerably close to that of the actual system, and the accuracy is better than the simple dominant pole method.

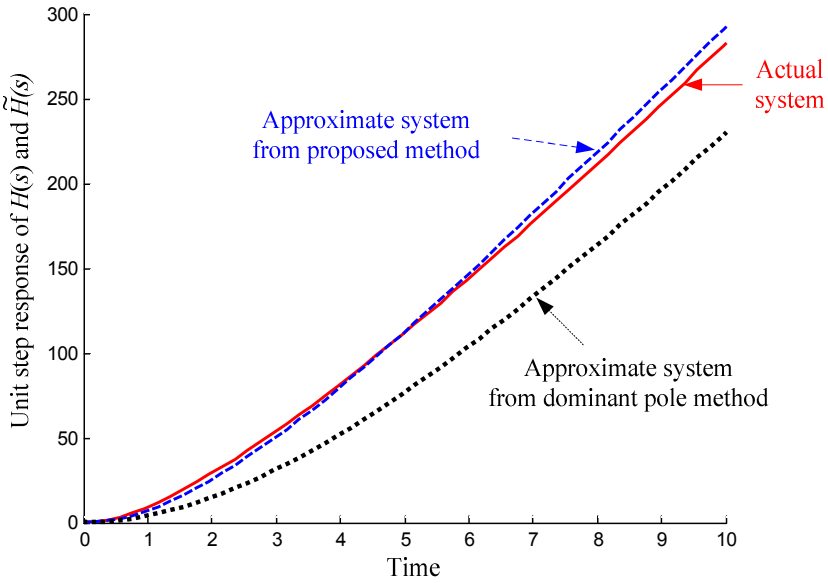

Figure 7.1 Unit step responses of the actual system and the approximate systems by the solution method and the dominant pole method.

7.3 Designing rules for the PBO

7.3.1 Simulation settings

Five cases of the price-based operation are simulated and compared. Since τ_A / c_A is equal to 2.25 and it is not a large value, the basic designing rule in (4.9) and the modified designing rule in (4.16) are used in composing the specific forms of the PBO in the simulations. Case I and Case II are determined from (4.9) for $\tau_c = 0.1$ minute and $\tau_c = 0.3$ minute, respectively. Case III and Case IV are constructed from the modified designing rule in (4.19) by adding the asymmetric damping of (4.15) for $\tau_{c,damp} = 0.05$ minute to Case I and Case II, respectively. Case V is a form of the PBO without the application of the design or tuning concept, and the parameters of the case are taken arbitrarily from [17] and [19]. The specific configurations of the PBO for each case are given in Table 7.2.

The simulations consist of two scenarios. The first one is the failure of the generation at the bus 30 (1,178 MW), which is similar to the step increase in the demand. This scenario shows the performance of the designing rules for the step change. The second one is the inclusion of small randomly changing demand. This simulation shows the performance with respect to the frequency control function. The random demand is generated every five seconds by the Wiener process so that about 99% of minute-to-minute change is within two percent of the total demand [31]. The simulations are performed with Matlab/Simulink, and the simulation time.

Table 7.2 Configuration of the PBO in the simulations for the designing rules.

		τ_c	$\tau_{c,damp}$	$G(s)$
Basic designing rule in (4.9)	Case I	0.1	-	$1.76 \cdot \left(1 + \frac{1}{2.65s} + 0.34s\right)$
	Case II	0.3	-	$0.25 \cdot \left(1 + \frac{1}{3.45s} + 0.78s\right)$
Modified designing rule in (4.16)	Case III	0.1	0.05	if $\text{sgn}(E \cdot \dot{E}) > 0$ Case I $+1.19s$ else Case I
	Case IV	0.3	0.05	if $\text{sgn}(E \cdot \dot{E}) > 0$ Case II $+1.19s$ else Case II
Without tuning	Case V	-	-	$0.1 \cdot \left(1 + \frac{1}{10s} + 3s\right)$

7.3.2 Results of a generation failure scenario

The simulation results of the generation failure scenario are shown in from Figure 7.2 to Figure 7.4. The figures are represented for a short duration around the instant of the generation failure to investigate the different shapes of variation in each case, although the simulations are performed for a sufficiently long time of 200 minutes. In the steady state, the total amount of generation (or demand) changes from 6828 MW before the generation failure to 5649 MW after the failure. Accordingly, the steady-state price also changes from \$39.43/MWh to \$39.75/MWh. Since the generation failure means the shortage of supply, the price rises to keep the balanced state, which conforms to the law of demand and supply in economics.

For Case V without any consideration of tuning, the price changes smoothly. However, the absolute maximum value of energy imbalance is the largest and the speed of the recovery to the nominal value is slower than the other cases where the proposed designing rules are used. This means that Case V requires the more capacity of AGC for the stable operation. Meanwhile, the responses in Case I show faster response than that in Case II by making τ_c smaller. However, the large gains of PID controller, which are determined from small value of τ_c, result in the oscillation of the energy imbalance, price, generation, and demand in Case I. Especially, as can be seen in Figure 7.2(a), the variation of generation in Case I is the largest. Considering the frequent small step changes in demand, this large variation is undesirable since it may put the bad effect on the physical systems such as the generators.

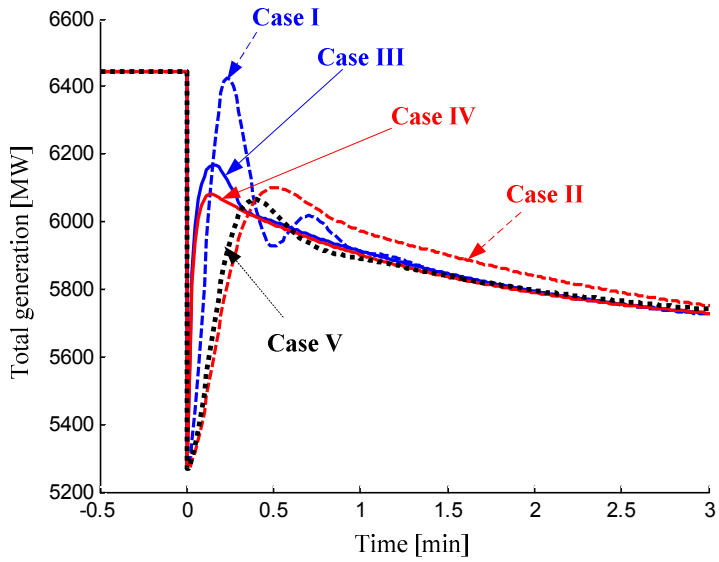

(a)

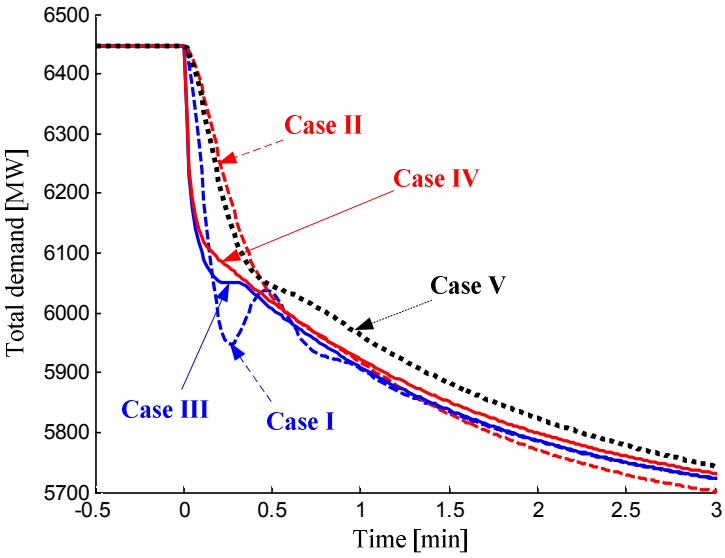

(b)

Figure 7.2 Simulation results of the generation failure scenario for designing rules. (a) Total amount of generation. (b) Total amount of demand.

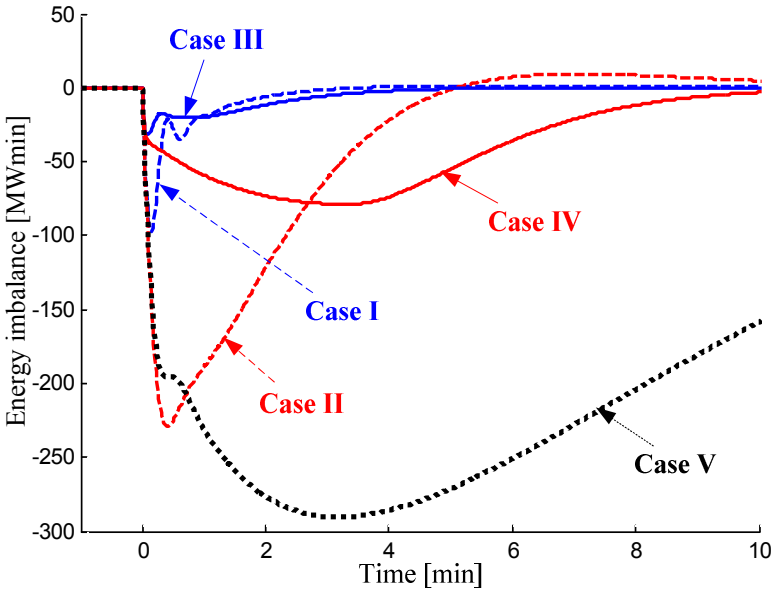

Figure 7.3 Simulation results of the generation failure scenario for designing rules: energy imbalance.

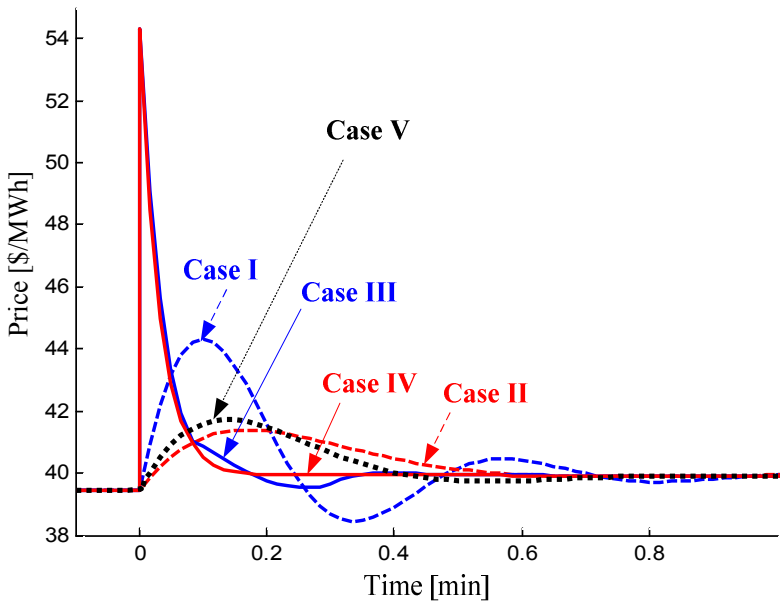

Figure 7.4 Simulation results of the generation failure scenario for designing rules: system marginal price.

For Case III and Case IV, the maximum deviation of the energy imbalance is reduced compared to Case I and Case II without the additional damping control. Actually, the maximum absolute values of the energy imbalance in each case are

$$\begin{aligned} &\text{Case I : 97.53,} \quad \text{Case II : 228.90} \\ &\text{Case III : 31.58,} \quad \text{Case IV : 78.72} \\ &\text{Case V : 290.40} \end{aligned} \tag{7.2}$$

where the unit is MWmin. It can be seen that the maximum deviation is reduced by 68% and 66% in Case III and Case IV over Case I and Case II, respectively, by using the modified designing rule with the asymmetric damping control. Moreover, the maximum absolute value in Case IV with $\tau_c = 0.3$ minute is even less than that of Case I with $\tau_c = 0.1$ minute by 21%. These results show that the addition of the asymmetric damping control not only reduces the variation of the energy imbalance, but also gives the same effect as the decrease of τ_c without causing the oscillation. As can be seen in Figure 7.4, there are price spikes in Case III and Case IV. However, it is around 38% increase from the price before the generation failure. Thus, considering the fact that the prices can rise a few times in dynamic pricing schemes such as time of use (TOU) pricing and critical peak pricing (CPP) [56], rather a high price rise in the contingency situation may not be of critical concern given the reduced variation of the energy imbalance or the enhancement of the frequency stability as in (7.2).

Finally, in order to get a feeling of the frequency deviation, the energy imbalance is translated into the frequency deviation with the relationship in

(2.5). For this purpose, the nominal frequency f_0 is set to 60 Hz. The system base of each bus is 100 MW, so that the total rating S_T can be computed as [31]

$$S_T = \sum_{k=30}^{39} S_k = \sum_{k=30}^{39} (100 \text{ MW}) = 1000 \text{ MW} \tag{7.3}$$

The inertia constants of each bus are taken from [55] and given in Table 7.3. Then, the weighted average of inertia constants H_T can be computed as [31]

$$H_T = \frac{\sum_{k=30}^{39} H_k S_k}{S_T} = 78.27 \text{ sec} \tag{7.4}$$

Then, from (2.5), the linear coefficient L_f in normal situation is determined as

$$L_f = \frac{f_0}{2H_T S_T} = 3.83 \times 10^{-4} \tag{7.5}$$

Table 7.3 Inertia constants of the 10 generator buses in the IEEE 39 bus network with respect to the system base of 100 MW.

Bus number Inertia constants (sec)				
30	31	32	33	34
42.0	30.3	35.8	28.6	26.0
35	36	37	38	39
34.8	26.4	24.3	34.5	500.0

However, in the contingency situation such as a generation failure of this case study, the generation loss should be considered in determining the values in (7.3), (7.4), and (7.5). In particular, (7.3) should be changed as

$$\hat{S}_T = \sum_{k=31}^{39} S_k = \sum_{k=31}^{39} (100 \text{ MW}) = 900 \text{ MW} \tag{7.6}$$

and (7.4) should be modified as

$$\hat{H}_T = \frac{\sum_{k=31}^{39} H_k S_k}{\hat{S}_T} = 82.30 \text{ sec} \tag{7.7}$$

where $\hat{S}_T$ and $\hat{H}_T$ are the total rating and the weighted average of inertia constants in the contingency of a generation failure. Then, the linear coefficient $\hat{L}_f$ in the contingency of a generation failure becomes

$$\hat{L}_f = \frac{f_0}{2\hat{H}_T \hat{S}_T} = 4.05 \times 10^{-4} \tag{7.8}$$

Although the frequency deviation is determined from the energy imbalance by applying $\hat{L}_f$ in the contingency, the PBO is still designed based on the normal situation. Thus, the actual frequency deviation translated from the energy imbalance is within the range between $L_f E$ and $\hat{L}_f E$. Then, the approximate values of the maximum absolute frequency deviation can be determined from (7.2) by averaging $L_f E$ and $\hat{L}_f E$, which are given as

Case I : 2.31 Hz, Case II : 5.41 Hz
Case III : 0.75 Hz, Case IV : 1.86 Hz (7.9)
Case V : 6.87 Hz

Then, the energy imbalance in Figure 7.3 can be represented as the frequency variation around the nominal frequency as given in Figure 7.5. It can be seen from (7.9) and Figure 7.5 that the frequency deviation is significant in Case II and Case V. In particular, the frequency deviation is over -5 Hz in Case II and over -6 Hz in Case V. This is because lost generation at the bus 30 is large enough to occupy around 16% of the total amount of generation before the failure.

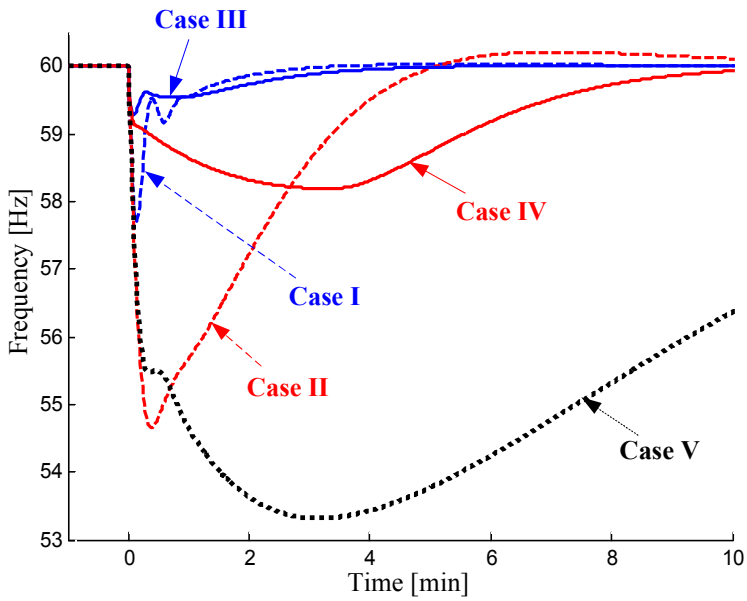

Figure 7.5 Simulation results of the generation failure scenario for designing rules: frequency computed from the energy imbalance.

7.3.3 Results of load frequency regulation scenario

In the scenario of load frequency regulation, the cumulative absolute energy imbalance for 60 minutes is determined for verifying the performance of the proposed designing rules. Due to the randomly changing demand, the average values of ten simulations are computed, and the results are as follows:

$$\begin{aligned} &\text{Case I} : 66.27, \quad \text{Case II} : 92.71 \\ &\text{Case III} : 32.56, \quad \text{Case IV} : 36.64 \\ &\text{Case V} : 84.21 \end{aligned} \tag{7.10}$$

where the unit is MWmin. The load frequency regulation corresponds to the normal situation. Thus, the results in (7.10) can be converted using L_f in (7.5) into the cumulative absolute frequency deviation as

$$\begin{aligned} &\text{Case I} : 1.52 \text{ Hz}, \quad \text{Case II} : 2.13 \text{ Hz} \\ &\text{Case III} : 0.75 \text{ Hz}, \quad \text{Case IV} : 0.84 \text{ Hz} \\ &\text{Case V} : 1.94 \text{ Hz} \end{aligned} \tag{7.11}$$

The time variation for one trial among ten are given in Figure 7.6. It can be seen from Figure 7.6 that, as the name ‘cumulative absolute value’ suggests, the values increase linearly over time. It can also be seen that the order of the performance in the frequency regulation function among the cases is maintained as same as the order in (7.10) or (7.11) from the start to the end of the simulation. This means that the cumulative absolute energy imbalance or the cumulative absolute frequency deviation is determined by the intrinsic property of the specific design of the PBO so that it can be used as the indicator of the performance in the frequency regulation function.

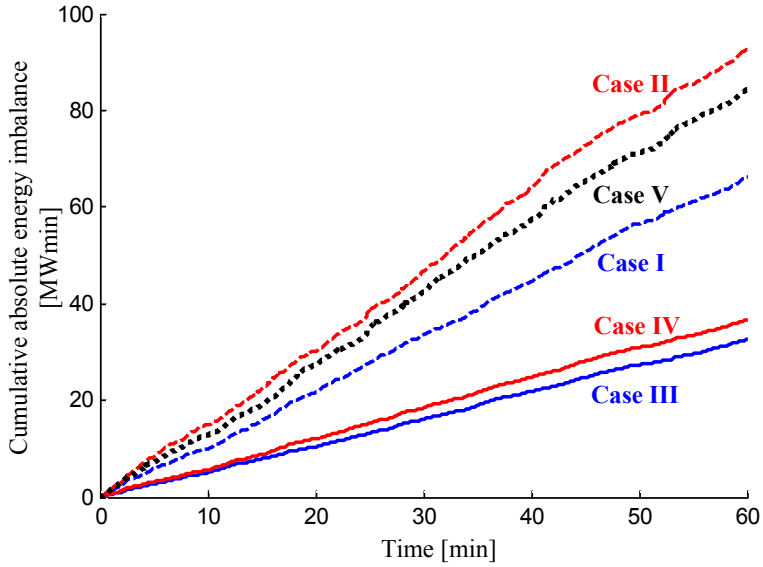

Figure 7.6 Simulation results of the frequency regulation scenario for designing rules: cumulative absolute value of the energy imbalance.

The results of Case I, Case III, and Case IV are better than that of Case V without tuning, but the result of Case II is worse even if the tuned design is applied. This can be explained by separating the price λ into the components from the proportional, integral, derivative, and additional damping controls. This is represented in Figure 7.7 and Figure 7.8 for Case II and Case IV, respectively. In order to investigate only the effect of the random demand, the component from integral control is subtracted by the steady-state price in Figure 7.7 and Figure 7.8. The values from the proportional and derivative controls are represented as they are because they are equal to zero in the steady state. It can be seen from Figure 7.7 that the component of the derivative control is dominant over the proportional and

integral components. This means that the performance of the PBO in the frequency regulation function depends mostly on the derivative control. Accidentally, it happens that the derivative gain in Case V arbitrarily selected without tuning concept, which is equal to 0.3, is a little larger than the derivative gain in Case II, which is equal to 0.19. This is the reason why the performance in the frequency regulation in Case V is better than Case II. This result implies that the basic designing rule in (4.9) or (4.11) is somewhat general to cover the various situations such as the frequent step changes. Therefore, it can be suggested that τ_c should be set as a smaller value in order to fast-tract the rapid and frequent changes in demand in the frequency regulation.

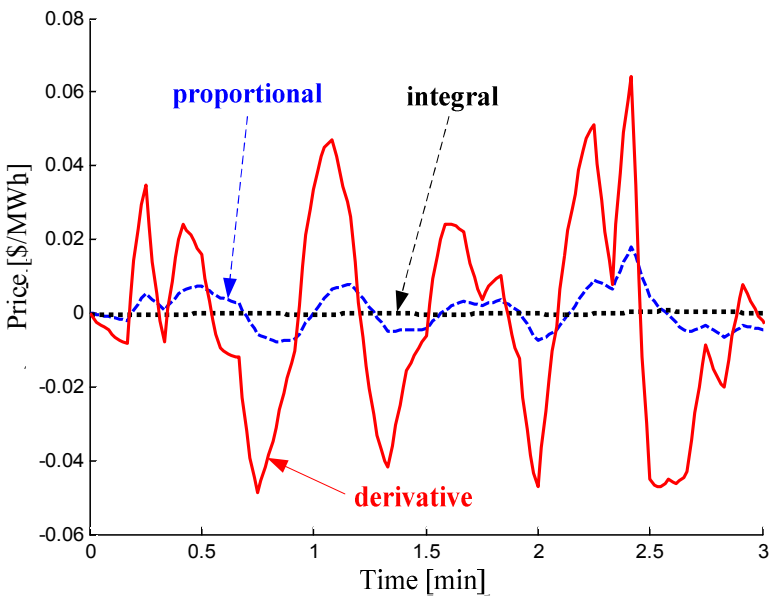

Figure 7.7 Simulation results of the frequency regulation scenario for designing rules: separated price components for Case II.

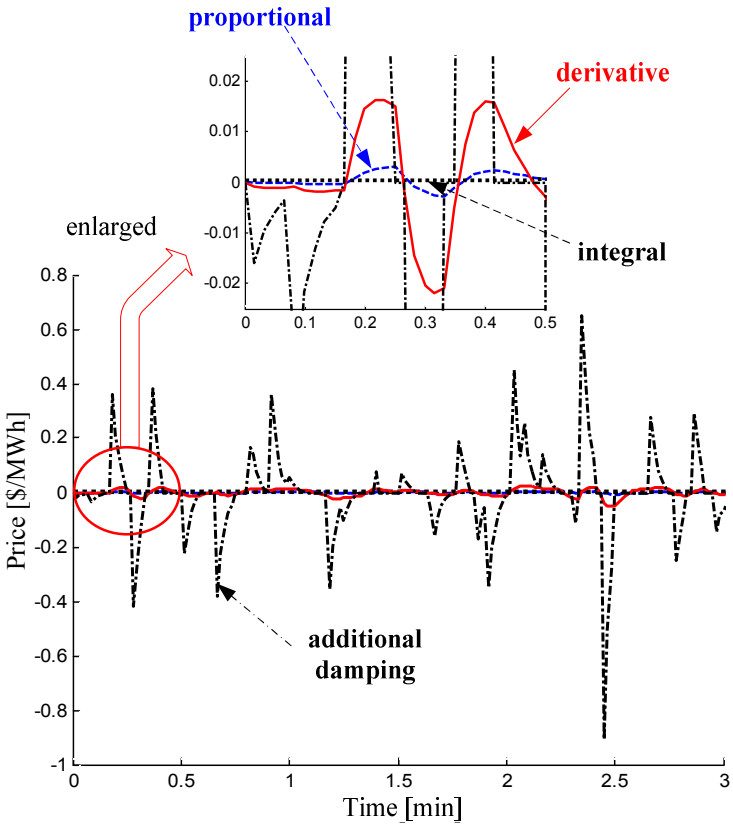

Figure 7.8 Simulation results of the frequency regulation scenario for designing rules: separated price components for Case IV.

On the other hand, as can be seen from Figure 7.8, the component from the additional damping control dominates over not only the values from the proportional and integral controls, but also the component from the basic derivative control, in the case of the modified designing rule. Since $\tau_{c,damp}$ is set to a smaller value than τ_c, the damping control augments the derivative control and improves the performance of the frequency regulation function. Actually, from the results in (7.10) or (7.11), the improvements can

be calculated as 51% and 60% for Case III and Case IV over Case I and Case II, respectively. The performance is improved by 61% and 56% for Case III and Case IV compared to Case V, respectively. Thus, the simulation results show that the modified designing rule performs much better in such a situation when the fast and frequent response is needed continuously as the load frequency regulation, rather than in the case when one sudden change happens like a generation failure or an abrupt demand change.

7.4 Effects of price information

7.4.1 Simulation settings

The effects of price information on the performance of the PBO in terms of the reduced frequency deviation can be achieved not only for well-designed PBO but also for any design without tuning, even though the performance becomes better if the PBO is appropriately designed. Thus, the designing rules are not applied to composing the forms of the PBO in this simulation. Instead, two cases are determined from [17] and [19] in a somewhat arbitrary sense, of which the specific forms of the PBO are given as

$$\begin{aligned} &\text{Case I} \ : G(s) = 0.1 \times \left(1 + \frac{1}{10s} \right) \\ &\text{Case II} : G(s) = 0.1 \times \left(1 + \frac{1}{10s} + 3s \right) \end{aligned} \tag{7.12}$$

Although various forms of the PBO are not used in the simulation, it is also investigated that the specific design of the PBO affects the performance by comparing the results of Case I and Case II.

7.4.2 Simulation results

The values of $\tilde{E}_{\max}$ with respect to the various values of λ_ε in Case I and Case II are given in Figure 7.9. The values of $\tilde{E}_{Init,\max}$ and $\tilde{E}^N_{Diff,\max}$ are determined as

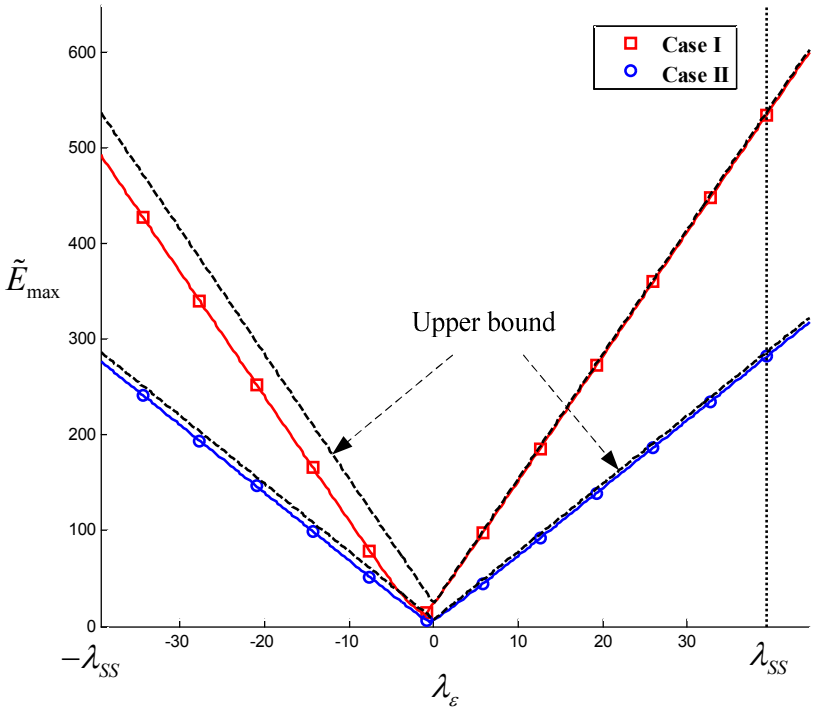

Figure 7.9 Simulation results for the effects of price information: the maximum absolute deviation of the energy imbalance ($\tilde{E}_{\max}$) in Case I and Case II together with the corresponding upper bounds.

$$\begin{aligned} &\text{Case I} : \tilde{E}_{Init,\max} = 23.90, \quad \tilde{E}^{N}_{Diff,\max} = 13.03 \\ &\text{Case II} : \tilde{E}_{Init,\max} = 7.38, \quad \tilde{E}^{N}_{Diff,\max} = 7.09 \end{aligned} \tag{7.13}$$

Then, the upper bounds of $\tilde{E}_{\max}$ in each case can be computed from (5.16), which are also represented as a dotted line in Figure 7.9.

It can be seen from Figure 7.9 that $\tilde{E}_{\max}$ shows a linear pattern in the range of $|\lambda_{\varepsilon}|$ far away from zero because of the small cancelling effect. However, due to the cancelling effect, the best price information is not zero

but $\lambda_0 = 38.43$ ($\lambda_\varepsilon = -1.00$) in Case I and $\lambda_0 = 38.98$ ($\lambda_\varepsilon = -0.44$) in Case II. To clarify the canceling effect in Case I, $\tilde{E}_{Init}(t)$ and $\tilde{E}^N_{Diff}(t)$ are shown in Figure 7.10, and the energy imbalance for some values of λ_ε are given in Figure 7.11. The best price information corresponds with $\lambda_\varepsilon = -1.00$. In that case when $\lambda_\varepsilon = -1.00$, the variation of $\tilde{E}(t)$ is evenly divided around zero so that the negative peak and the positive peak are equal to each other, as can be seen from Figure 7.11(b). If λ_ε is greater than this value, the magnitude of the positive peak becomes larger than that of the negative peak. Thus, larger positive peak increases the value of $\tilde{E}_{\max}$ for $\lambda_\varepsilon = 0$, which is the reason why $\tilde{E}_{\max}$ is not the smallest when $\lambda_\varepsilon = 0$ or when the price information is exactly equal to the steady-state price.

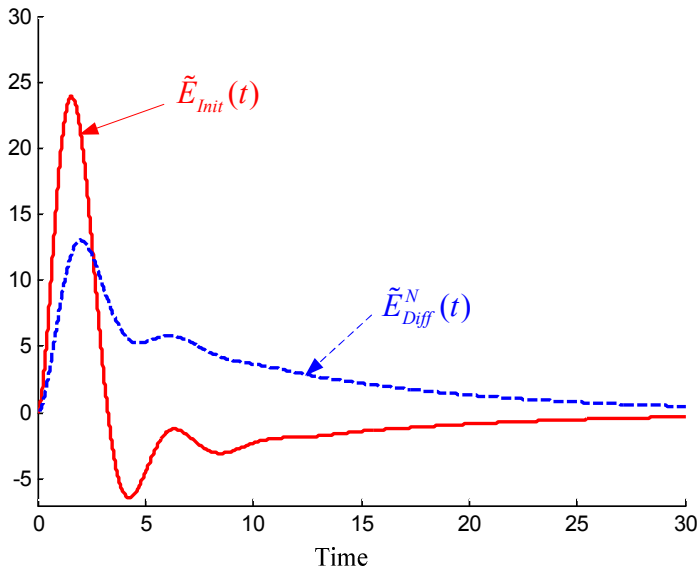

Figure 7.10 Simulation results for the effects of price information: $\tilde{E}_{Init}(t)$ and $\tilde{E}^N_{Dist}(t)$ in Case I.

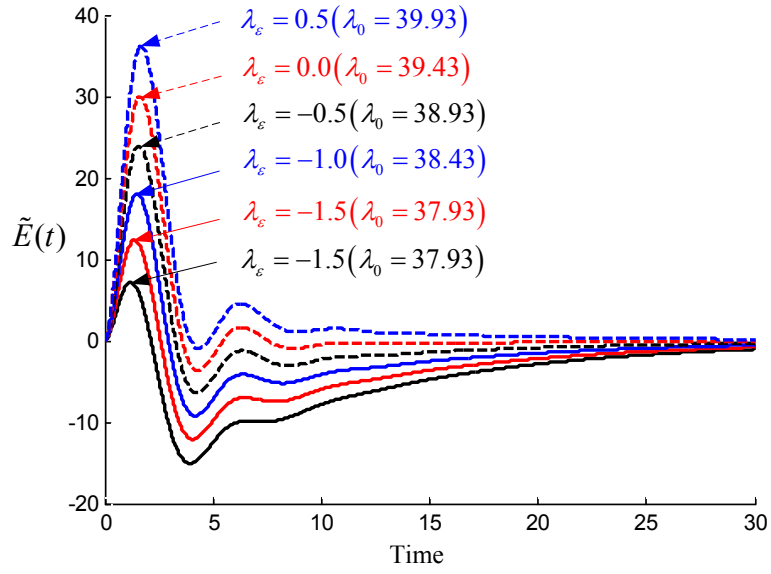

(a)

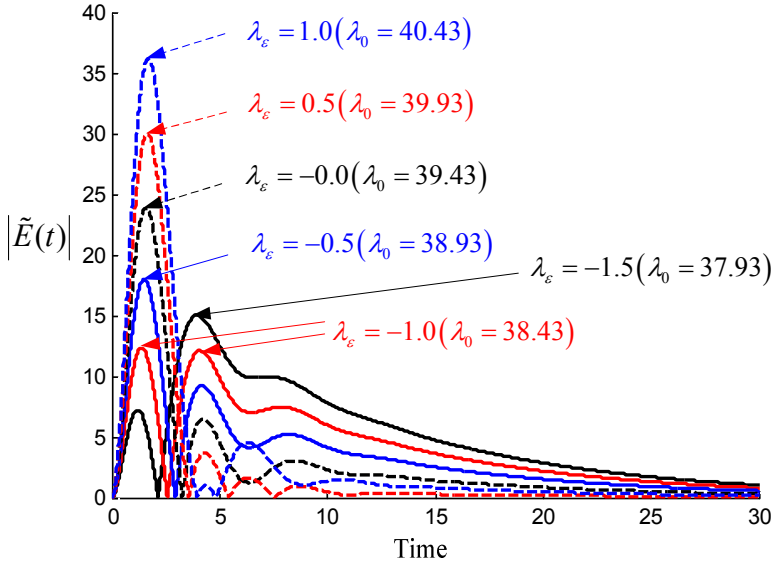

(b)

Figure 7.11 Simulation results for the effects of price information. (a) $\tilde{E}(t)$ in Case I. (b) $\left|\tilde{E}(t)\right|$ in Case I.

Lastly, quantitative analysis is done about how much the price information can reduce the energy imbalance or the frequency deviation. With the price information of $\lambda_0 = \lambda_{SS}$, $\tilde{E}_{\max}$ is reduced by 97.51% (from 492.90 to 12.28) in Case I and 98.05% (from 277.10 to 5.40) in Case II compared to the case without using the price information. When talking about available sources of the price information in Chapter 5, it is mentioned that the accuracy is around 8% and 4% error when the price information is obtained from the futures market and the forecasting technique, respectively [47, 49]. In particular, when $\lambda_\varepsilon = \pm 3.15$, which corresponds to the price information with 8% error, the improvements are

$$\begin{aligned} &\text{Case I} : 94.34\% \ (\lambda_\varepsilon = -3.15),\ 87.00\% \ (\lambda_\varepsilon = 3.15) \\ &\text{Case II} : 92.13\% \ (\lambda_\varepsilon = -3.15),\ 90.38\% \ (\lambda_\varepsilon = 3.15) \end{aligned} \tag{7.14}$$

Therefore, it can be concluded from (7.14) that considerable reduction of the energy imbalance (or the frequency deviation) can be achieved by the proposed scheme with practically available price information. Consequently, the suitable use of price information can result in the improved frequency stability of the PBO.

Chapter 8. Case Study II

In this case study, the framework for the optimal PBO with congestion management in Chapter 6 is simulated and verified. The simulations are also based on the IEEE 39 bus network [55]. However, different from the case study in Chapter 7, the line congestion is considered so that the specific network parameters need to be used in this case study. The IEEE 39 bus network is shown in Figure 8.1, in which the generations and the loads are also specified.

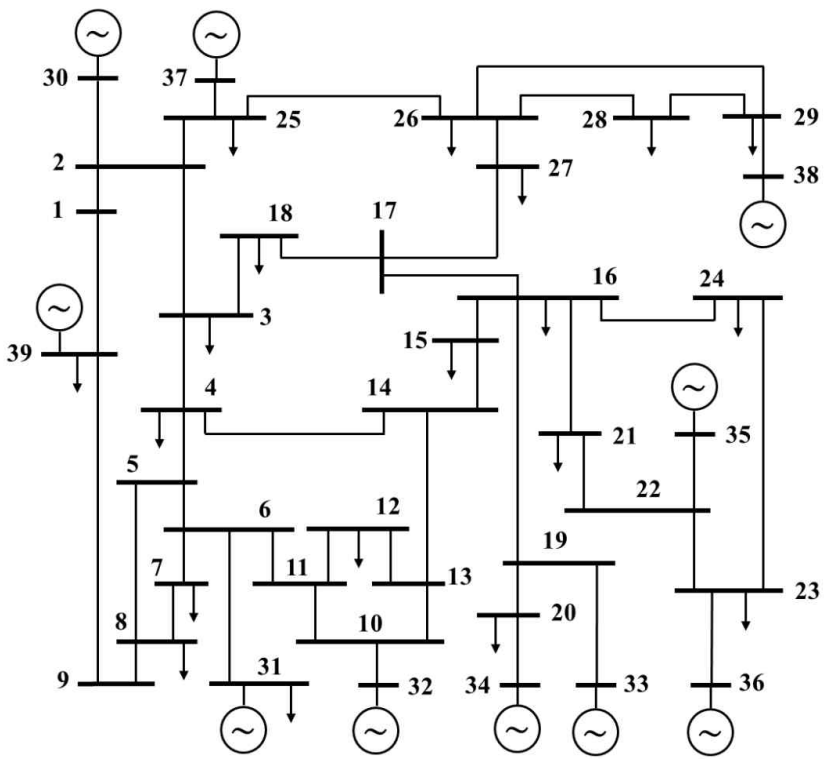

Figure 8.1 One-line diagram of the IEEE 39 bus network.

8.1 Simulation settings

8.1.1 Common configuration

The parameter values of the power market dynamics are explicitly derived from the generation cost functions. Thus, only the generation is assumed to be responsive to the prices, and the demand is assumed as the constant. The strategic coefficients, the operational coefficient for the price update, and the cost functions and are taken from [23] and [57], respectively. The system base is assumed as 100 MW. Thus, the parameters of the market dynamics are adjusted with respect to the system base, which are given in Table 8.1. A set of constant demand is the same as the data in [55], which are given in Table 8.2. The maximum generation limits at each generator bus are also taken from [55], which are given in Table 8.1. The quantities of generation in the basic case without any violation of the maximum generation limit and the maximum power flow limit are obtained from the OPF function of Matpower [54], which are given in Table 8.3. The nodal prices at all buses are equal to \$15.87/MWh in the basic case. It is assumed that there is no line resistance or line loss. The values of line reactances and the maximum power flow limits of each line are taken from [54] and [55], which are shown in Table 8.4. As stated in [55], the bus 31 is assumed as the slack bus in this case study.

Two simulation scenarios are composed. The first scenario is a generation failure at the bus 33 at $t = 0$ [58]. It results in the violation of the maximum generation limit of the bus 38. The second scenario is the tripping

of line 21-22 at $t = 0$ [59]. This one consists of three events; that is, the violation of the maximum generation limit of the bus 38, the congestion in the line 16-19, and the congestion in the line 23-24. The simulations are performed with Matlab/Simulink and Matpower [54].

Table 8.1 Parameter values of the maximum generation limits and the power market dynamics with 10 suppliers in the IEEE 39 bus network used in the simulations for the framework.

Bus	Maximum generation (MW)	τ_g (min)	c_g ($/MW^{2}h)	b_g ($/MWh)
30	350	35/60	3.86	6.9
31	650	35/60	2.22	3.7
32	800	25/60	2.08	2.8
33	750	30/60	1.76	4.7
34	650	25/60	2.56	2.8
35	750	30/60	1.88	3.7
36	750	30/60	1.98	4.8
37	700	30/60	2.26	3.6
38	900	30/60	1.42	3.7
39	1200	35/60	1.28	3.9

Table 8.2 Constant loads of the IEEE 39 bus network used in the simulations for the framework.

Bus	Load (MW)	Bus	Load (MW)	Bus	Load (MW)	Bus	Load (MW)
1	-	11	-	21	274.0	31	9.2
2	-	12	7.5	22	-	32	-
3	322.0	13	-	23	247.5	33	-
4	500.0	14	-	24	308.6	34	-
5	-	15	320.0	25	224.0	35	-
6	-	16	329.0	26	139.0	36	-
7	233.8	17	-	27	281.0	37	-
8	522.0	18	158.0	28	206.0	38	-
9	-	19	-	29	283.5	39	1104.0
10	-	20	628.0	30	-		

Table 8.3 Quantities of generation in the basic case without any violation of constraints obtained from the OPF method used in the simulations for the framework.

Bus	Generation (MW)	Bus	Generation (MW)
30	232.45	35	647.49
31	548.32	36	559.23
32	628.50	37	543.04
33	634.81	38	857.23
34	510.65	39	653.47

Table 8.4 Line reactances and maximum power flow limits of the transmission lines of the IEEE 39 bus network used in the simulations for the framework.

From bus(i)	To bus(j)	$x_{i,j}$	$P_{f,i-j}^{\max}$	From bus(i)	To bus(j)	$x_{i,j}$	$P_{f,i-j}^{\max}$
1	2	0.0411	600	14	15	0.0217	600
1	39	0.0250	1000	15	16	0.0094	600
2	3	0.0151	500	16	17	0.0089	600
2	25	0.0086	500	16	19	0.0195	600
2	30	0.0181	900	16	21	0.0135	600
3	4	0.0213	500	16	24	0.0059	600

(Continued)

Table 8.4 (Continued) Line reactances and maximum power flow limits of the transmission lines of the IEEE 39 bus network used in the simulations for the framework.

From bus(i)	To bus(j)	$x_{i,j}$	$P_{f,i-j}^{\max}$	From bus(i)	To bus(j)	$x_{i,j}$	$P_{f,i-j}^{\max}$
3	18	0.0133	500	17	18	0.0082	600
4	5	0.0128	600	17	27	0.0173	600
4	14	0.0129	500	19	20	0.0138	900
5	6	0.0026	1200	19	33	0.0142	900
5	8	0.0112	900	20	34	0.0180	900
6	7	0.0092	900	21	22	0.0140	900
6	11	0.0082	480	22	23	0.0096	600
6	31	0.0250	1800	22	35	0.0143	900
7	8	0.0046	900	23	24	0.0350	600
8	9	0.0363	900	23	36	0.0272	900
9	39	0.0250	900	25	26	0.0323	600
10	11	0.0043	600	25	37	0.0232	900
10	13	0.0043	600	26	27	0.0147	600
10	32	0.0200	900	26	28	0.0474	600
11	12	0.0435	500	26	29	0.0625	600
12	13	0.0435	500	28	29	0.0151	600
13	14	0.0101	600	29	38	0.0156	1200

8.1.2 Configuration in a generation failure scenario

Since there is no congestion in this scenario, only the power/energy balancing controller is considered. The form of the power/energy balancing controller is constructed from the basic designing rule in (4.9) or (4.11). By the solution method described in Chapter 3, the approximate target system for the power market dynamics in Table 8.3 is determined as

$$\tilde{H}(s) = \frac{1}{s(0.0527s + 0.1955)} \tag{8.1}$$

The value of $\tau_A / c_A = 0.27$ is not so large a value. Thus, the basic designing rule in (4.9) is suitable for composing the balancing controller. Three designs of the power/energy balancing controller are constructed for three values of τ_c, that is, $\tau_c = 0.2$ minute (fast), $\tau_c = 0.4$ minute (normal), and $\tau_c = 0.6$ minute (slow). The specific forms of the power/energy balancing controllers are given in Table 8.5.

Table 8.5 Three designs of the power/energy balancing controller used in the simulations of the generation failure scenario for the framework.

	τ_c (min)	Power/energy balancing controller $G_\lambda(s)$
Case A-I	0.2 (fast)	$1.31\times\left(1+\frac{1}{1.07s}+0.20s\right)$
Case A-II	0.4 (normal)	$0.57\times\left(1+\frac{1}{1.87s}+0.23s\right)$
Case A-III	0.6 (slow)	$0.36\times\left(1+\frac{1}{2.67s}+0.24s\right)$

8.1.3 Configuration in a line trip scenario

Since the congestions occur in two lines, the congestion management controllers for the corresponding lines should be designed as well as the power/energy balancing controller. The controller in Case A-II (normal) of the generation failure scenario is used as the power/energy balancing controller, which is shown again for convenience as follows:

$$G_\lambda(s)=0.57\times\left(1+\frac{1}{1.87s}+0.23s\right) \tag{8.2}$$

As the congestion management controller, three designs are composed based on the selected balancing controller. In Case B-I, the tuning concept is not applied to composing the congestion management controller so that the congestion management controller is equal to the balancing controller. In Case

B-II, the designing procedure is performed based on (6.27). The value of k_L is set to 3 for all the lines by trials and errors. Then, the congestion management controllers are determined as

$$G_{\mu,l}(s) = -k_{L,}G_{\lambda}(s|T_D = 0) = -1.71\times\left(1+\frac{1}{1.87s}\right) \tag{8.3}$$

Case B-I and Case B-II are composed in order to investigate the need for tuning of the congestion management controller separate from the balancing controller. Lastly, unit step changes of the congestion prices from zero to the OPF solutions are used in Case B-III instead of the form of PID controller. The purpose of Case B-III is to verify the optimality characteristics of the framework. Three designs for the congestion management controller are shown in Table 8.6.

Table 8.6 Three designs of the congestion management controller used in the simulations of the line trip scenario for the framework.

	k_L	Congestion management controller $G_{\mu,l}(s)$
Case B-I	1	$-0.57\times\left(1+\frac{1}{1.87s}\right)$
Case B-II	3	$-1.71\times\left(1+\frac{1}{1.87s}\right)$
Case B-III	-	$\mu_{16-19} = 0.11u(t)$ $\mu_{23-24} = 4.43u(t)$

8.2 Simulation results

8.2.1 Results of a generation failure scenario

The simulation results of the total amount of generation, the energy imbalance, and nodal prices are shown in Figure 8.2. The same nodal prices are provided to all the buses because of no congestion, which change from \$15.87/MWh before the failure to \$17.41/MWh after the failure. Naturally, it can be seen from Figure 8.2 that the shapes of variation in the total generation, the energy imbalance, and the nodal prices are different according to the design of the balancing controller in the framework. In particular, high rise in the prices at the instant of the failure results in faster recovery of the total generation and the energy imbalance to the normal states. Thus, it can be stated that there is a trade-off between the recovery speed for the failure event and the peak rise in the nodal prices incurred from the recovery process. As another aspect, it is necessary to investigate the results in Case A-I. Although the energy imbalance is the smallest, there is a small oscillation in the total generation and the price. Thus, it can be also stated that there is another trade-off between the recovery speed and the smooth change of the total generation and the energy imbalance. Consequently, the target system in (6.13) or (6.14) can be important information in the design process for deciding a suitable point between the conflicting properties of various types of trade-off.

However, it should be noted that the focus of the simulation in this case study is not on good-and-bad of a certain design, but on the fact that any design can be used in the proposed framework for the optimal PBO once it

guarantees the convergence. In other words, the steady-state values in the framework are equal to the optimal solution of the OPF method. Actually, the total generation becomes equal to the constant total demand; the price converges to the new steady-state price of $17.41/MWh; the energy imbalance converges to zero; for all three designs of the balancing controllers. Thus, it can be suggested that the framework can be generally used with any design of the PBO and it can satisfy the optimality conditions at the same time.

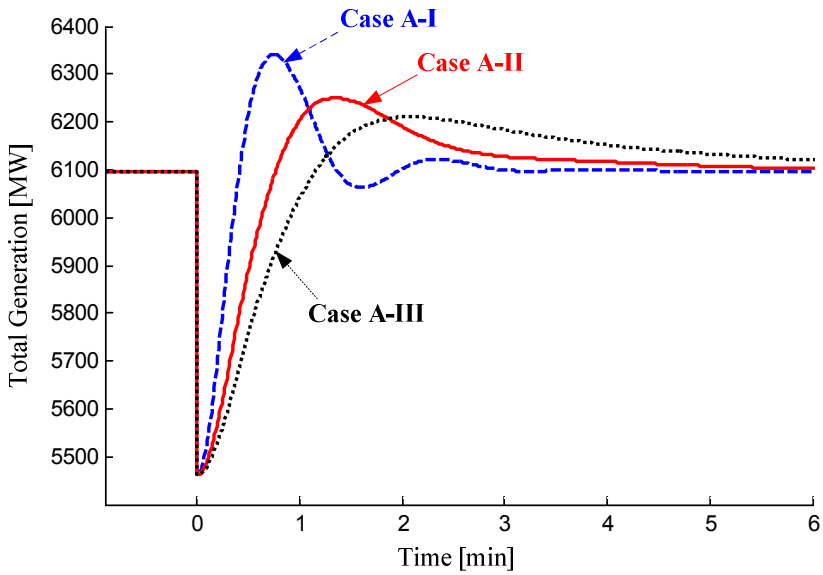

(a)

Figure 8.2 Simulation results of the generation failure scenario for the framework. (a) Total amount of generation.

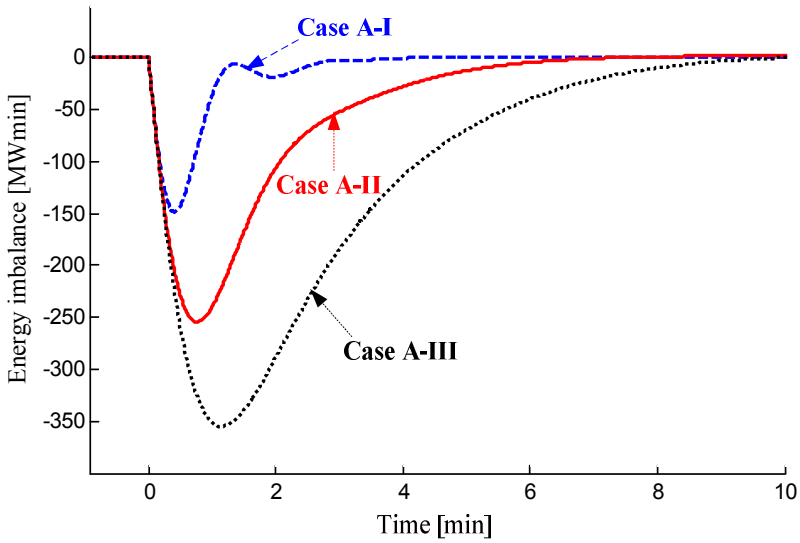

(b)

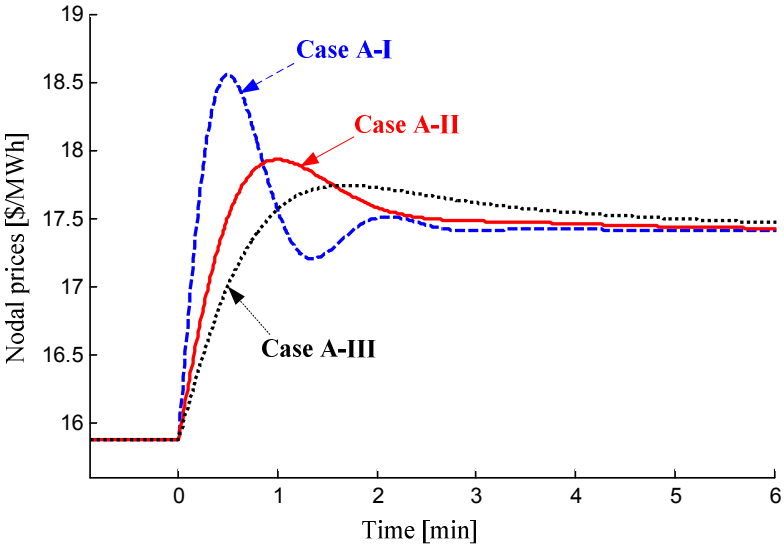

(c)

Figure 8.2 (Continued) Simulation results of the generation failure scenario for the framework. (b) Energy imbalance. (c) Nodal prices.

8.2.2 Results of line trip scenario

The simulation results are shown in from Figure 8.3 to Figure 8.6; the amount of generation is in Figure 8.3; the energy imbalance is in Figure 8.4; power flows both in the line 19-16 and the line 23-24 are in Figure 8.5; congestion prices for two congested lines of 19-16 and 23-24 are in Figure 8.6. Even without the event such as a generation failure, there occurs the power/energy imbalance due to the variation of generation quantities for relieving the congestion in the lines of 19-16 and 23-24. However, the imbalance is very small compared the generation failure event as shown in Figure 8.2(b).

The congestion is resolved the slowest in Case B-I. Thus, comparing Case B-II, it can be concluded that the appropriately designed congestion management controllers are needed to achieve better performance in the congestion management. Moreover, when comparing Case B-III, it can be seen that the use of simple unit step functions based on OPF solution is better than the real-time congestion management controllers which are not properly designed.

On the contrary, when Case B-II and Case B-III are compared, it cannot be certainly said that the one is superior to the other for the performance of the congestion management function. To be specific, the congestion is managed the fast in Case B-III for the line 23-24. In contrast, for the line 19-16, the time duration of the congestion management in Case B-III is equivalent to that in Case B-III. However, a variation of the power generation and the energy imbalance is larger in Case B-III than in Case B-II as shown in

Figure 8.3 and Figure 8.4, which means the more stable operation with respect to the aspect of the frequency stability. Thus, this analysis illustrates that a properly designed congestion management controller performs better than the simple application of the OPF solution.

Regardless of the comparison of the performance among the cases, it is meaningful to analyze the relationship between the power/energy balancing and the congestion management functions. The fast resolution of the congestion results from the fast variation and the high overshoot of power generation as shown in Figure 8.3, which results from the fast rise of the congestion prices as can be seen from Figure 8.6. However, the fast variation of power generation induces larger energy imbalance as can be seen from Figure 8.4. Thus, it can be noted that the better performance in the congestion management can be achieved at the expense of the energy imbalance or the frequency stability. This is a kind of trade-off between the balancing and congestion management. In other words, it is possible that each transmission system operator is individually in charge of the congestion management in the corresponding line within the framework. In addition, it is certain that each congestion management controller can be separately designed. However, if the congestion management controller is designed extremely on the aspect of managing the corresponding line, the power/energy balancing or the frequency stability can be threatened. Consequently, a policy or a rule should exist in a decentralized environment which appropriately coordinates the operation of the ISO and the TSO's.

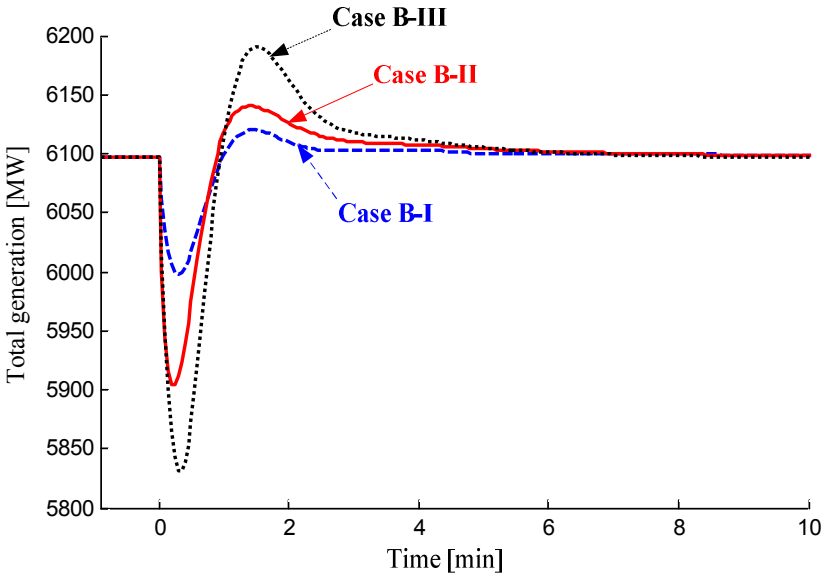

Figure 8.3 Simulation results of the line trip scenario for the framework: total amount of generation.

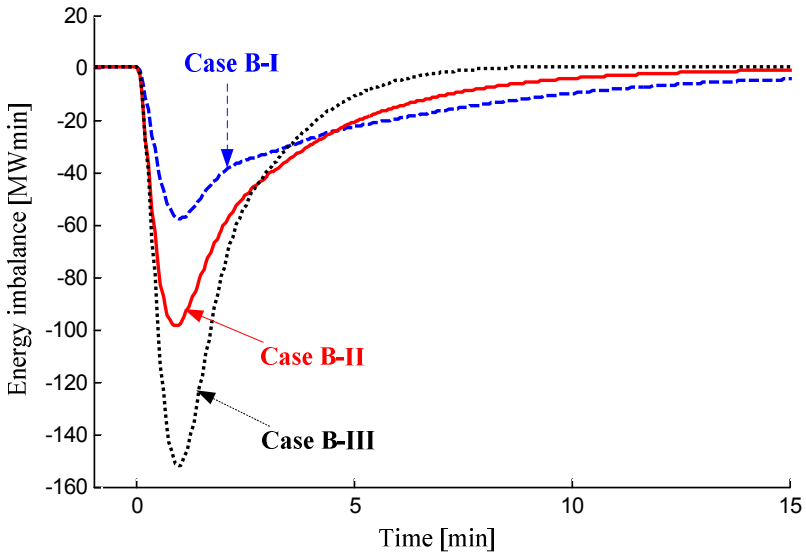

Figure 8.4 Simulation results of the line trip scenario for the framework: energy imbalance.

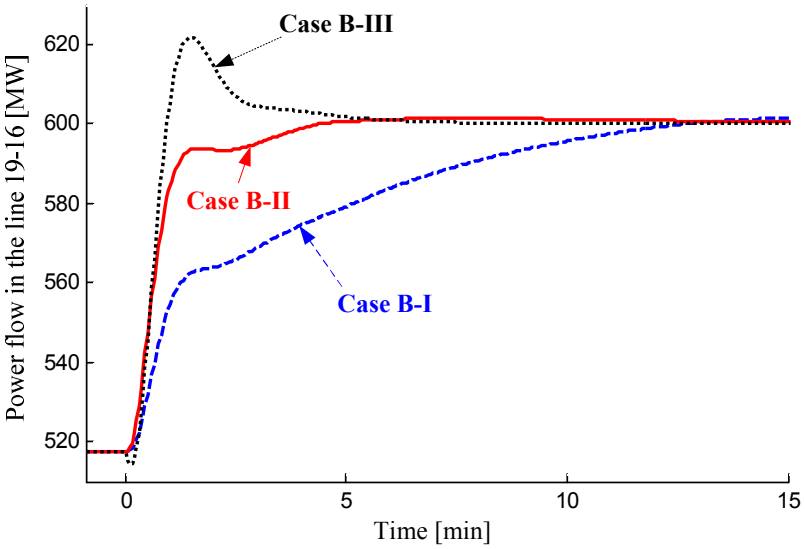

(a)

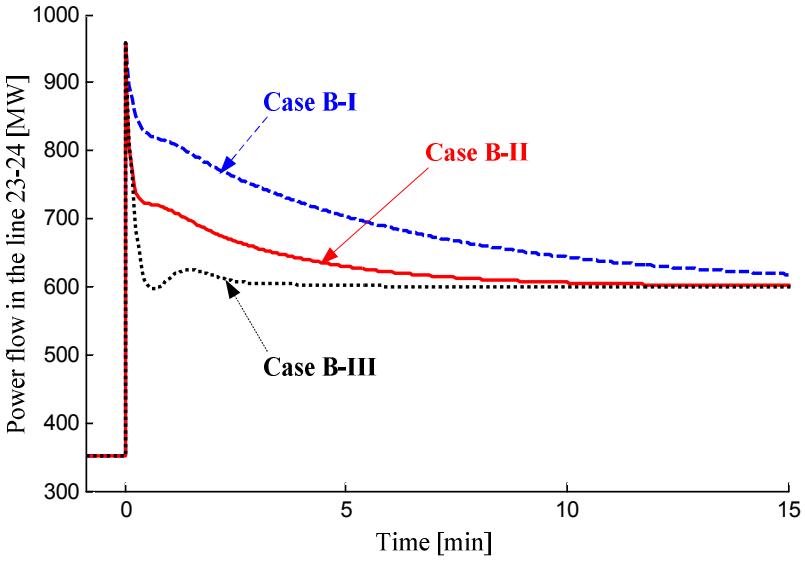

(b)

Figure 8.5 Simulation results of the line trip scenario for the framework. (a) Power flow in the line 19-16. (b) Power flow in the line 23-24.

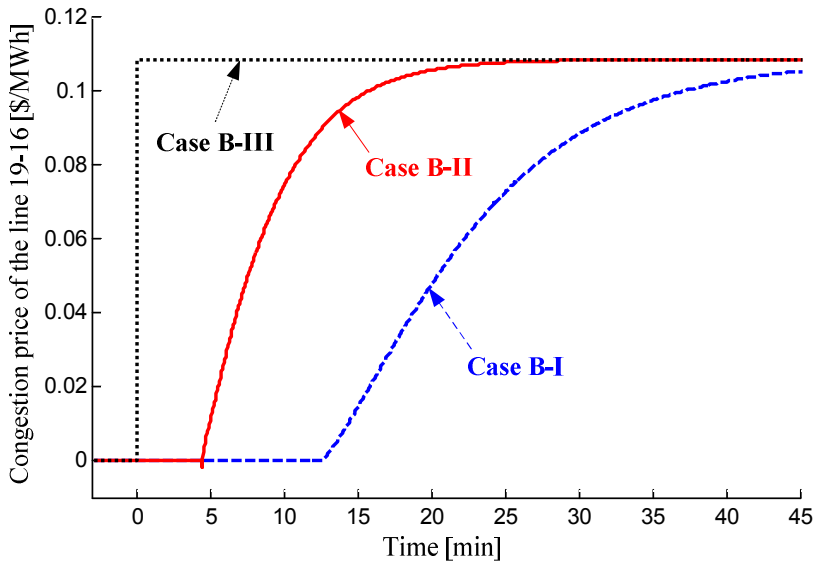

(a)

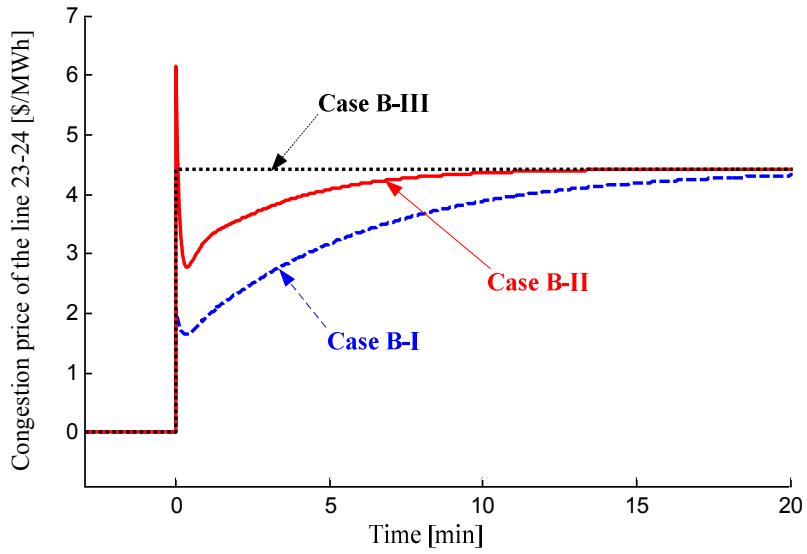

(b)

Figure 8.6 Simulation results of the line trip scenario for the framework. (a) Congestion prices of the line 19-16. (b) Congestion prices of the line 23-24.

The big difference of the framework from the OPF method can be seen from Figure 8.6(a). Since the framework is based on the real-time feedback control mechanism, the congestion prices of the line 19-16 begin to increase from zero right after the moment of the congestion, which is $t = 12.66$ minutes in Case B-I or $t = 4.43$ minutes in Case B-II, compared that the congestion prices jump from zero to the OPF solution at $t = 0$ in Case B-III. This is because, in the OPF method of Case B-III, only the final values in the steady state can be found and the exact time instant when the congestion occurs cannot be known in advance. Thus, the framework is very suitable for the real-time power system operation.

Similar to the generation failure scenario, the focus of the framework is not only on the performance of the specific design, but also on the convergence characteristics compared to the optimal solution. Firstly, the total generation becomes equal to the constant total demand in all three cases as shown in Figure 8.3. Secondly, the energy imbalance returns to zero as shown in Figure 8.4. The congestion prices of the line 19-16 and 23-23 converge to \$0.11/MWh and \$4.43/MWh, respectively, which are equal to the values from the OPF method. Both nodal prices at all buses and the generation quantities at ten generator buses converge also to the OPF solution. This result is shown in the selected buses of 31 and 35 in Figure 8.7 and Figure 8.8, respectively. It should be noted from the figures that, although the variation differs in shape with respect to the design of the congestion management controllers, they converge to the same optimal solution from the OPF method in all three cases.

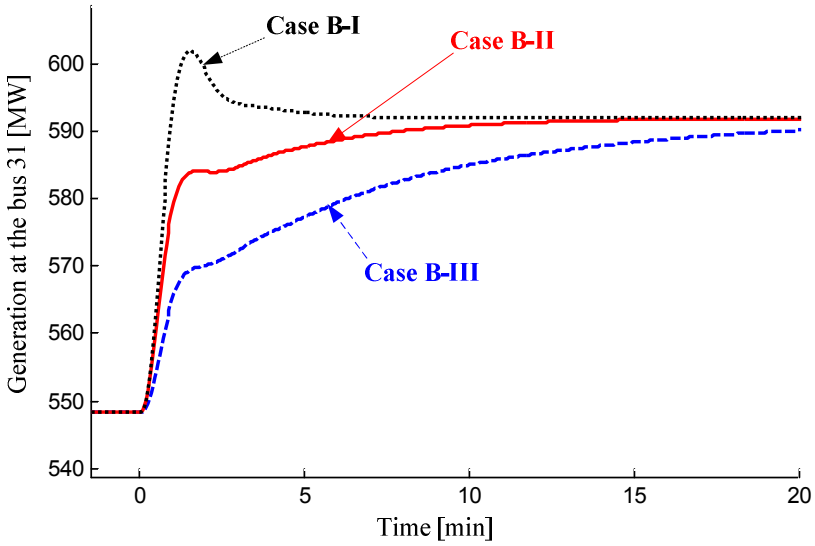

(a)

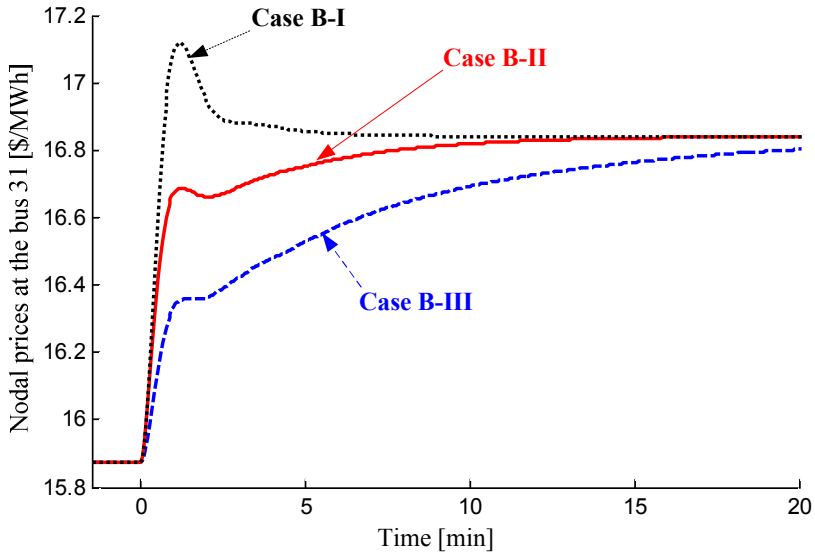

(b)

Figure 8.7 Simulation results for the selected bus of 31 of the line trip scenario for the framework. (a) Power generation. (b) Nodal prices.

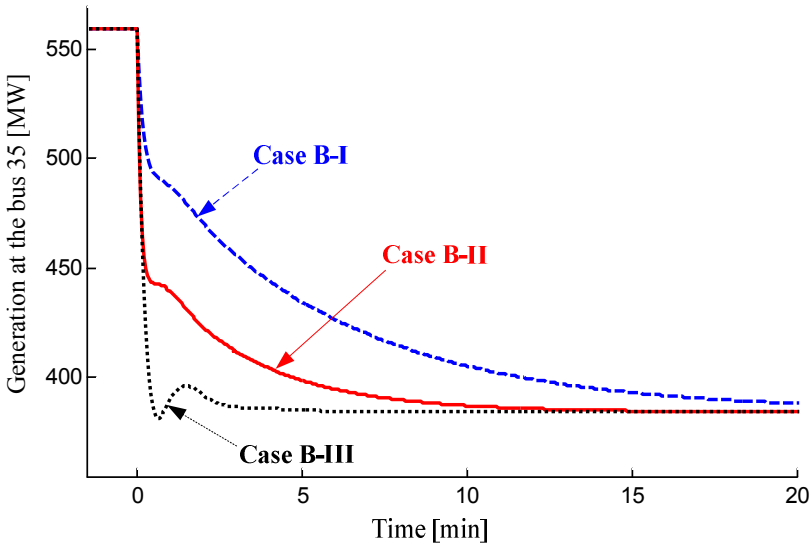

(a)

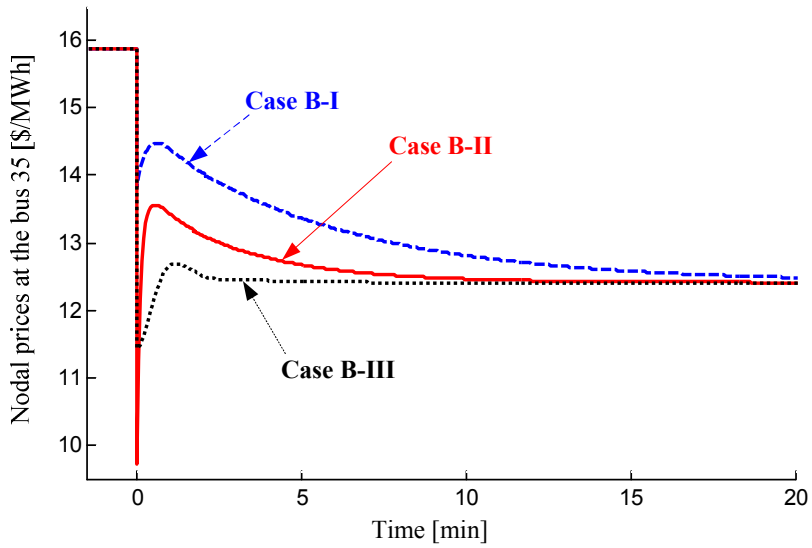

(b)

Figure 8.8 Simulation results for the selected bus of 35 of the line trip scenario for the framework. (a) Power generation. (b) Nodal prices.

Chapter 9. Conclusions and Future Works

9.1 Conclusions

The objectives of the power system operation are to balance the power, maintain the system frequency to the nominal value, and to manage the line congestion. Not to speak of the existing schemes for the power system operation, the price-based operation, which is proposed as an alternative to the centralized ones in a decentralized and deregulated environment, should satisfy those objectives. It is the most important task in the PBO to determine the appropriate electricity prices. Thus, analyzing and designing methods for the PBO is necessary to guide the determination of the price signals and to provide insights for the dynamic results. Despite the considerable number of previous researches on analyzing and designing the PBO, it has not sufficiently been handled to apply design concept considering the dynamic performance in view of the frequency stability. Thus, various designing methods and the structures for the PBO have been presented in this dissertation.

Before presenting the specific methods for analyzing and designing the PBO, the possibility of the power market dynamics in the continuous-time domain is described. When deriving the continuous-time model of the PBO, they are assumed that there are a large number of the participants and that the superposition of the asynchronous responses of them can be approximately represented as the continuous function. And then, in the process of deriving

the designing methods for the PBO, the feedback control mechanism in the control engineering is usefully adopted. In other words, the PBO is interpreted as the controller within the feedback control structure, and then the problem of designing the PBO becomes equivalent to the familiar problem of designing or tuning the controller. After formalizing the feedback control structure for the PBO, researches on three major topics of the dissertation have been conducted based on it; that is, designing rules for the PBO without the congestion management, a method for and the effects of using the price information, and a general framework for the optimal PBO providing both the balancing and the congestion management functions. All the topics are based on the power market dynamics expressed as a set of differential equations. The power market dynamics are based on the perfect competition, and the equilibrium is determined when the marginal cost and the marginal benefit are equal to each other as same as the theory in economics.

The designing rules for the PBO are derived under the assumption of no line congestion, and derived by using the tuning rules for PID controller. Since most of the tuning rules are based on the typical system with simple forms, the approximation methods are firstly considered. By exploiting the form of the power market dynamics, an approximation method based on the definition of the time constant is composed. After determining the approximate target system, the application of a selected tuning rule results in the basic tuning rule. By supplementing an asymmetric damping control to the basic tuning rule, the modified designing rule is composed in order to enhance the dynamic characteristics for the frequency control. The modified designing

rule effectively shows the important property that a specific form of the PBO is not limited to the typical PID controller within the feedback control structure for designing the PBO. The presented designing rules are verified through the case study using the IEEE 39 bus network for two scenarios of a generation failure and frequent small changes of demand. The results show that the PBO designed by the designing rules is better than that without the application of them in view of the frequency stability. Moreover, the modified tuning rule performs even better than the basic tuning rule. It is also verified that the improvement of the frequency control is achieved by the high rise in the price, which forms a trade-off between them and should be carefully considered in the design of the PBO. From the investigation into the separate components of the price, it is identified that the component of the derivative control dominates other components at the instant of the changed situation.

As a method for further improving the dynamic performance in view of the frequency stability, a new structure for the PBO using price information as a kind of price offset is constructed. The price information can be obtained from the futures electricity market and various price forecasting methods. The effects of the price information on the maximum deviation of the energy imbalance are quantitatively analyzed. Although the exact value of the maximum deviation cannot be determined, the upper bound of it is analytically derived. The upper bound shows that the maximum deviation is likely to be reduced linearly to the difference between the price information and the system marginal price in the steady state. However, there occurs cancelling between the components forming the energy imbalance in the

vicinity of the steady-state price. Thus, it is found that the actual maximum deviation is the smallest when the price information is a little greater or less than the steady-state price, not when it is exactly equal to the steady-state price. The quantitative effects of the price information are verified through the case study using the IEEE 39 bus network. The reduction of the maximum deviation of the energy imbalance is significant, which results in the considerable improvements in the frequency stability. The use of price information gives the desirable effect regardless of whether the PBO is appropriately designed or not. However, it is shown that the maximum deviation of the energy imbalance is related to the specific design of the PBO, so that more improvement can be obtained from the suitably designed PBO. It is also verified in the case study that the actual maximum deviation is the smallest when the error of the price information is not zero.

Finally, a general framework for the optimal design of the PBO is constructed. The framework consists of the substructures derived from the optimal conditions of the OPF method. Not only that the power/energy balancing and the congestion management functions are successfully performed within the framework, but it is also guaranteed that the converged values in the steady state should be equal to the optimal solutions of the OPF method. The PBO in the framework includes the power/energy balancing controller and the congestion management controller, which generate corresponding components of the nodal prices. The framework is suitable in a decentralized environment in the sense that each congestion management controller can be separately designed and operated. The effectiveness of the

proposed framework is verified through the simple example using the 6 bus network and the case study using the IEEE 39 bus network. Two scenarios of a generation failure and a line trip are configured, and specific forms of the PBO are composed including the designed ones and the arbitrary ones in each case. The results show the fundamental property of the framework that the converged values are all equal to the optimal solution irrespective of the specific design of the PBO, even though the time variation differs by the designs. A few kinds of the trade-off in the PBO are identified such as; between the recovery speed to the normal state and the smooth change of the variables such as the nodal prices; between the power/energy balancing and the congestion management functions.

The significance of this research can be summarized as that it can give an insight over the dynamic phenomena on the aspects of both the market and the physical power systems. To be specific, the contributions can be described as follows. Firstly, a structure is constructed in which electricity prices can be generated based on the important status of the power systems such as the system frequency and the power flows. Since the method for generating the prices is not limited to a specific form, various methods can be compared within the described structure. Furthermore, a new pricing scheme as a kind of policy can be composed based on the engineering method for generating the prices, and the dynamic phenomena resulting from the pricing scheme can be predicted by the analysis of the transient behavior of the feedback control system. Secondly, the dissertation demonstrates a method for finding the relationship between the price information in the electricity market and the

physical power system operation. Thus, the basis for the reconfiguration of market structure and operation can be found from the physical power systems, and vice versa. Lastly, it suggests the way how a decentralized system should be configured and operated. In addition, the effects of the various interactions among the independent entities on the aspects of the power system operation including the frequency stability and the congestion management can be investigated within the presented framework.

9.2 Future works

The essential point from which the research in this dissertation starts is the power market dynamics. However, they are continuous functions which can hardly be implemented in the PBO in the real world. Thus, empirical further researches should be performed in order to verify that a large number of discrete asynchronous changes of both the participants' behavior and the price signal can be approximately represented as the differential equations as in the power market dynamics. In this process, the cases for abnormal behavior of the participants are also necessary to be investigated. The abnormal cases include the exercise of market power resulting from monopoly or oligopoly, and cheating or gaming contrary to the actual cost/benefit. The analysis and appropriate design of the PBO in the abnormal cases can be performed by following the same procedures in this dissertation. Thus, various methods and structures in this dissertation can be the significant starting point even in the abnormal cases just as the methods for the linear systems can be the basis of the derivation of the methods for the nonlinear systems.

In the same vein, the power market dynamics have a limitation on capturing phenomena in the real world. For example, when a sudden change occurs such as step decrease of generation due to a generation failure, the initial time delay of the response just after the sudden change cannot be avoided. Additionally, even though the time duration between the consecutive asynchronous price signals can be considerably reduced by the improved communication capability, inherent discrete property of the price signal

cannot be changed. Despite these limitations of the power market dynamics, the results based on them in this dissertation still have significant meaning for providing the insights and guide in the PBO. Moreover, various methods and structures in this dissertation can constitute a useful tool for analyzing and designing the PBO. However, more efforts should be made in order for the time variation expected in the analysis to be as similar as possible to the observation in the real world. Thus, just as common improving process of the analysis tool, various aspects of the real world, including time delay and discrete price signals, should be reflected in analyzing and designing methods for the PBO as well as in modifying the power market dynamics.

In the framework for the optimal PBO, only the active power is considered in the formulation of the OPF method. Thus, the DC OPF method for the active power is used in finding the solution, and nodal prices as the control signals are also the values of the active power. However, voltage constraints related to the reactive power are other important conditions to be considered. If the voltage constraints are considered, the solution of the OPF method considered in this dissertation should be modified. As a result, a further research is necessary to extend the framework in this dissertation so that voltage constraints are considered in it; the AC OPF method is used; and the values of the reactive power are determined and used as other price signals.

Similar to the current schemes for the power system operation, the power market dynamics consist of generations and loads. However, it has been a big issue recently the introduction of new systems such as renewable energy resources and energy storage systems. The installed amount of new systems is

not so large at this point compared to the capacity of the whole grid. However, the number is likely to increase exponentially after a certain point. Thus, the power market dynamics should be modified considering the operation of new system components, and the designing rules should be accordingly adjusted in order to reflect the effects of them on the power system operation.

Finally, the provision of the price signal and the introduction of the new systems are suitable within relatively small areas. This small and independent power grid is called as a micro-grid, which is another hot topic within the power system research area. Micro-grid can be a fundamental entity in a decentralized environment. This is consistent with the property of the PBO supporting the independent design and operation. Thus, it is significant and meaning to perform a research on the integration of the PBO into the structure of micro-grid.

Bibliography

[1] R. D. Christie, B. F. Wollenberg, and I. Wangensteen, "Transmission management in the deregulated environment," *Proc. IEEE*, vol. 88, no. 2, pp. 170-195, 2000.

[2] Y. R. Sood, N. P. Padhy, and H. Gupta, "Wheeling of power under deregulated environment of power system-a bibliographical survey," *IEEE Trans. Power Syst.*, vol. 17, no. 3, pp. 870-878, 2002.

[3] A. S. De Vany, and W. D. Walls, "Price dynamics in a network of decentralized power markets," *J. Regul. Econ.*, vol. 15, no. 2, pp. 123-140, 1999.

[4] A. Rudkevich, M. Duckworth, and R. Rosen, "Modeling electricity pricing in a deregulated generation industry: the potential for oligopoly pricing in a poolco," *The Energy J.*, vol. 19, no. 3, pp. 19-48, 1998.

[5] C. Bendel and D. Nestle, "Decentralized Electrical Power generators in the low voltage grid–development of a technical and economical integration strategy," *Int. J. Distributed Energy Resour.*, vol. 1, no. 2, pp. 63-70, 2005.

[6] P. Giabardo, M. Zugno, P. Pinson et al., "Feedback, competition and stochasticity in a day ahead electricity market," *Energy Econ.*, vol. 32, no. 2, pp. 292-301, 2010.

[7] D. Garber, W. W. Hogan, and L. Ruff, "An efficient electricity market: using a pool to support real competition," *Electr. J.*, vol. 7, no. 7, pp. 48-60, 1994.

[8] C. Yu, X. Zhao, F. Wen, C. Chung, T. Chung, and M. Huang, “Pricing and procurement of operating reserves in competitive pool-based electricity markets,” *Electr. Power Syst. Res.*, vol. 73, no. 1, pp. 37-43, 2005.

[9] F. Liu, Y. H. Song, J. Ma, S. Mei, and Q. Lu, “Optimal load frequency control in restructured power systems,” *IEE Proc. Gener., Transm. and Distribution*, vol. 150, no. 1, pp. 87–95, 2003.

[10] Y.-H. Song and X.-F. Wang, *Operation of Market-oriented Power Systems*, London: Springer, 2003.

[11] M. Shahidehpour, H. Yamin, and Z. Li, *Market Operations in Electric Power Systems*, NY: John Wiley & Sons, 2002.

[12] F. C. Schweppe, M. C. Caramanis, R. D. Tabors, and R. E. Bohn, *Spot Pricing of Electricity*, MA: Kluwer Academic Publishers, 1988.

[13] A. W. Berger and F. C. Schweppe, “Real time pricing to assist in load frequency control,” *IEEE Trans. Power Syst.*, vol. 4, no. 3, pp. 920-926, 1989.

[14] G. Gutierrez-Alcaraz and G. B. Sheble, “Decentralized electricity market price dynamics,” in *PES General Meeting*, 2004, pp. 274-279.

[15] A. Jokic, M. Lazar, and P. P. J. van den Bosch, “Real-time control of power systems using nodal prices,” *Int. J. Electr. Power Energy Syst.*, vol. 31, no. 9, pp. 522-530, 2009.

[16] J. Kumar and G. Sheble, “Auction market simulator for price based operation,” *IEEE Trans. Power Syst.*, vol. 13, no. 1, pp. 250-255, 1998.

[17] F. L. Alvarado, *The Dynamics of Power System Markets*, Technical

Report PSERC-97-01, University of Wisconsin-Madison, 1997.

[18] F. Alvarado, "The stability of power system markets," *IEEE Trans. Power Syst.*, vol. 14, no. 2, pp. 505-511, 1999.

[19] A. Jokic, E. H. M. Wittebol, and P. P. J. van den Bosch, "Dynamic market behavior of autonomous network-based power systems," *Eur. Trans. Electr. Power*, vol. 16, no. 5, pp. 533-544, 2006.

[20] A. Syothert and I. MacLeod, "Competitive bidding as a control problem," *IEEE Trans. Power Syst.*, vol. 15, no. 1, pp. 88-94, 2000.

[21] Y. F Liu, Y. X. Ni, and F. F. Wu, "Control Theory Application in Power Market Stability Analysis," in *Proceedings of the International Conference on Electric Utility Deregulation*, 2004, pp. 562-569.

[22] J. Nutaro and V. Protopopescu, "The impact of market clearing time and price signal delay on the stability of electric power markets," *IEEE Trans. Power Syst.*, vol. 24, no. 3, pp. 1337-1345, 2009.

[23] F. L. Alvarado, J. Meng, C. L. DeMarco et al., "Stability analysis of interconnected power systems coupled with market dynamics," *IEEE Trans. Power Syst.*, vol. 16, no. 4, pp. 695-701, 2001.

[24] H. Glatvitsch and F. Alvarado, "Management of multiple congested conditions in unbundled operation of a power system," *IEEE Trans. Power Syst.*, vol. 13, no. 3, pp. 1013-1019, 1998.

[25] F. L. Alvarado, "Controlling power systems with price signals," *Decis. Support Syst.*, vol. 40, pp. 495-504, 2005.

[26] A. J. Wood and B. F. Wollenberg, *Power Generation, Operation, and Control*, 2nd ed., NY: Wiley, 1996.

[27] A. Bergen and V. Vittal, *Power System Analysis*, 2nd ed., NJ: Prentice-Hall, 2000.

[28] NERC, *Balancing and Frequency Control*, North American Electric Reliability Corporation, Atlanta, GA, Jan. 2011.

[29] X. Ma, D. Sun, and K. Cheung, "Energy and reserve dispatch in a multi-zone electricity market," *IEEE Trans. Power Syst.*, vol. 14, no. 3, pp. 913-919, 1999.

[30] R. Baldick, "Electricity market equilibrium models: the effect of parametrization," *IEEE Trans. Power Syst.*, vol. 17, no. 4, pp. 1170-1176, 2002.

[31] G. Andersson, *Dynamics and Control of Electric Power Systems*, Lecture 227-0528-00, ETH, Zurich, Feb. 2012.

[32] K. Ogata, *Modern Control Engineering*, 3rd ed., NJ: Prentice-Hall, 1997.

[33] G. F. Franklin, J. D. Powell, and B. Emami-Naeini, *Feedback Control of Dynamic Systems*, 3rd ed., Addison-Wesley, 1994.

[34] C.-T. Chen, *Linear System Theory and Design*, 3rd ed., NY:Oxford University Press, 1999.

[35] H. K. Khalil, *Nonlinear Systems*, 3rd ed., NJ:Prentice Hall, 2002.

[36] A. Gomez-Exposito, A. J. Conejo, and C. Canizares, *Electric Energy Systems: Analysis and Operation*, FL: CRC Press, 2008.

[37] N. Martins, L. T. G. Lima, and H. J. C. P. Pinto, "Computing dominant poles of power system transfer functions," *IEEE Trans. Power Syst.*, vol. 11, no. 1, pp. 162-170, 1996.

[38] Y. G. Jin, S. Y. Lee, S. W. Kim, and Y. T. Yoon, "Designing rule for price-based operation with reliability enhancement by reducing the frequency deviation," *IEEE Trans. Power Syst.*, vol. 28, no. 4, pp. 4365-4372, 2013.

[39] J. G. Ziegler and N. B. Nichols, "Optimum settings for automatic controllers," *Trans. ASME*, vol. 64, pp. 759-768, 1942.

[40] P. Cominos and N. Munro, "PID controllers: recent tuning methods and design to specification," *IEE Proc.-Control Theory Appl.*, vol. 149, no. 1, pp. 46-53, 2002.

[41] S. Skogestad, "Simple analytic rules for model reduction and PID controller tuning," *J. Process Control*, vol. 13, no. 4, pp. 291-309, 2003.

[42] D. E. Rivera, M. Morari, and S. Skogestad, "Internal model control. 4. PID controller design," *Ind. Eng. Chem. Process Des. Dev.*, vol. 25, no. 1, pp. 252-265, 1986.

[43] C. A. Smith and A. B. Corripio, *Principles and Practice of Automatic Process Control*, NY: Wiley, 1985.

[44] UCTE OpHB-Team, *UCTE Operation Handbook Policy 1: Load-Frequency Control and Performance*, UCTE, Jul. 2004.

[45] NERC, *Reliability Standards for the Bulk Electric Systems of North America*, North American Electric Reliability Corporation, Atlanta, GA, Nov. 2012.

[46] J. C. Hull, *Options, Futures and Other Derivatives*, 7th ed., NJ:Prentice-Hall, 2009.

[47] C. Redl, R. Haas, C. Huber, and B. Bohm, "Price formation in electricity forward markets and the relevance of systematic forecast errors," *Energy Econ.*, vol. 31, no. 3, pp. 356-364, 2009.

[48] S. K. Aggarwal, L. M. Saini, and A. Kumar, "Electricity price forecasting in deregulated markets: A review and evaluation," *Int. J. Electr. Power Energy Syst.*, vol. 31, no. 1, pp. 13-22, 2009.

[49] F. J. Nogales, J. Contreras, A. J. Conejo, and R. Espinola, "Forecasting next-day electricity prices by time series models," *IEEE Trans. Power Syst.*, vo. 17, no. 2, pp. 342-348, 2002.

[50] J. Johnston and J. DiNardo, *Econometric Methods*, 4th ed., McGraw-Hill, 1997.

[51] F. Genoese, M. Genoese, and M. Wietschel, "Occurrence of negative prices on the German spot market for electricity and their influence on balancing power markets," in *International Conference on the European Energy Market*, 2010, pp. 1-6.

[52] E. Fanonea, A. Gambab, and M. Prokopczukc, "The case of negative day-ahead electricity prices," *Energy Econ.,* vol. 35, pp. 22-34, 2013.

[53] S. Boyd and L. Vandenberghe*, Convex Optimization*, NY:Cambridge University Press, 2004.

[54] R. D. Zimmerman, C. E. Murillo-Sanchez, and R. J. Thomas, "Matpower: Steady-State Operations, Planning and Analysis Tools for Power Systems Research and Education," *IEEE Trans. Power Syst.*, vol. 26, no. 1, pp. 12–19, 2011.

[55] M. A. Pai, *Energy Function Analysis for Power System Stability*, MA: Kluwer, 1989.

[56] A. Faruqui and S. George, "Quantifying customer response to dynamic pricing," *Electr. J.*, vol. 18, no. 4, pp. 53–63, 2005.

[57] T. B. Nguyen, and M. A. Pai, "Dynamic security-constrained rescheduling of power systems using trajectory sensitivities," *IEEE Trans. Power Syst.*, vol. 18, no. 2, pp. 848-854, 2003.

[58] Z. Zhong, "Power systems frequency dynamic monitoring system design and applications," PhD. dissertation, Dept. Elect. Comput. Eng., Virginia Polytechnic Institute and State Univ., Blacksburg, VA, USA, Jul. 2005.

[59] H. R. Cai, C. Y. Chung, and K. P. Wong, "Application of differential evolution algorithm for transient stability constrained optimal power flow," *IEEE Trans. Power Syst.*, vol. 23, no. 2, pp. 719-728, 2008.

초 록

가격 기반의 전력시스템 운영 방법은 분산화된 탈규제 환경에서 기존의 중앙집중형 운영 방식을 대신할 수 있는 하나의 대안으로 제시되었다. 가격 기반 운영 방법에서는 변화하는 가격 신호를 통해 자기 이익의 최대화를 우선으로 하는 독립적인 참여자들을 조정하게 된다. 가격 기반 운영 방법에서 가장 중요한 것은 적절한 가격 신호를 정하는 것이지만, 이것은 상당히 어려운 과제 중 하나이다. 따라서, 가격 신호의 결정에 도움을 주고 동적인 현상에 대한 해석과 통찰을 제공하기 위한 가격 기반 운영 방법에 대한 분석 및 설계 방법이 필요하다. 본 논문에서는 주파수 안정도 관점에서의 동적인 성능을 향상시키는 것을 목적으로 하는 가격 기반의 전력시스템 운영 방법의 분석 및 설계에 대한 다양한 기법들을 제시하고자 한다.

우선 공급자와 소비자의 수가 매우 많고 중첩된 비동기 이산 응답을 연속함수로 근사시킬 수 있다는 가정 하에 가격 기반 운영 방법의 연속시간 모델을 규정한다. 그리고 기존 연구에서 제안되었던 전력시장 동역학 방정식을 피드백 제어 구조로 정형화하고, 가격 기반 운영 방법이 피드백 제어 구조에서 제어기에 해당함을 보였다. 그리고, 피드백 제어 구조의 대상 시스템을 제어기 설계 기법에서 주로 다루는 전형적인 형태로 단순화시키기 위해 시정수의 정의에 근거한 근사화 기법을 구성하였다. 선택한

제어기 설계 기법을 근사된 대상 시스템에 적용함으로써 가격 기반 운영 방법에 대한 기본 설계 기법을 유도하였다. 여기에 보조적인 감폭 제어를 부가함으로써, 주파수 제어 성능이 향상된 개선된 설계 기법을 구성하였다.

주파수 안정도 관점에서의 동적인 성능을 더 향상시키는 방법으로서 사전적인 가격 정보를 활용하는 새로운 피드백 제어 구조를 제안하였다. 새로운 구조에서 가격 정보는 제어기 신호에 대한 일종의 오프셋으로 작용한다. 가격 정보가 주파수 변화의 최대폭에 미치는 영향에 대한 정량적 분석을 수행하였다. 그 결과 가격 정보의 균형 가격 대비 정확도에 선형적으로 비례하여 주파수 변화의 최대폭이 감소한다는 것과 구성성분간의 상쇄 현상으로 인해 주파수 변화의 최대폭이 감소할 때는 가격 정보가 균형 가격과 같을 때가 아니라 약간 크거나 작을 때라는 것을 확인하였다.

가격 기반의 최적 운영방법 설계를 위한 체계를 구성하였다. 제안된 설계 체계에서는 기본적인 수렴 특성만 보장된다면 가격 기반 운영 방법이 어떻게 설계되더라도, 전력 평형과 송전 혼잡 해소의 기능이 수행될 뿐만 아니라, 안정상태에서의 수렴값이 최적해와 같아진다. 따라서, 설계 체계 내에서는 최적 운영이 보장되는 것이다. 또한 설계 체계에서는 송전 혼잡 해소 기능에 대한 설계와 운영이 개별적으로 이루어지므로, 분산화된 환경에서의 가격 기반 운영 방법 설계에 매우 적합한 구조를 가지고 있다.

IEEE 39-버스 전력망을 이용한 두 가지 시뮬레이션을 통해 제안된 기법들의 유효성을 확인하였다. 설계 기법을 적용한 경우에 주파수 안정도가 개선되고, 기본적인 설계 기법보다는 개선된 설계 기법을 적용한 경우에 더 많이 개선되었다. 사전적인 가격 정보를 활용하는 경우에는 가격 기반 운영 방법 설계에 관계없이 주파수 제어 성능이 상당히 개선되었다. 또한, 설계 체계에 대한 시뮬레이션 결과로부터 가격 기반 운영 방법 설계에 따라 주파수 제어 성능을 차이가 나지만, 설계 체계 내에서 사고 상황이 모두 정상 상태로 회복되었고 변경된 안정 상태도 최적 운영점과 동일하였다. 주요 변수에 대한 시뮬레이션 결과를 분석함으로써, 정상 상태로의 회복 속도와 전력 가격과 같은 주요 변수의 변화 속도, 그리고 전력 균형 기능과 송전 혼잡 제어 기능간에는 일종의 트레이드오프 관계가 성립함을 보여주었다.

주요어: 전력 시스템 운영, 전력 가격, 주파수 제어, 송전 혼잡 제어, 최적 조류 계산, 제어기 설계.

학 번: 2010-31001